11-21-2019

Shake Table Experiments on Multi-Story Aluminum Structures Using Scaled Ground Motions.

Biraj Joshi

SHAKE TABLE EXPERIMENTS ON MULTI-STORY ALUMINUM STRUCTURES USING SCALED GROUND MOTIONS

By

Biraj Joshi

A Thesis

Submitted in Partial Fulfillment of the

Requirements for the Degree of

Master of Science

Major: Civil Engineering

The University of Memphis

December 2019

ACKNOWLEDGMENTS

First and foremost, I would like to express my gratitude to my academic and research advisor, Dr. Charles V. Camp, without whom this work would not have seen the light of day. I would like to thank him for his direction and support throughout the course of this study. I would also like to acknowledge my thesis advising committee members: Dr. Shahram Pezeshk for his guidance and for providing me with the necessary data acquisition system, which was an essential part of the study, and Dr. Roger Meier for his advice and recommendations on improving the scope and script of this work. This work would have never been possible without them.

I am grateful to Chris Johnson and Barry Wymore for preparing the structural components used in this study at the University of Memphis's engineering shop.

My special thanks go to Melish Kayastha for lending his helpful hand in assembling the model structures at the research lab. Finally, I would like to thank the University of Memphis for funding the necessary materials that were needed for carrying out the experiments.

ABSTRACT

A shake table is a device used to simulate the seismic waves during an earthquake event and test the stability of the structure after an event. This table can be helpful in testing structural components or models. The primary objective of this study is to operate and verify the functionality of the shake table present at the Department of Civil Engineering's structure research lab. The System Communication Software (SCSW), present at the University of Memphis's Department of Civil Engineering lab, operates the shake table unidirectionally and requires ground motions to be uploaded to the software. Pacific Earthquake Engineering Research (PEER) provides strong ground motion data that was used to extract several ground motions for selection and scaling purposes for the study. As per ASCE 7-16, Chapter 16.2, non-linear response history analysis is applied to select and scale the motions. In addition to the ASCE provisions, the Spectral-Matching procedure in the frequency domain is practiced in scaling or matching of the ground motions for this study.

The ground motions to be uploaded needs to be either load or displacement controlled. The extracted scaled ground motions as acceleration time histories are converted into displacement time histories and are uploaded to the SCSW software to control the shake table to displace. The scaled models are mounted on the shake table using bolted connections. Accelerometers are clamped on every story of the scaled model to measure the acceleration while being subjected to scaled ground motion. The data acquired from the accelerometers are raw, unprocessed, and thus need to be filtered for unwanted components or noise. The final processed and corrected accelerations are then compared with the output response at every story of all the scaled models from the 2D SAP2000 model for validation of the functionality of the shake table.

TABLE OF CONTENTS

LIST OF FIGURES

Chapter 1. Introduction

Shake tables can be extremely helpful in testing structural components or models to the point of failure of the structural system. A shake table is a device used to simulate the seismic waves during an earthquake event and test the stability and functionality of the structure after an event. Shake tables are typically driven by a series of hydraulic actuators to recreate motions in one, two, or three dimensions. A model of the structure is placed on a shake table capable of simulating seismic loads in order to record and analyze the structure's response to those loads. The simulated shake table ground motions must be selected considering site soil characteristics, fault type, earthquake magnitude, and rupture distance.

Following the scaling of the ground motion and the application of the motion to the specimen, the structural dynamic behavior can be studied. A data acquisition system capable of recording the response in terms of acceleration is utilized to record the structural response. The data recorded during a shake table simulation are not free of unwanted noise, and hence, measures are taken to filter unwanted features.

The Department of Civil Engineering at the University of Memphis recently constructed a 1D shake table. The capabilities and performance of the shake table have not been verified. In this study, three-, four- and five-story scaled aluminum models are subjected to 1D ground motions using a shake table, and the performance and the seismic response of the specimen under such loading are recorded. The experimental results are compared to numerical simulations using SAP2000 to verify the operational performance of the shake table system. A set of scaled ground

motions are applied to structural models on the shake table and to SAP2000 two-dimensional models. The SAP2000 model allows one degree of freedom in the direction of the lateral force of the shake table.

The objective of the study is to operate and verify the functionality of the shake table at the Department of Civil Engineering's structure research lab. The following steps were taken to accomplish these objectives.

- Set up a structural system at the structure research lab and document the progressions and findings, which could be used for further research and experiment purposes.
- Develop and assemble 3D multi-story scaled moment frame models on a 1D shake table.
- Select and scale a suitable suite of ground motions.
- Baseline correct and filter the accelerations acquired from the data acquisition system.
- Validate the structural response of the scaled models with the 2D SAP2000 model.

1.2 Literature Review

Any structure to be constructed in a high seismic zone needs to be designed in accordance with seismic design codes. The design of such structures as a normal load-bearing structure leaves it vulnerable to collapse during strong ground motions. Earthquakes are unpredictable, and it takes special measures to design a structure that will reside in a high seismic zone. Seismic design codes such as the American Society of Civil Engineers (ASCE) 7-16 incorporate specifications and guidelines to account for linear as well as nonlinear behavior of the structure and allows for the design of buildings to withstand ground motions.

The seismic response of a structure can be determined by performing linear static, non-linear static, linear dynamic, and nonlinear dynamic analyses. Linear static analysis, also known as the equivalent static method, is useful in the case of regular structures undergoing regular loading conditions. Nonlinear static analysis considers the inelastic behavior of the structure, which is an improvement over linear static analysis. In the past, seismic design of structures was performed assuming linear behavior of the structure, which is not the case. Under seismic loadings, a structure is expected to show nonlinear behavior that is not considered while performing simple linear static analysis.

A nonlinear response history analysis considers the force redistribution and the dissipation of energy among the structural members when it comes under lateral forces (Riddell et al. 1996). Nonlinear response history analysis, also known as nonlinear modal time history analysis, estimates the seismic response of a structure for several modes as a function of modal load vectors (Tokoro et al. 2004).

A time history analysis approach is used for the evaluation of the response of a structure under dynamic loading according to a specific time function whereas response spectrum analysis is a dynamic statistical approach that indicates the maximum response of a structure to seismic loads by estimating the pseudo acceleration, velocity, and displacement as a function of the fundamental period of the structure.

It is highly unlikely to have recorded ground motions for every site under various conditions. Also, the specific seismic design parameters do not necessarily have to be constant within the same region. Ground motion selection and scaling play a vital role in designing a structure at a site where there are limited ground motions available. Over 40 methods are described in the literature for the selection and scaling of earthquake ground motions. The ASCE 7-16 seismic design code has a provision to select and scale ground motions based on site characteristics, earthquake magnitude, rupture distance, and the target spectrum for a specific site considering a specific range of periods.

ASCE 7-16 allows for the selection of a series of ground motions based on amplitude scaling or spectral matching. For scaling purposes, a target response spectrum is developed using one of the following methods: Method 1 deals with the development of a single response spectrum; Method 2 deals with the generation of two or more site-specific target response spectra (ASCE 7-16).

In addition to the ASCE 7-16 provisions, spectral matching in the frequency domain can also be applied to scale or match the response spectrum of a suite of ground motions to a predefined target spectrum. The spectral matching process can either be done by ground motion modification itself in the time domain as suggested in the RspMatch2005 program, or in the frequency domain using the computer code: Response Spectra and Acceleration Scaling (RASCAL). This computer

code generates the Fourier amplitude spectrum of the accelerogram and scales it by the ratio of the target spectrum to the response spectrum at the natural frequency of the structure. The scaling is done iteratively by the code until the response and target spectra overlap each other. (Shahbazian and Pezeshk, 2010).

It is of utmost importance to understand the effects of earthquakes on structures in order to refine seismic design codes. The cost of repairing the damage done by strong ground motions greatly exceeds the cost of erecting a structure capable of withstanding such strong motions. In order to study and analyze the dynamic behavior of a structure or its components, an earthquake simulator or a shake table can be used to simulate earthquake ground motions (Wang 2002).

The selection of a suitable set of ground motions is a prerequisite for performing a reliable structural analysis during the application of strong ground motions (Sextos 2014). The selection and scaling of ground motions have a key role in seismic load definition and serve as an interface between seismology and engineering (Baker 2007). The purpose of the selection and scaling is to realistically represent aspects of the nonlinear response during the design phase. It is highly unlikely to have ground motions for every site and condition (Thrainsson et al. 2000). So, the selection and scaling of ground motions from other sites sharing similar attributes and characteristics are used.

The Ground Motion Selection and Modification (GMSM) Program from the Pacific Earthquake Engineering Research (PEER) has categorized the methods for selecting and scaling ground motions (Haselton 2009). Over 40 methods exist for selection, modification, and scaling of the ground motions in the published literature. One of these methods is described in ASCE 7-16 Chapter 16 (Sextos 2014).

Seismic provisions for selection and scaling per ASCE 7-16 include guidelines for designing structures using nonlinear response history analysis. The structural response to a set of ground motions is evaluated through numerical integration of equations of motion in the response history analysis (Mulchandani 2018). Seismic design codes define shaking of the ground in the form of a response spectrum given in terms of accelerations and allow spectrally matched ground motions for linear as well as nonlinear time-domain analysis. The ground motions must be organized in such a way that they match the design response spectrum for all or a portion of a specified range of time of interest. Amplitude scaling can be done in either time or frequency domain. (Fahjan 2008).

Matching a single ground motion to the design response spectrum does not adequately represent the actual movement, which is a drawback of using only one ground motion for design purposes (Naeim and Kelly, 1999). A strong global ground motion database and records have made it possible to select and scale the motions for many, if not all, conditions (Bommer et al. 2003). The records having similar earthquake parameters such as magnitude, rupture distance, and site classification can be used for design or test purposes. ASCE 7-16 requires eleven ground motions sharing similar earthquake parameters to be selected and then scaled to meet the target response spectrum.

Another method for selecting and scaling ground motions is spectral-matching, performed in the frequency domain. In order to get some degree of agreement between target and response spectrum of any ground motion, the response spectrum of the motion must be reformed (Shahbazian and Pezeshk, 2010). The RASCAL computer code uses the approach of scaling the modulus of the Fourier spectral density by the ratio of target to response spectrum until the spectrum of

scaled ground motion is close to the target response spectrum. RASCAL follows the iterative scaling of the Fourier Amplitude Spectrum by the ratio at the fundamental frequency such that a degree of agreement is reached between the target spectrum and response spectrum.

The ground motions extracted from the PEER database are reviewed and processed in a consistent manner and require no additional processing after extraction (Darragh et al. 2013). The ground motions processed by PEER have two major objectives: reducing the random noise in the signals and correcting for the instrument measuring the motion.

Prior to filtering, a length of zeroes needs to be added before and after the ground motion (zero-padding) to prevent unwanted deviations or distortions in the displacement time history (Boore 2005). Not implementing zero-padding results in unreasonable and inappropriate ground motions. In addition, zero-padding expands the time history so that the total number of points in the record is an integer power of two. The Fast Fourier Transform (FFT) algorithm used to convert time into the frequency domain, works best if the number of points is an integer power of two.

Ground motion observations are of great importance in earthquake engineering. Obtaining a credible ground motion record and processing those motions is an important task. The velocity and displacement time history obtained as a result of the integration of acceleration often exhibits baseline drift (Tao 2015). Baseline drift is a linear or nonlinear addition to the spectrum that causes expected zero measurements to gain some positive value. Although modern digital instruments have a higher dynamic range, wider frequency bandwidth, and lower noise level, baseline drift cannot be completely removed. Data acquired from the accelerometers are highly influenced by the proximity of electric generators or any vibratory machines. Instrument noise and background noise in the surrounding environment are other factors that require correction of the drift error.

Baseline correction and filtering are required for the generated acceleration time histories as the scaled motion might have very high energy content, and an excessive number of cycles (Abrahamson 1992). Other sources of baseline error include instrument errors, background noise, initial value error, and manipulation errors. Baseline initialization, also known as baseline adjustment, suggests subtracting the mean value of the prior ground motion application part for 20 seconds (Boore 1999). It is one of several methods for applying baseline correction. Low-frequency noise also causes baseline drift. A high-cut filtering method is effective in eliminating the impacts of low-frequency noise (Trifunac 1971).

Accelerograms obtained from accelerometers are not absolute replicas of a seismic signal and contain a fair amount of noise (Boore et al. 2004). Given the arbitrary nature of the noise, obtaining an uncontaminated and actual signal is next to impossible (Athanasiou et al. 2017). Signal processing or filtering is an essential step that aims to remove the effects of noise in strong ground motions. Low-frequency noise is a trait of background noise, instrument errors, and drifts (Chiu 1997), and their effects can be minimized using low-cut filters or high-pass filters. The automated digitization of the records may lead to erroneous spikes throughout the acquired data (Alexander 2013). The effects of low-frequency noise can be more critical than high-frequency noise as they impact the response quantities such as velocity and displacement (Athanasiou et al. 2017). The main purpose of processing ground motions is to optimize the signal-to-noise ratio, which is the comparison between the desired signal and unwanted background noise (Boore et al. 2004).

Chapter 2. Experimental Setup

This chapter deals with the assembly of the multi-story structures, the setup of the experiments, and the components used in performing the test. Also, this chapter describes the system and software environment used to acquire the data.

Several different components were assembled to form a shake table system to perform a dynamic test:

1) Shore Western 92E Series single-ended actuator,

2) Shake table testbed,

3) Multi-story structural models, and

4) Data acquisition system.

2.1 Shore Western 92E Series Single-Ended Actuator

Figure 2 shows a Shore Western 92E Series single-ended actuator is used to apply a unidirectional load. The compact-sized single series actuator is best suited for static low-cycle structural and component testing and is sized for a 10 in stroke and a force rating of 10 kips. The actuator is connected to the shake table at one end, enabling the table to move as per the loading cycles applied to the actuator. The actuator is connected to the shake table and is equipped with a linear variable differential transducer (LVDT) and a load cell and can be displacement or load controlled. In this study, the acceleration-based ground motions extracted from the PEER are integrated into the displacement domain to drive a displacement-controlled test.

Figure 1. 92E series single-ended Shore Western actuator

2.2 Shake Table

The shake table used in this study has an aluminum rectangular base plate measuring 48.5 in. x 40 in x 4 in., that moves in one direction and is capable of displacing ± 5 in from the mean position. The table is driven by the Shore Western 92E hydraulic actuator, which is connected to one end of the base plate, providing the means to simulate ground motions. The base of the shake table rests on a set of linear roller bearings that support the loads and allow the table to move unidirectionally upon the application of the desired load.

2.3 Multi-story Structural Models

A scaled structural model is expected to show scaled dynamic properties and behavior of an actual structure. For this study, three-story, four-story, and five-story structures were assembled using essential structural components and connections. Figure 2 shows the three structural models. The three-story model consists of four aluminum slabs, each measuring 18 in. x 18 in. x 1 in., that are assembled with four aluminum columns, each measuring 36 in. x 2 in. x 0.125 in. The four-story model consists of five aluminum slabs with the same dimensions, that are assembled with four aluminum columns, each measuring 48 in. x 2 in. x 0.125 in. The five-story model consists of six aluminum slabs that are assembled with four aluminum columns, each measuring 60 in. x 2 in. x 0.125 in. The models are positioned on the shake table such that the load is applied in the

weak direction of the columns. Two 0.25 in. diameter bolts were used at every slab-column connection with the help of a 2 in. x 1 in. x 0.5 in. washer block and lock washers. The columns are attached to the slabs such that the structure is subjected to in-plane loading via scaled ground motions, and out-of-plane motion is almost negligible. The base slab is linked with the shake table itself using four 1 in. diameter cap head bolts and washer blocks to ensure rigid connections between the columns and the floor slabs. Lock washers are placed under the head of the 0.25 in. bolts to maintain a preload and prevents loosening and crushing of the bolt. The total self-weights of the three-story, four-story, and five-story structures are approximately 133.2 lb., 166.8 lb., and 200.4 lb., respectively.

(a) (b) (c)

Figure 2. Aluminum structural model (a) three-story, (b) four-story, and (c) five-story

2.4 Data Acquisition System

Data acquisition systems typically measure real-world information and record data capable of being manipulated by a computer. Data acquisition devices, application software, sensors, and filters are the main components of a data acquisition system. Upon application of the scaled ground motion to the scaled structures, it is expected that the models will respond to the dynamic loads. A data acquisition system is essential to acquire those responses. Data in the form of acceleration will be acquired for further analysis and study. Two-dimensional SAP2000 models will be developed and analyzed considering nonlinear time history analysis and compared to the recorded structural responses of the models on the shake table.

Figure 3 shows an ultra-low frequency, high sensitivity seismic accelerometer made by Wilcoxon (Model 731A). These are clamped on every story of the scaled model to record the accelerations during the application of simulated ground motions. These seismic accelerometers have a maximum peak amplitude of 0.5g and a sensitivity of 10 V/g and are connected by 16-ft cables to a battery-powered power unit/amplifier with a switchable low-pass filter of 450 Hz or 100 Hz frequency and a switchable output system for recording acceleration or velocity. The power unit/amplifier further enhances the capabilities of the seismic accelerometers by providing signal amplification, filtering, and signal integration.

Figure 3. Wilcoxon (Model 731A) seismic accelerometer with cable and power unit

A measurement and automation explorer (MAX) is required in order to configure and customize the number of channels for this data acquisition system, to provide access to these components, and to run test panels. National Instrument's MAX can be used to customize the configuration and run the VXI system. Figure 4 shows the VXI Mainframe with controllers (CT-100C) and is used as a modular instrument having enhanced monitoring capabilities equipped to shelter a number of channels as required. These interconnected components, which perform the analog operation, require a programming software development environment to produce and store the output in the desired format.

Figure 5 shows the user interface of the Keysight VEE Pro 9.33 (Visual Engineering Environment) graphical dataflow programming development environment that enables users to measure, analyze, and report outputs generated using seismic accelerometers. The software development environment is optimized in the automation of measurement devices such as data acquisition equipment and source devices. The VEE Pro 9.33 identifies the instrument managers, creates a

sequence with input and output parameters, generates waveforms in time or frequency domain, and stores the data for the desired time range and block size in text format.

Figure 4. VXI Mainframe (CT-100C)

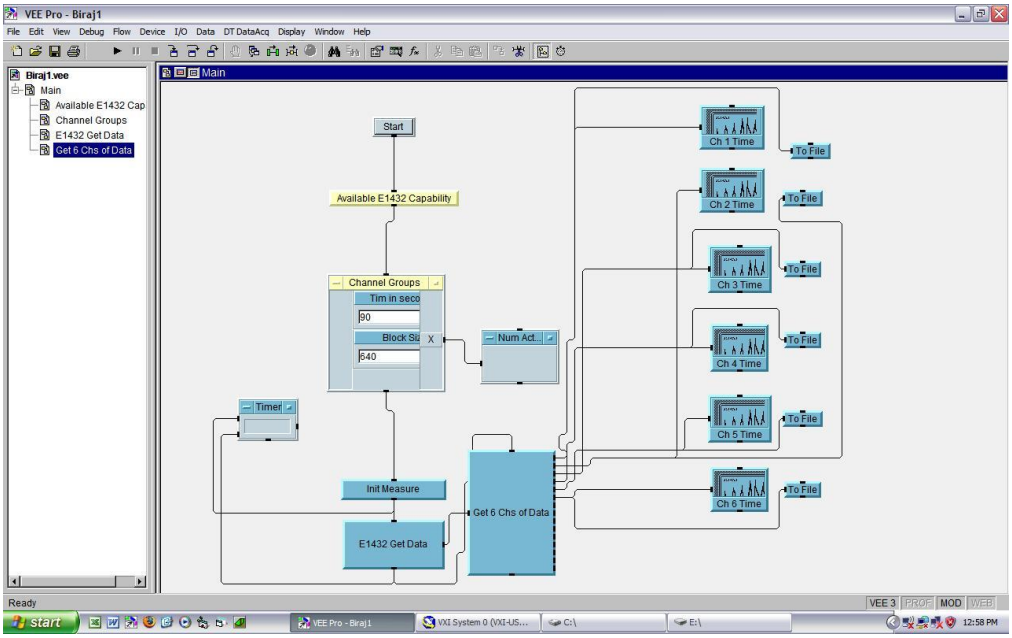

Figure 5. VEE Pro command window with a programming flowchart

Chapter 3. Methodology

3.1 Generating 2D SAP2000 models

SAP2000 is a powerful finite element (FE) analysis program that can be used to model, analyze, and design structures. In addition, SAP2000 can analyze and evaluate the dynamic structural response to various time-dependent loadings. In this study, SAP2000 models will provide insights on how the scaled structures behave under the application of scaled ground motions and are used to verify the recorded behavior of the models on the shake table.

Two-dimensional SAP2000 models were generated to visualize and estimate the fundamental period and mode shapes of the scaled aluminum structures. Figure 6 shows a drawing of the three-story scaled model, which is composed of four 18 in. x 18 in. x 1 in. slabs and four 36 in. x 2 in. x 0.125 in. columns assembled using bolt connection. The 2D SAP2000 model represents just half of the structure with 9 in.. x 1 in. beams instead of slabs. Figure 7 shows the 2D SAP2000 topology of the scaled model. Figures 8-10 show the first three mode shapes of the three-story model determined from the SAP2000 analysis. Similarly, Figure 11 shows a drawing of the four-story scaled aluminum structure. Figure 12 shows the 2D SAP2000 topology of the four-story scaled model. Figures 13-15 show the first three mode shapes of the four-story model determined from the SAP2000 analysis. Figure 16 shows a drawing of the five-story scaled aluminum structure. Figure 17 shows the 2D SAP2000 topology of the five-story scaled model. Figures 18-20 show the first three mode shapes of the five-story model determined from the SAP2000 analysis.

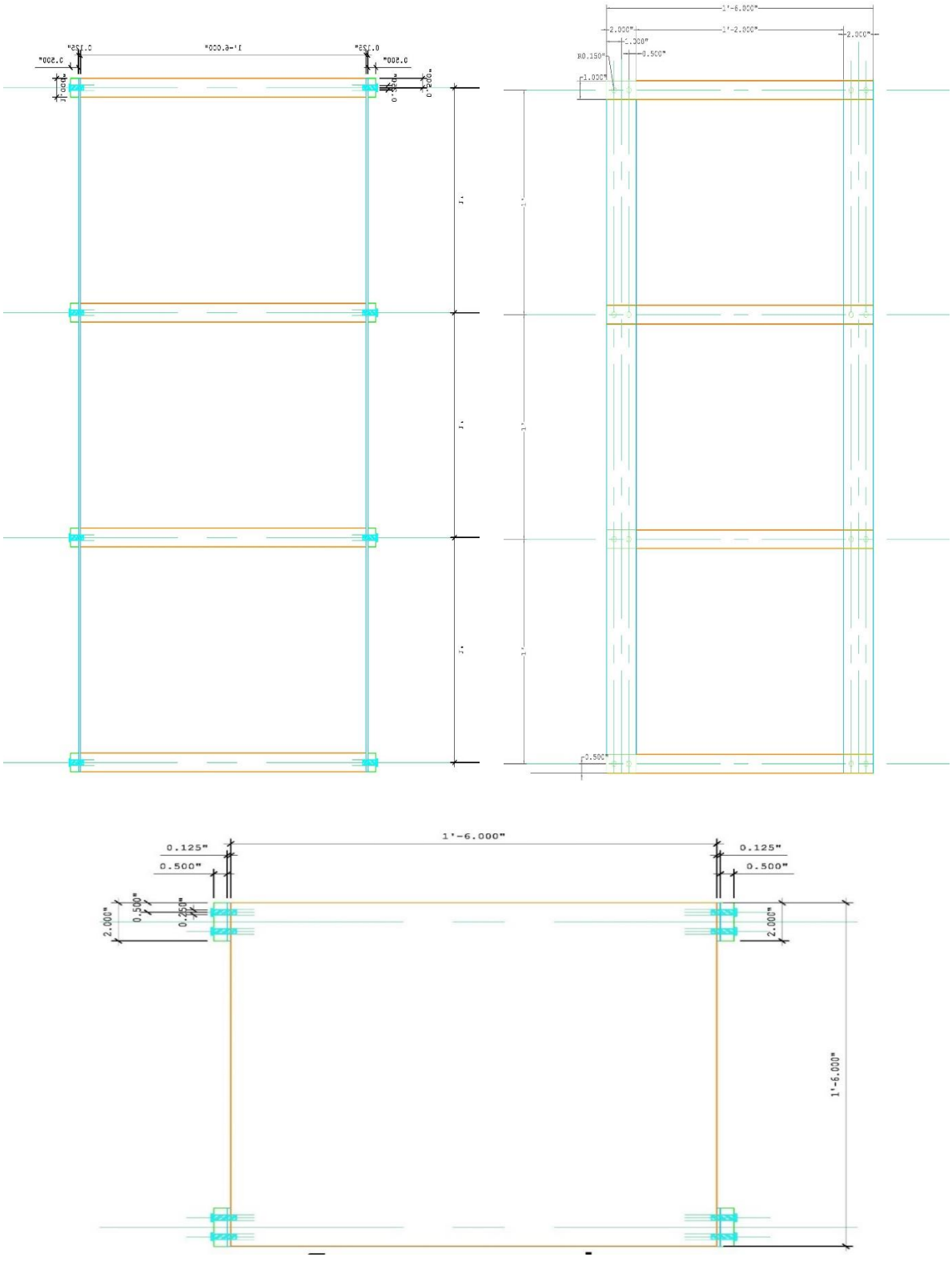

Figure 6. Elevation (top) and plan (bottom) and views of the three-story scaled structure

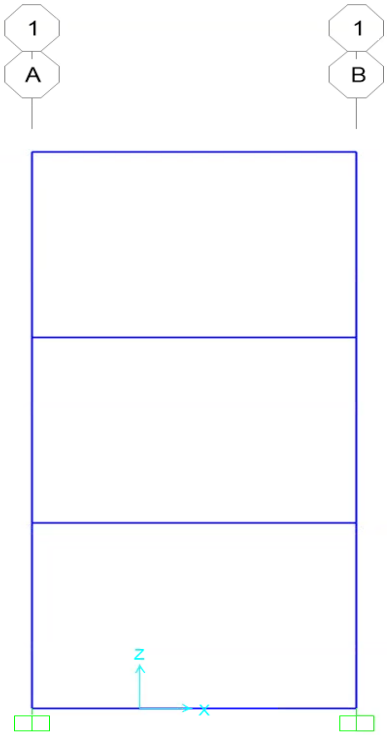

Figure 7. 2D SAP2000 model of the three-story structure

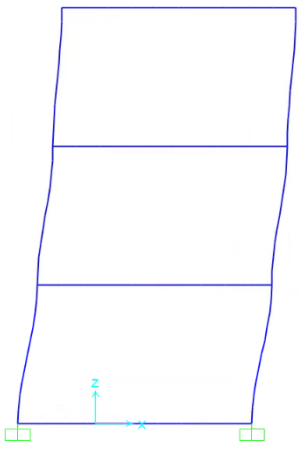

Figure 8. First mode
(T_1= 0.429 sec, f_1= 2.327 Hz)

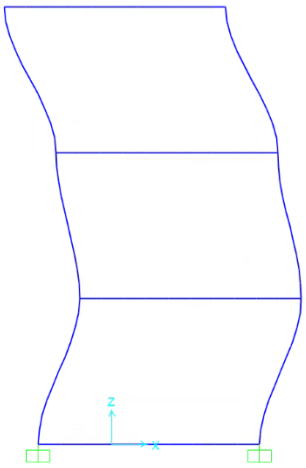

Figure 9. Second mode
(T_2= 0.153 sec f_2= 6.511 Hz)

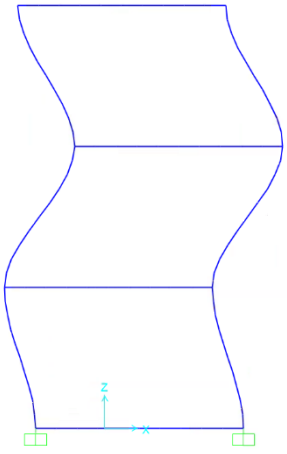

Figure 10. Third mode
(T_3= 0.106 sec, f_3= 9.389 Hz)

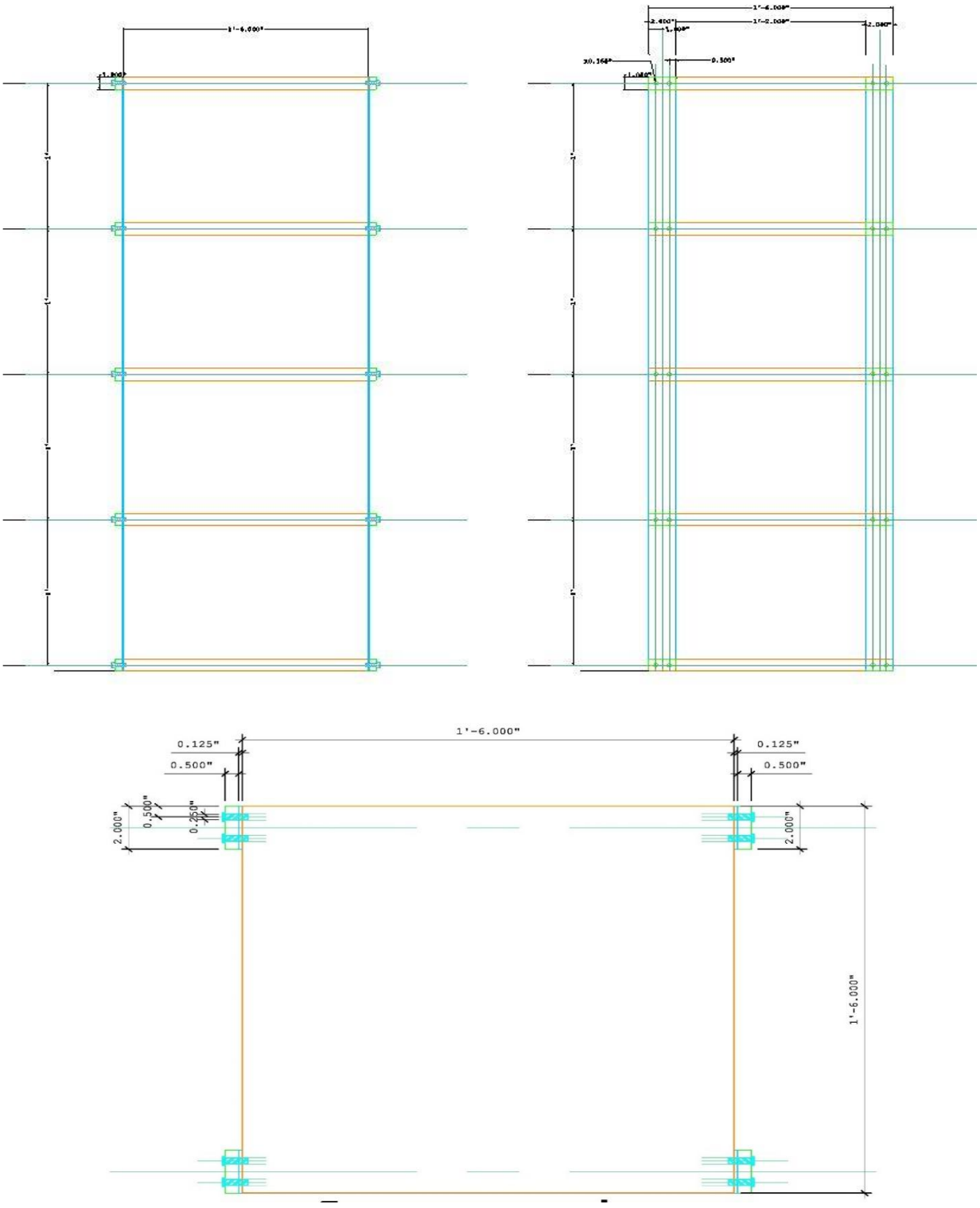

Figure 11. Elevation (top) and plan (bottom) and views of the four-story scaled structure

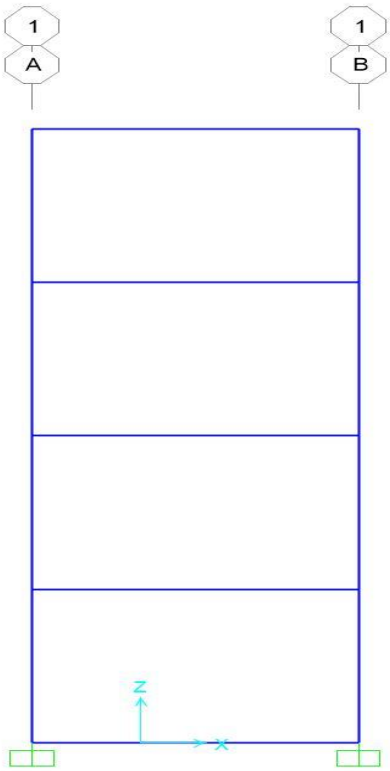

Figure 12. 2D SAP2000 model of the four-story structure

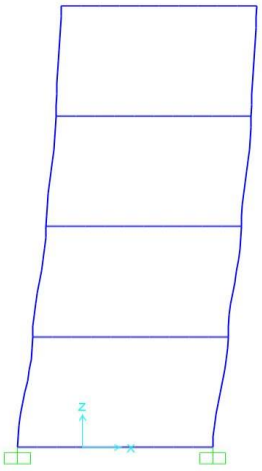

Figure 13. First mode
(T_1= 0.551 sec, f_1= 1.814 Hz)

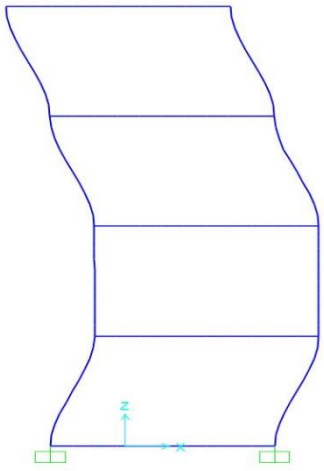

Figure 14. Second mode
(T_2= 0.1915 sec f_2= 5.22 Hz)

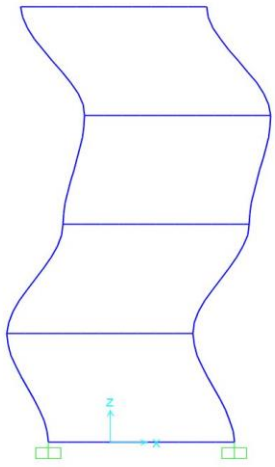

Figure 15. Third mode
(T_3= 0.125 sec, f_3= 7.988 Hz)

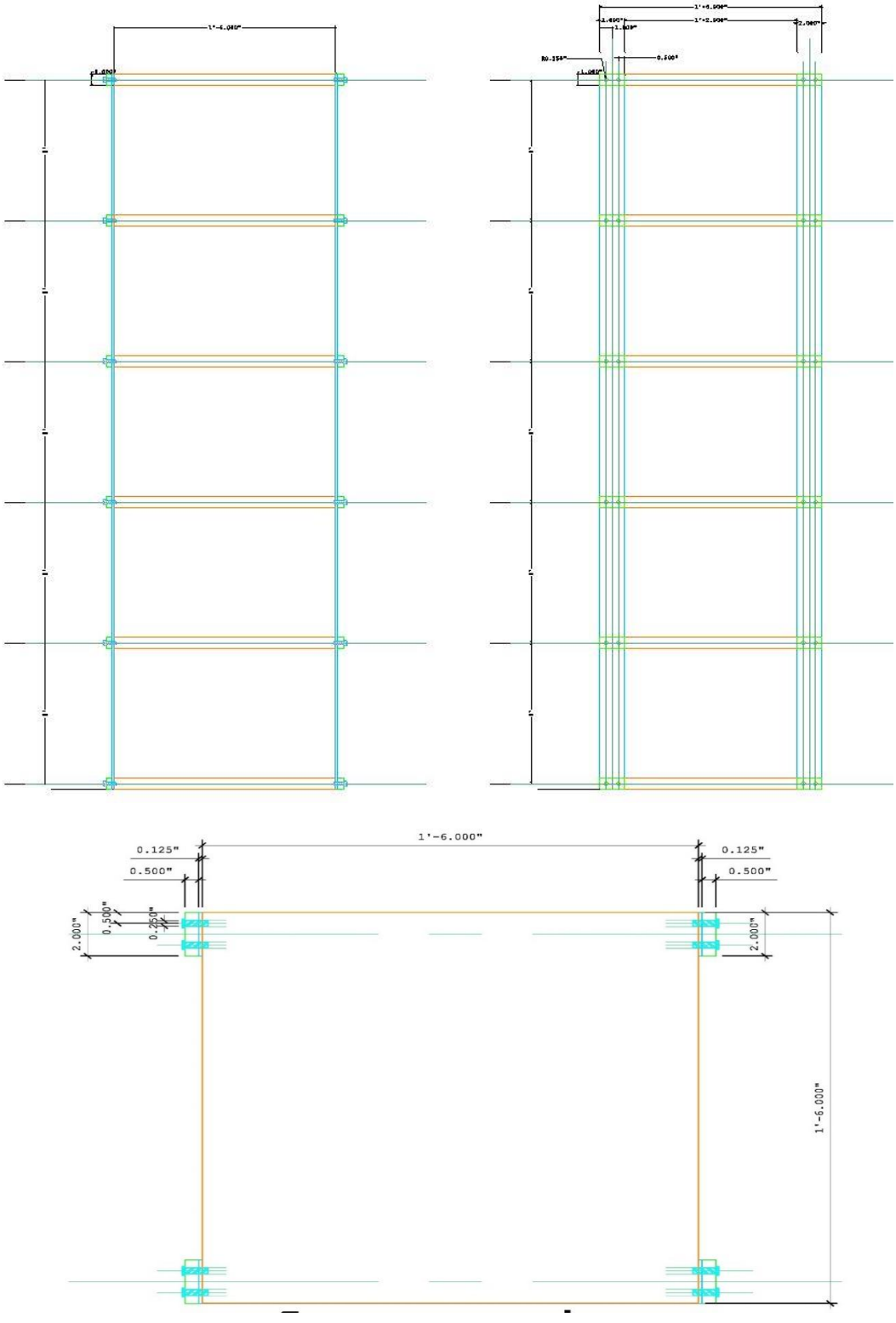

Figure 16. Elevation (top) and plan (bottom) and views of the five-story scaled structure

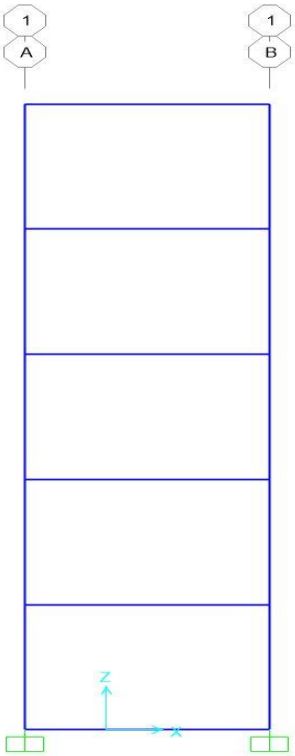

Figure 17. 2D SAP2000 model of the five-story structure

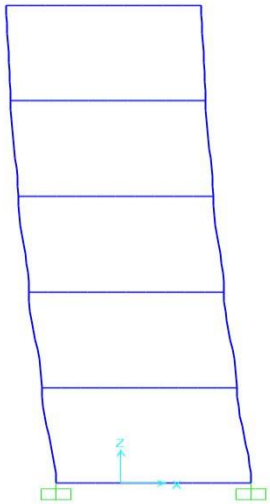

Figure 18. First mode
(T_1= 0.672 sec, f_1= 1.486 Hz)

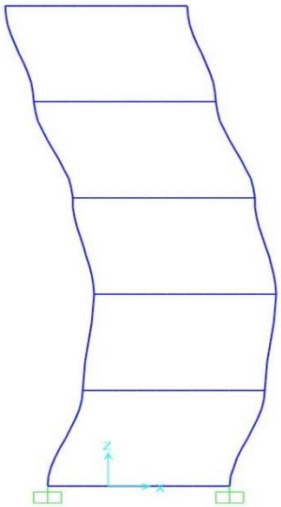

Figure 19. Second mode
(T_2= 0.230 sec f_2= 4.336 Hz)

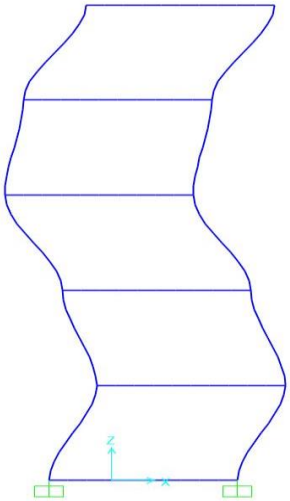

Figure 20. Third mode
(T_3= 0.146 sec, f_3= 6.830 Hz)

3.2 Selecting and Scaling of Ground Motions

Nonlinear response history analysis is performed to get the response of the scaled structure while applying a dynamic load. Acceleration histories (accelerograms) are selected to satisfy design code requirements and soil conditions at a specific site. Due to the increase of available strong ground motion databases, selecting and scaling recorded accelerograms can be performed in various ways. In this study, measures provided in Chapter 16.2 of ASCE 7-16 are employed for selecting and then scaling the ground motions. The best-fitted ground motion time histories are selected and classified by considering the earthquake magnitude, site-to-source distance, and site soil conditions. The code considers the similarity in magnitude and rupture distance and mechanism for selecting eleven ground motions. A period range of 0.2T to 2T, where T is the fundamental period of the structure, is considered ideal to scale the ground motion. The selected eleven ground motions are scaled in such a way that the average spectrum does not fall below 90% of the target spectrum for any period within the period range of interest.

3.2.1 Selection of Ground Motions

Table 1 lists the eleven ground motions that were extracted from the PEER Ground Motion Database. These ground motions are selected such that they are consistent with the magnitudes, source characteristics, fault distances, and site conditions controlling the target spectrum. In prior versions of the code, ASCE 7-05 suggests selecting three ground motions for analysis purposes, whereas ASCE 7-10 suggests selecting seven ground motions for analysis purposes. If three ground motions are selected, the maximum value of the peak response is used for analysis and design purposes. The average value of seven or eleven motions, as suggested by ASCE 7-16, is used for analysis purposes. The New Madrid fault system consists of two types of faults: A strike-slip fault oriented to the northeast and a reverse fault oriented to the northwest. This study considers the strike-slip mechanism.

Table 1. Select ground motions for the PEER database

SN	Event	Magnitude	Rupture Distance (km)	Mechanism
1	North California	6.5	27.02	Strike-slip
2	Imperial Valley	6.53	31.92	Strike-slip
3	Superstition Hills	6.54	27	Strike-slip
4	Landers	7.28	26.96	Strike-slip
5	Kobe	6.9	28.08	Strike-slip
6	Irpinia	6.9	29.8	Strike-slip
7	Hector	7.13	31.06	Strike-slip
8	Cape Mendocino	7.01	31.46	Strike-slip
9	Tottori	6.6	28.82	Strike-slip
10	El Mayor	7.2	26.55	Strike-slip
11	Darfield	7	31.41	Strike-slip

3.2.2 Scaling of the Ground Motions:

A response spectrum can be defined as a plot of responses such as displacement, velocity, and acceleration versus the natural vibration period of the system. A response spectrum plots the maximum response of a series of oscillators allowing only a single-degree-of-freedom at a certain level of damping with respect to time or frequency. These spectra are considered to be a valuable tool in earthquake engineering. ASCE 7-16 allows the generation of a target spectrum by multiplying the design response spectrum by 1.5 as per Chapter 11.4.7. Figure 21 shows the design response spectrum with defining parameters.

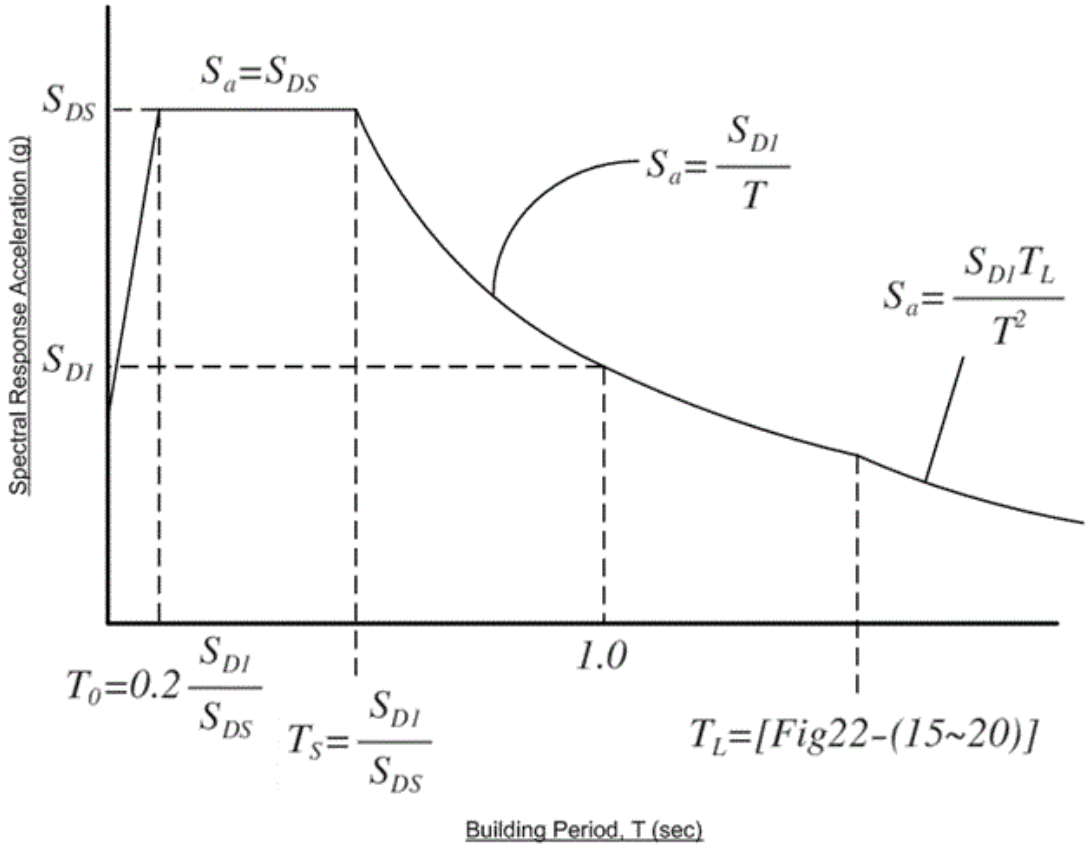

Figure 21. Design response spectrum with generating parameters (ASCE 7-16)

The parameters listed in Figure 21 are defined as:

F_a = short-period site coefficient (at 0.2-s period)

F_v = long-period site coefficient (at 1.0-s period)

S_S = mapped Maximum Considered Earthquake Response (MCER), 5% damped, spectral response acceleration parameter at short periods

S_1 = mapped MCER spectral response acceleration parameter at a period of 1 s

S_{D1} = design, 5% damped, spectral response acceleration parameter at a period of 1 sec

S_{DS} = design, 5% damped, spectral response acceleration parameter at short periods

S_{M1} = MCER, 5% damped, spectral response acceleration parameter at a period of 1 s adjusted for site class effects

S_{MS} = MCER, 5% damped, spectral response acceleration parameter at short periods adjusted for site class effects.

United States Geological Survey (USGS) generates the Maximum Considered Earthquake (MCE), also known as the target spectrum, based on different parameters. Site class, mapped acceleration parameters, and site coefficients are used to generate the design response spectrum. Figure 22 shows a summary of the USGS Report with the Target and Design Response Spectrum generated using ASCE 7-16 recommended seismic provisions with the help of Office of Statewide Health Planning and Development (OSHPD) Seismic Design Maps Tool.

As per ASCE 7-16 Chapter 16.2.3.1, the period range for scaling or matching lies between 0.2T to 2T. In this study, the fundamental period was 0.429 sec, which makes the period 0.0858 sec to 0.6435 sec, our range of interest.

Figure 23 shows the Target Response Spectrum of a specific site in Memphis, which is the Design Response Spectrum multiplied by a factor of safety of 1.5. Figure 24 shows the 5% Damped Response Spectra of eleven selected ground motions for the period range of interest.

OSHPD

3566 Bristerwood Dr, Memphis, TN 38111, USA

Latitude, Longitude: 35.1151099, -89.94281860000001

Date	8/17/2019, 10:56:45 AM
Design Code Reference Document	ASCE7-16
Risk Category	II
Site Class	D - Stiff Soil

Type	Value	Description
S_S	0.925	MCE_R ground motion. (for 0.2 second period)
S_1	0.311	MCE_R ground motion. (for 1.0s period)
S_{MS}	1.045	Site-modified spectral acceleration value
S_{M1}	null -See Section 11.4.8	Site-modified spectral acceleration value
S_{DS}	0.697	Numeric seismic design value at 0.2 second SA
S_{D1}	null -See Section 11.4.8	Numeric seismic design value at 1.0 second SA

Type	Value	Description
SDC	null -See Section 11.4.8	Seismic design category
F_a	1.13	Site amplification factor at 0.2 second
F_v	null -See Section 11.4.8	Site amplification factor at 1.0 second
PGA	0.556	MCE_G peak ground acceleration
F_{PGA}	1.1	Site amplification factor at PGA
PGA_M	0.611	Site modified peak ground acceleration
T_L	12	Long-period transition period in seconds
SsRT	0.925	Probabilistic risk-targeted ground motion. (0.2 second)
SsUH	1.059	Factored uniform-hazard (2% probability of exceedance in 50 years) spectral acceleration
SsD	2.501	Factored deterministic acceleration value. (0.2 second)
S1RT	0.311	Probabilistic risk-targeted ground motion. (1.0 second)
S1UH	0.355	Factored uniform-hazard (2% probability of exceedance in 50 years) spectral acceleration.
S1D	0.797	Factored deterministic acceleration value. (1.0 second)
PGAd	1.341	Factored deterministic acceleration value. (Peak Ground Acceleration)
C_{RS}	0.873	Mapped value of the risk coefficient at short periods

Figure 22. USGS Design Response Spectrum generated using OSHPD

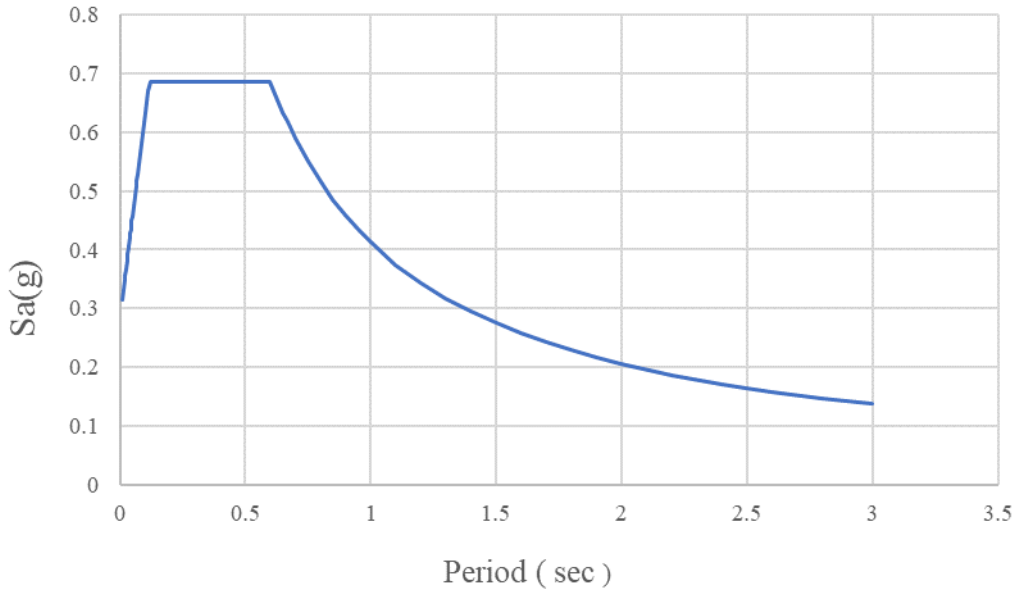

Figure 23. Target response spectrum generated using Excel

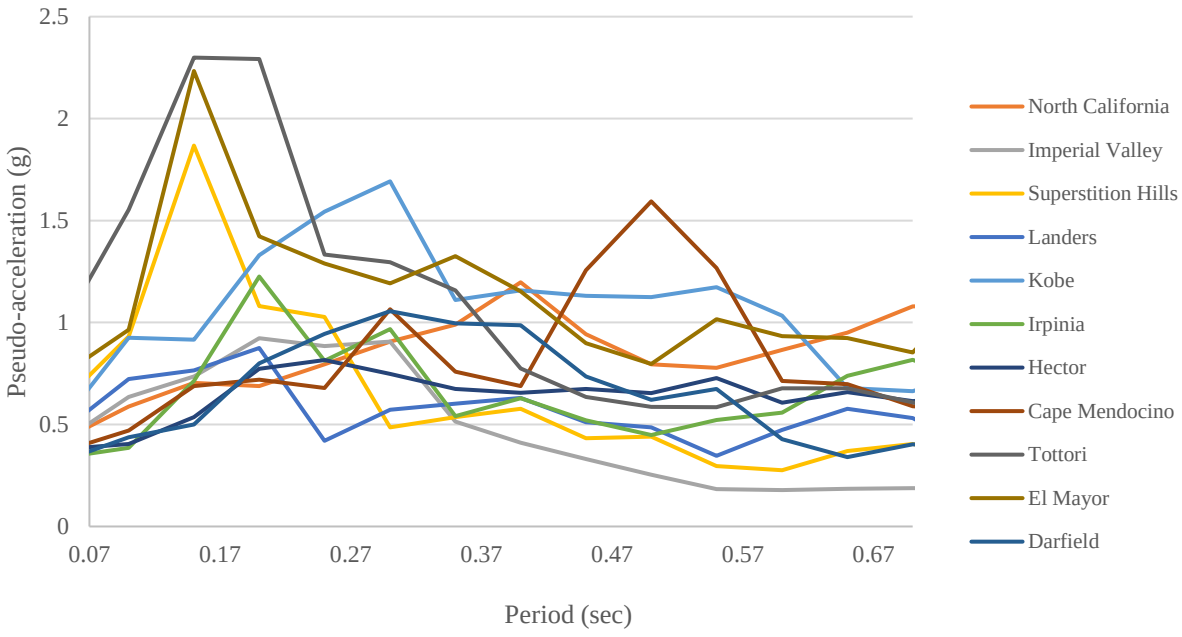

Figure 24. Response spectrum of eleven ground motions for a specific time range

Chapter 4. Data Acquisition

After selecting and scaling a suite of ground motions, the scaled motion is applied to the structure using the shake table and 92E series single-ended actuator. ASCE 7-16 suggests selecting eleven ground motions for scaling purposes based on several characteristics, but only one ground motion is necessary to study, analyze, and design a structure on a specific site condition. Generally, the average value of the eleven selected motions is considered for analysis purposes. Keeping in mind several constraints, such as the limits of the shake table displacement and the maximum amplitude range of the accelerometers used, the ground motion experienced in the Imperial Valley (1979) is selected to be applied in this study.

The total time of Imperial Valley Ground motion was observed to be 116.385 seconds, and the peak ground acceleration after the scaling of the motion was 0.372g, and it occurred at 24.28 seconds. The maximum displacement was found to be 10.352 cm at 24.235 seconds. The time interval between the records is 0.005 sec.

The actuator connected to the table, which is equipped with an LVDT and a load cell, can either be displacement or load controlled. In this study, the scaled ground motions in the acceleration domain, extracted from PEER, are integrated twice to convert them into the displacement domain. Figures 25 and 26 show the unscaled and scaled ground motions for acceleration and displacement, respectively, experienced at a station in the Imperial valley extracted from the PEER database.

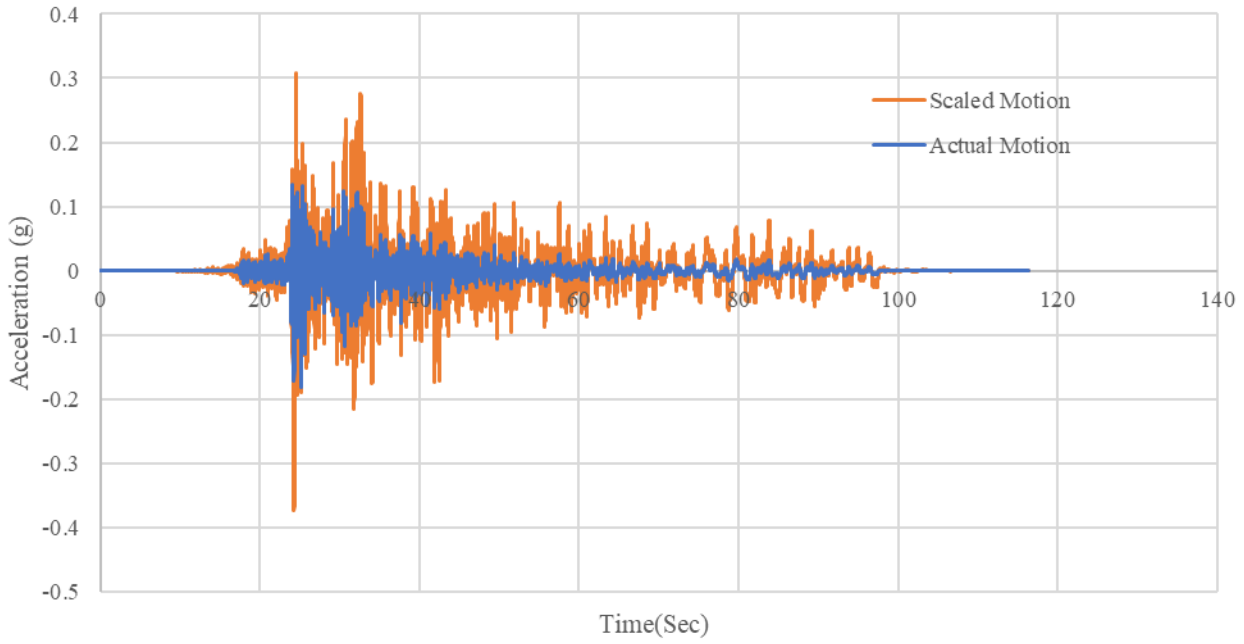

Figure 25. Imperial Valley ground motion (acceleration)

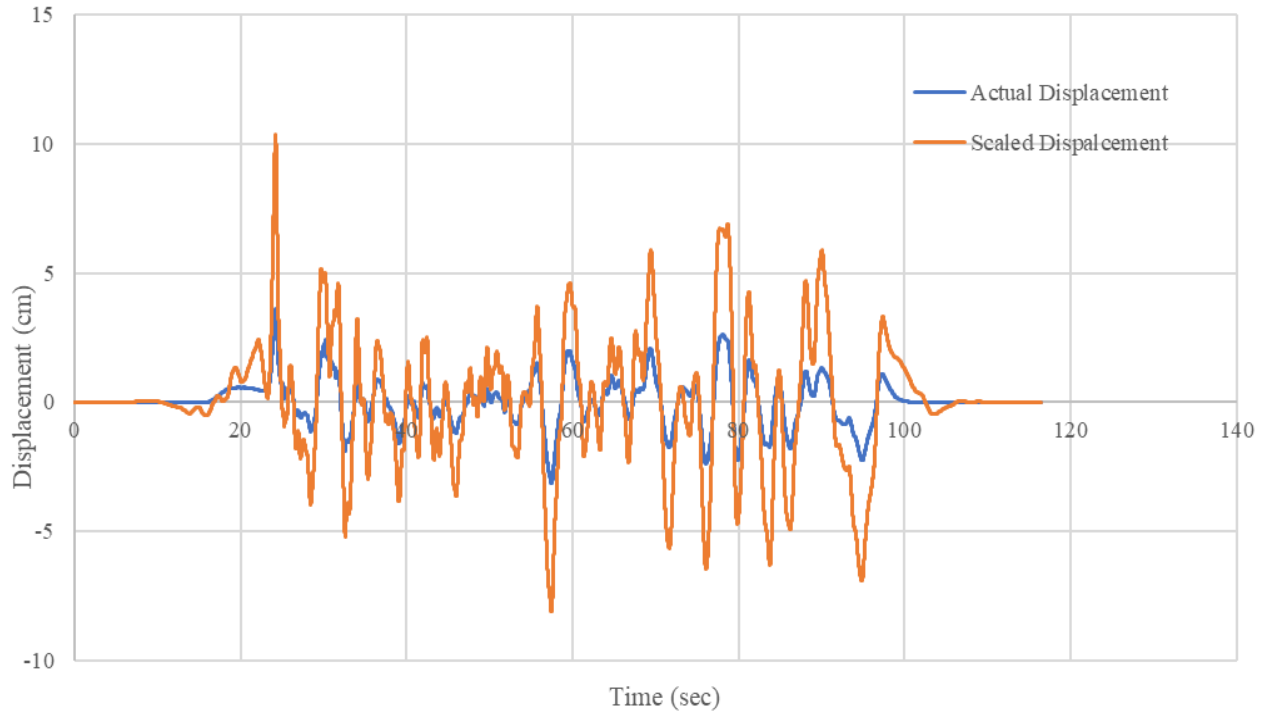

Figure 26. Imperial Valley ground motion (displacement)

After the application of the motion to the structure, it is expected to displace in the direction of application of the load. As explained earlier, the Wilcoxon accelerometers mounted on every story of the structure provide raw, unfiltered acceleration measurements that need to be processed for unwanted components.

Figure 27 shows the raw acceleration record on the application of the ground motion as recorded by the accelerometer clamped at the base of the shake table without any structure or additional mass mounted on the table.

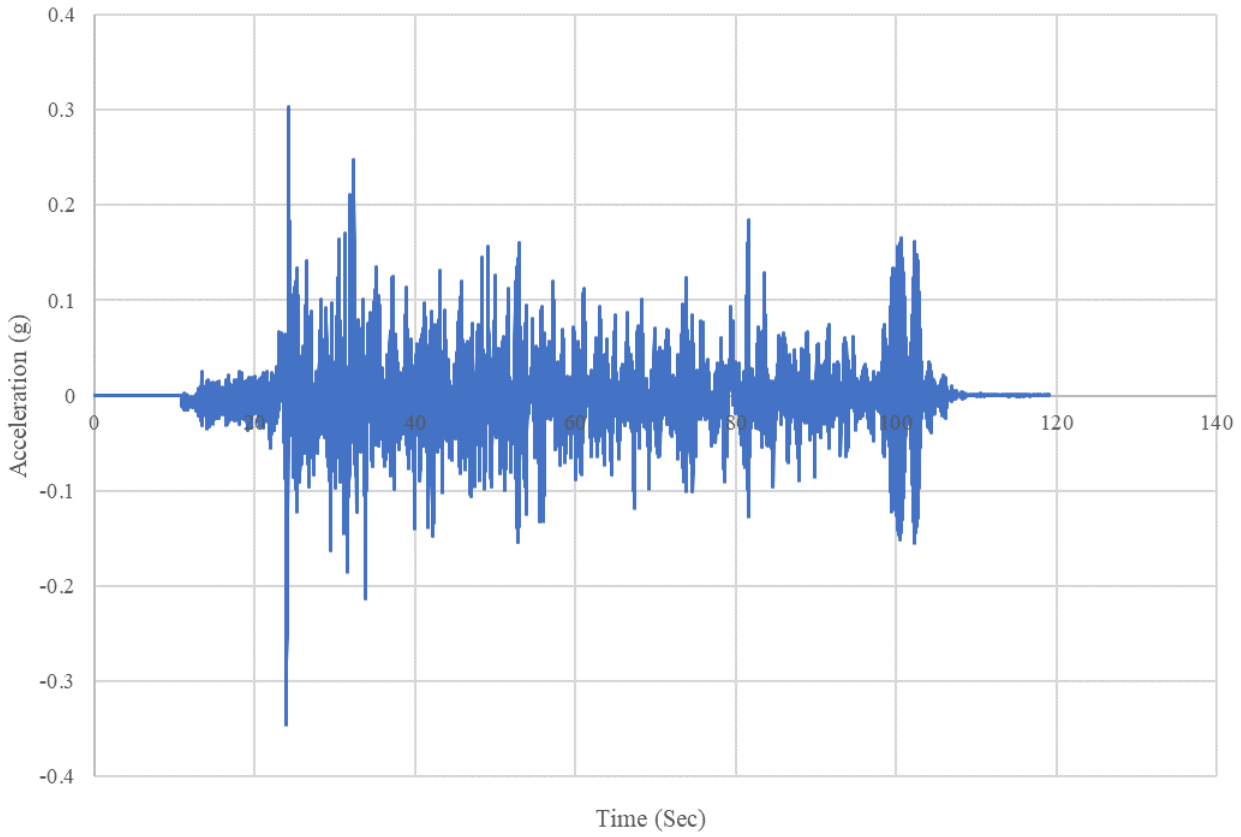

Figure 27. Unprocessed acceleration record at the base of the shake table

4.1 Baseline Correction and Filtering of the Acquired Data

It is assumed that the initial values of displacement and velocity are generally zero so as to attain the displacement and velocity-time histories; however, this might not be the case. Baseline drift occurs in a time history due to this assumption. The displacement history obtained by integrating the acceleration twice generally shifts from the actual baseline resulting in inconsistency and unreliability of the data acquired. Baseline drift is a linear or nonlinear addition to the spectra, which causes the expected zero measurements to gain some positive values. Baseline correction can be applied to ground motions in several ways. The method adopted in this study subtracts the mean value of the prior ground motion application part for 20 seconds, as suggested by Boore (2005). The method is commonly known as baseline initialization or adjustment.

The data acquired from the data acquisition system also contains unwanted components or features that need to be filtered. The processing of the motion is done to eliminate random noise that is generated with the recorded data. Some frequencies that are either too low or too high makeup for the unwanted feature in the acquired data.

A linear continuous-time filter removes frequencies that do not contribute to the data and allows other frequencies to pass into the data. Several filters based on polynomial functions are used to filter the response. The Chebyshev filter is commonly used in signal processing of the ground motions. The steepness of the transfer function and increase in passband or stopband ripple is an advantage of this filter over others. Although the Butterworth filter has less steepness and maximally flat frequency response in comparison to the Chebyshev filter, it is considered to have greater phase response than the Chebyshev filter. The maximally flat magnitude filter is designed in such a way that they form no ripples in the passband ("Filter (signal processing")," Wikipedia). Both types of filters are used in this study to process retrieved acceleration records.

The drifts associated with integrating the acceleration twice to get displacement appears as a low-frequency noise in the data. A high pass filter can remove such low-frequency noise; however, there remains the difficulty in getting the peak displacement. Zero padding can be used to add zeros before and after the ground motions of interest, generally in the frequency domain, to address the drifts.

Below are the steps for filtering ground motions.

1. The desired ground motion is zero-padded using the following relationship

   $T_{Zpad} = 1.5n/f_c$

   where T_{Zpad} is the length of zeros to be added, n is the order of the Butterworth filter, and f_c is the filter corner frequency
2. The time history in the time domain is converted into the frequency domain using a Fast Fourier Transform (FFT).
3. Displacements are obtained by integrating the accelerations twice.
4. The third-order polynomial trend is removed from the displacement.
5. With the help of a half-cosine function, the start, as well as the end of the displacement history, is tapered.
6. Baseline correction is applied if necessary.
7. The Butterworth filter is applied with the required filter order.
8. Accelerations are obtained by differentiating the displacements twice.
9. The padding is removed to generate final processed ground motions.

These steps are performed using MATLAB scripts, presented in the Appendix. An FFT is required to decompose any data recorded originally as a function of time into a function of frequency. A Fourier series gives information on how the amplitude of any ground motion is distributed with respect to frequency. Using FFT, a built-in MATLAB function, the acceleration records are converted into the frequency domain. A Fourier amplitude spectrum, which deals with the amplitude and frequency content of the time history, is generated using a sampling frequency of 200 Hz, i.e. $\Delta t = 0.005$ sec, and Nyquist frequency of 100 Hz.

Figure 28 shows the Fourier amplitude spectrum of the base of the shake table and indicates that the frequencies below 0.1 Hz are too low, whereas the frequencies above 10 Hz are too high. These frequencies act as corner frequencies in the application of a suitable filter to the records. The bandpass filter allows only the records within these frequencies to pass and rejects the records above or below the designated frequencies. Figure 29 shows the original scaled Imperial Valley ground motion and the corrected and processed, recorded ground motion at the table without any models mounted.

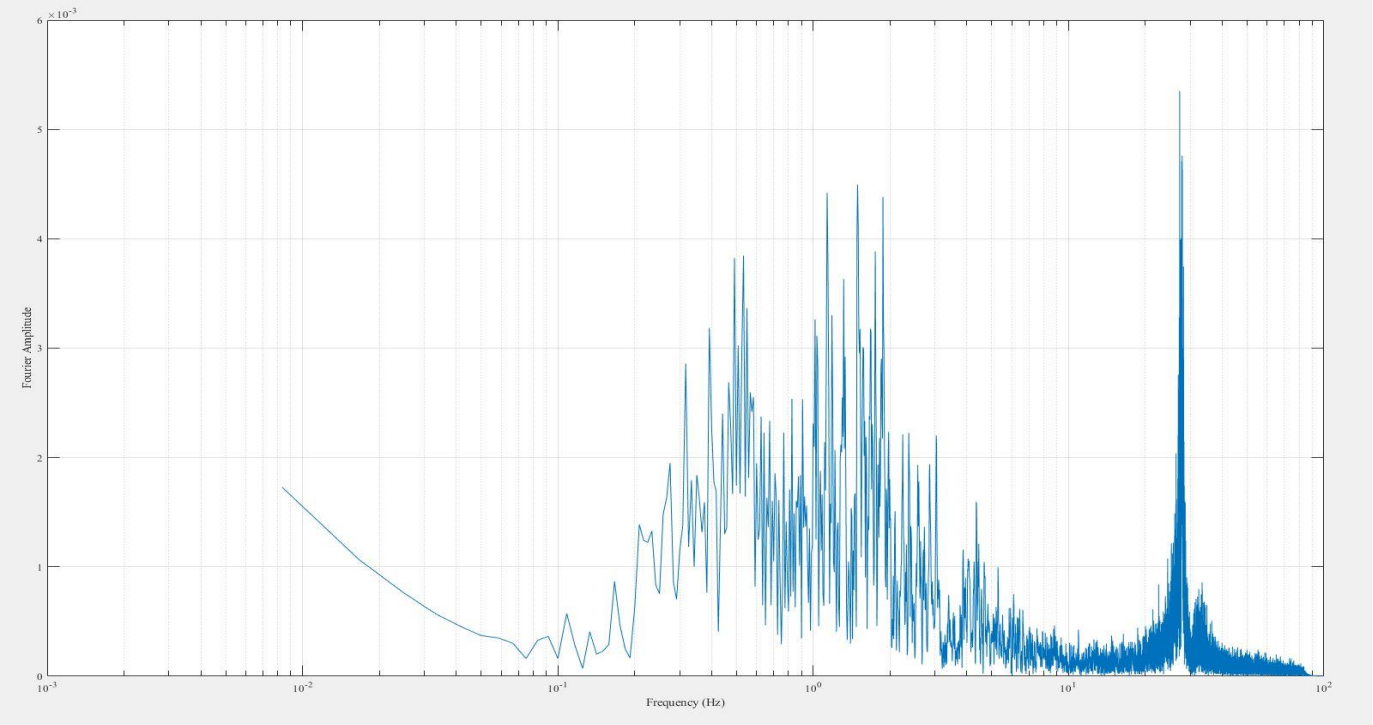

Figure 28. Fourier amplitude spectrum of the base of the shake table

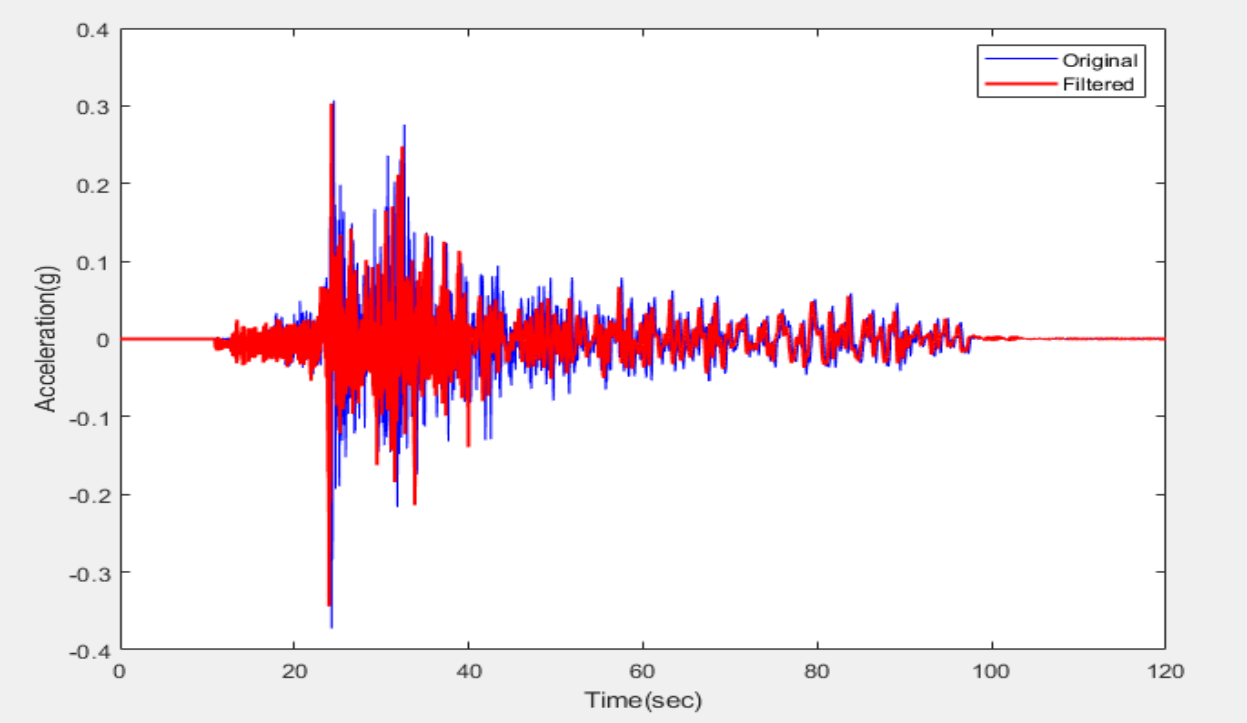

Figure 29. Original and scaled Imperial Valley ground motion

Chapter 5. Analysis and Results

The study and analysis of structural responses such as acceleration, velocity, and displacement are of great importance to the earthquake and structural engineering communities. These responses determine the sustainability, strength, reliability, and safety of the occupants in events of various hazards. The characteristics of a structure, such as its configuration, height, and weight, affect its seismic performance.

Newton's second law of motion states that force (inertial) equals mass times acceleration. The forces on a structure are reduced as the mass/self-weight of the structure is reduced. The three-story model is expected to perform better on the application of ground motion than the four and five-story models as the self-weight of the three-story model is less than the others. With an increase in the height and mass of the building, the fundamental or natural period of the building increases and as well as the responses of the building under seismic forces. The purpose of this study is to extract such responses from every story of the structural models simultaneously, analyze and compare the responses acquired from the data acquisition system at the structure's research lab to the SAP2000 non-linear time history analysis responses and validate the functionality of the shake table.

Upon application of the scaled Imperial Valley ground motion to the multi-story structures mounted on the shake table, structural responses such as acceleration are recorded at every story simultaneously. This chapter illustrates the raw, unprocessed as well as final and processed records and acceleration obtained from non-linear time history analysis using SAP2000, for every story of all the structural models.

5.1 Three-Story Structural Responses

After assembling the three-story model and clamping the accelerometers at every story, the scaled Imperial Valley motion is applied to the structure. Figure 30 shows the experimental setup of the three-story model and the data acquisition system. An accelerometer is clamped to the shake table to account for the records on the ground floor. The raw acceleration data recorded with this system is presented in further chapter sections.

Figure 30. Experimental setup for three-story model

5.1.1 Ground Floor

Figure 31 shows the raw and unrefined acceleration as a function of time on the ground floor of the model. The peak ground acceleration (PGA) of this unprocessed accelerogram is 0.362g and occurs at 24.275 sec. The unusual spikes that occur throughout the graph are due to the unwanted low and high-frequency noise in the recorded accelerogram. These spikes corrupt the record and need to be filtered out.

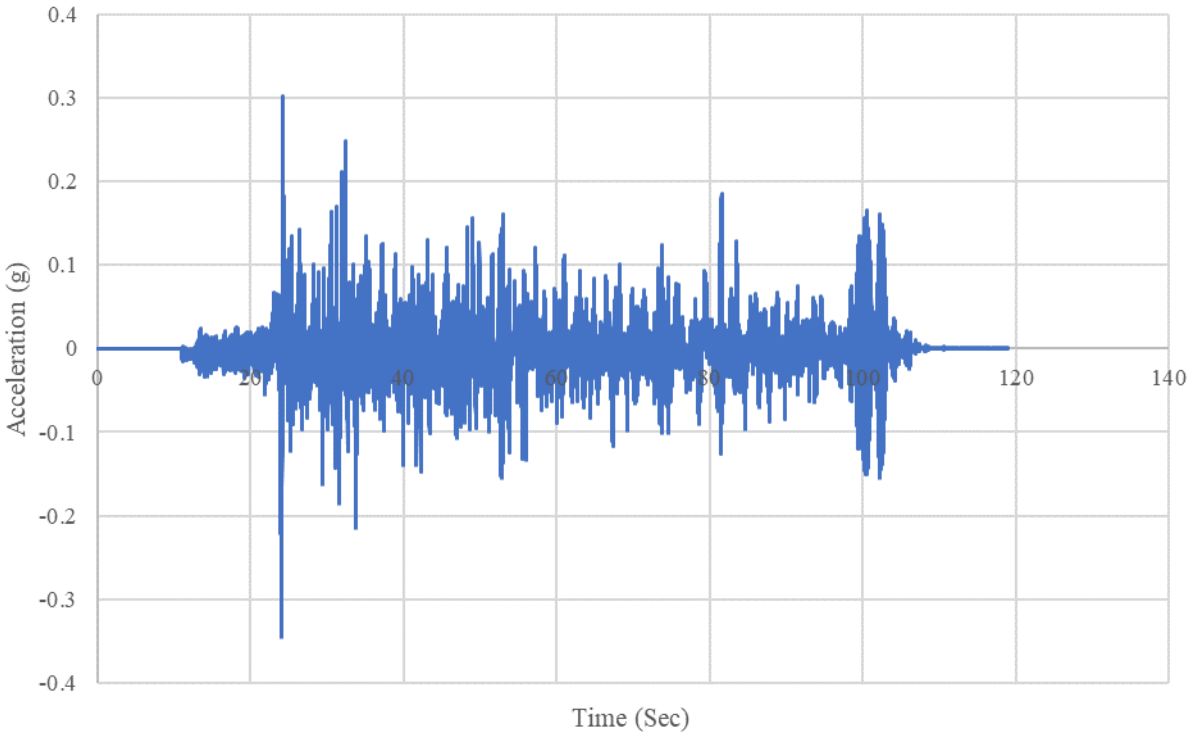

Figure 31. Raw accelerogram recorded at the ground floor

Figure 32 shows the processed record after application of baseline correction and filtering and the actual ground motion as extracted from the PEER database that is applied to the structural model. The PGA of the processed motion is 0.368g, occurring at 23.98 seconds, whereas the PGA of the actual motion is 0.37g, occurring at 24.27 seconds. Although the PGA of the processed motion is very close to the actual motion, there seems to be a discrepancy in the time of occurrence,

which can be attributed to the slight delay in the startup time of the data acquisition system. Figure 33 shows the Energy flux plots, which is a build-up of Specific Energy Density(SED) of the actual and recorded motion. Energy density can be defined as the amount of energy stored in any system. Specific Energy Density, one of the ground motion parameters, is the square of velocity at a time-integrated over a certain range. The SED of the actual motion is observed to be 5115.145 cm^2/sec, and the SED of the recorded motion is observed to be 5012.842 cm^2/sec.

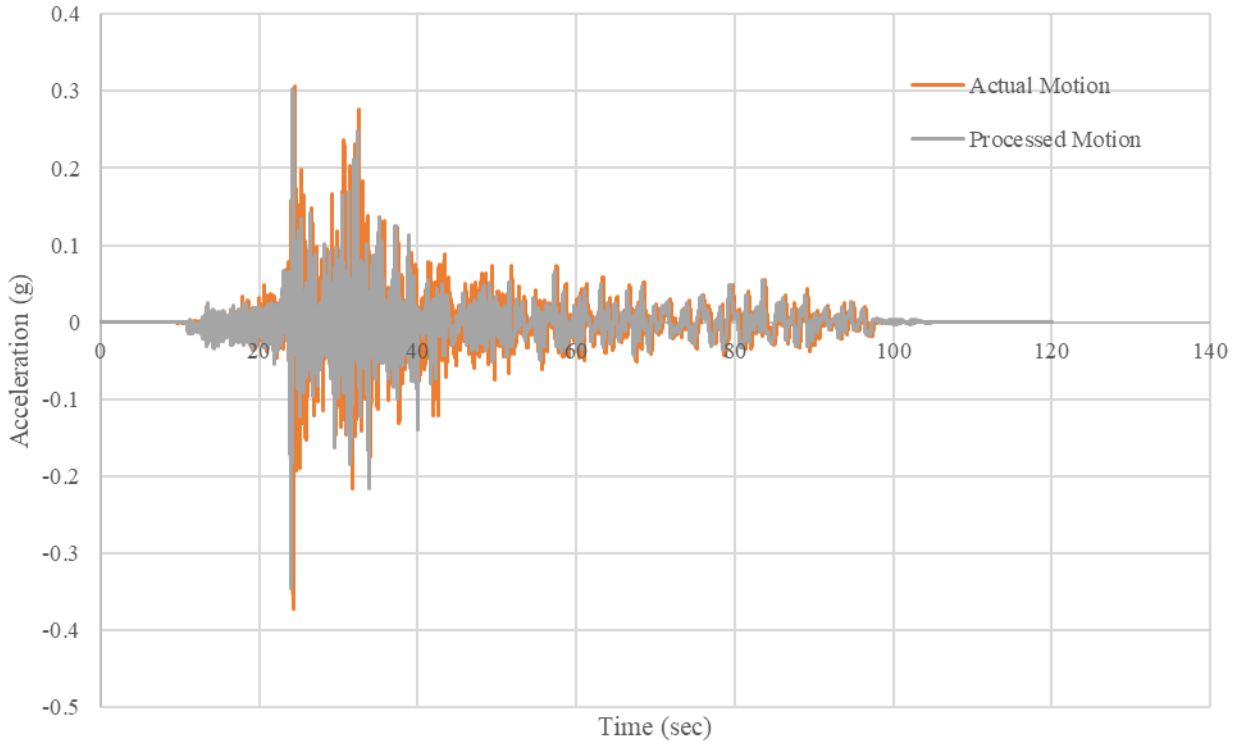

Figure 32. Actual and Final processed accelerogram recorded at the ground floor

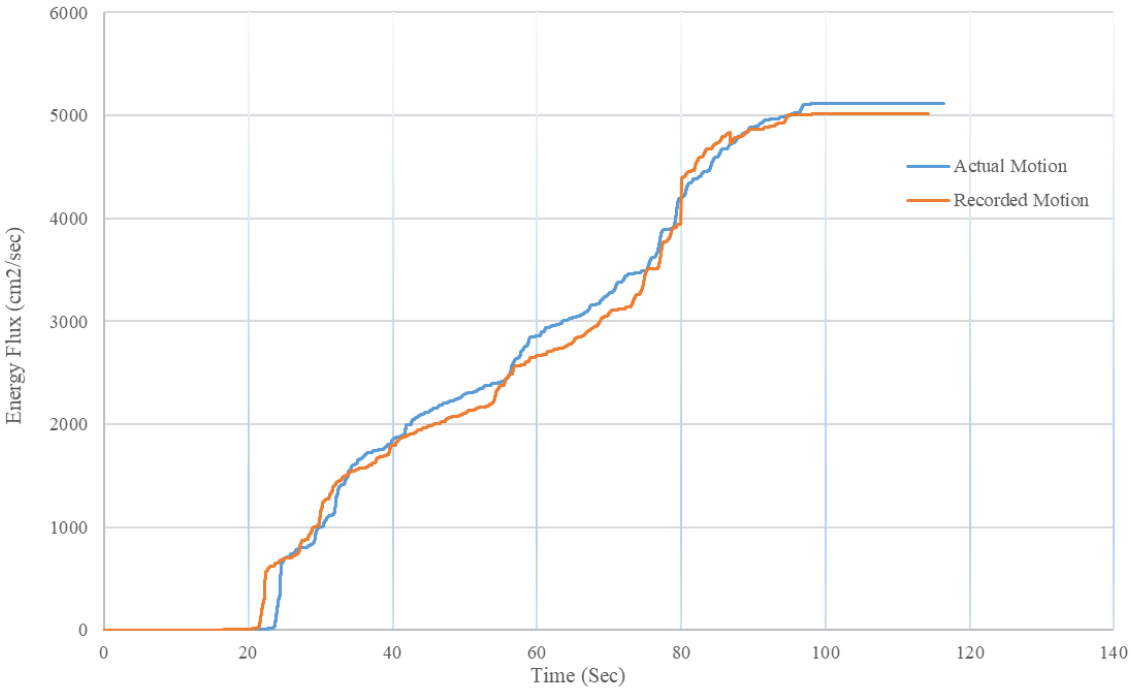

Figure 33. Actual and Recorded Energy Flux Plot at the ground floor

The Wilcoxon seismic accelerometers used for this study have built-in low-pass filtering that eliminates high frequencies. The Imperial Valley motion has high-frequency content in the earlier part of the time history in comparison to the later part. As seen in Figure 32, the processed motion keeps up with the actual ground motion in the latter part of the time history but does not match as well in the earlier part of the motion.

5.1.2 First Floor

Figure 34 shows the raw and unprocessed acceleration history on the first floor of the model. The PGA of this unprocessed accelerogram is 0.381g and occurs at 28.485 sec.

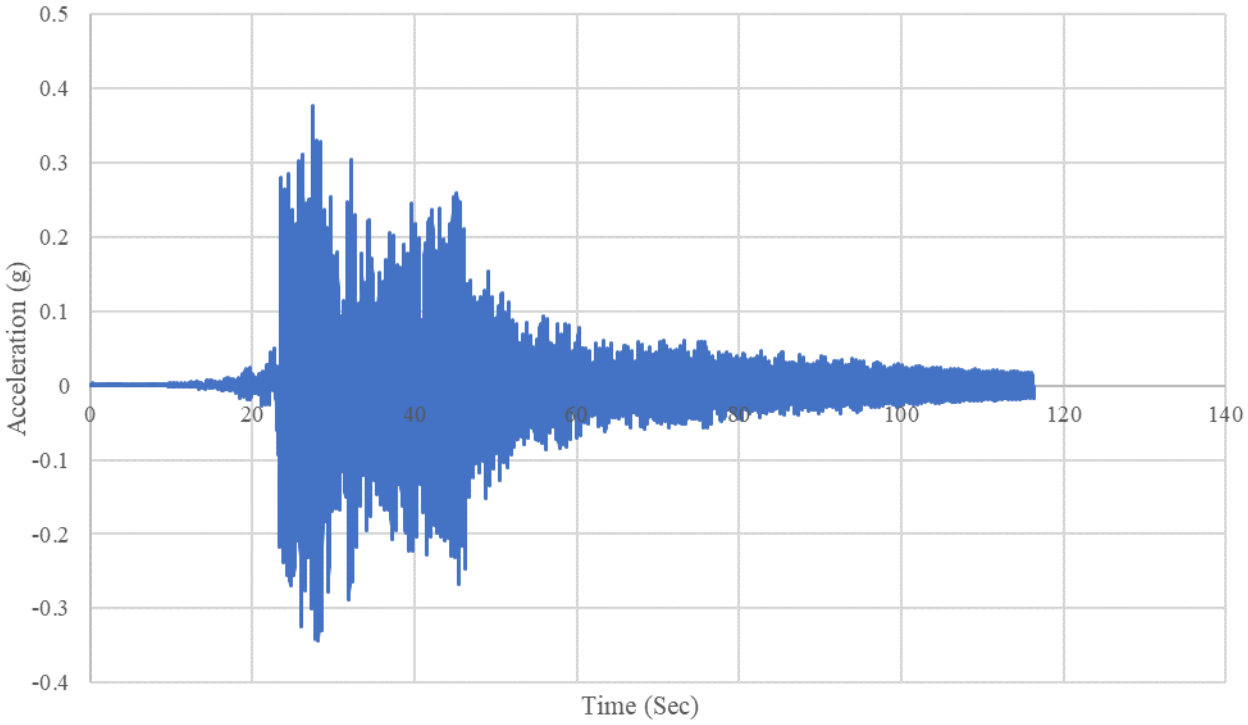

Figure 34. Raw accelerogram recorded at the first floor

Figure 35 shows the processed record after application of baseline correction and filtering and the accelerogram at the first story predicted by a 2D three-story, SAP2000 model. The PGA of the processed motion is 0.376g and occurs at 28.6 seconds; whereas, the PGA of the SAP2000 model is 0.38g and occurs at 29.12 seconds. Although close, the SAP2000 model seems to have overestimated the peak acceleration by 0.004g. Figure 36 shows the energy flux plots of the SAP2000 model and the recorded motion of the first floor. The SED of the recorded motion is observed to be 6649.689 cm^2/sec, and the SED of the SAP2000 model is observed to be 6516.695 cm^2/sec.

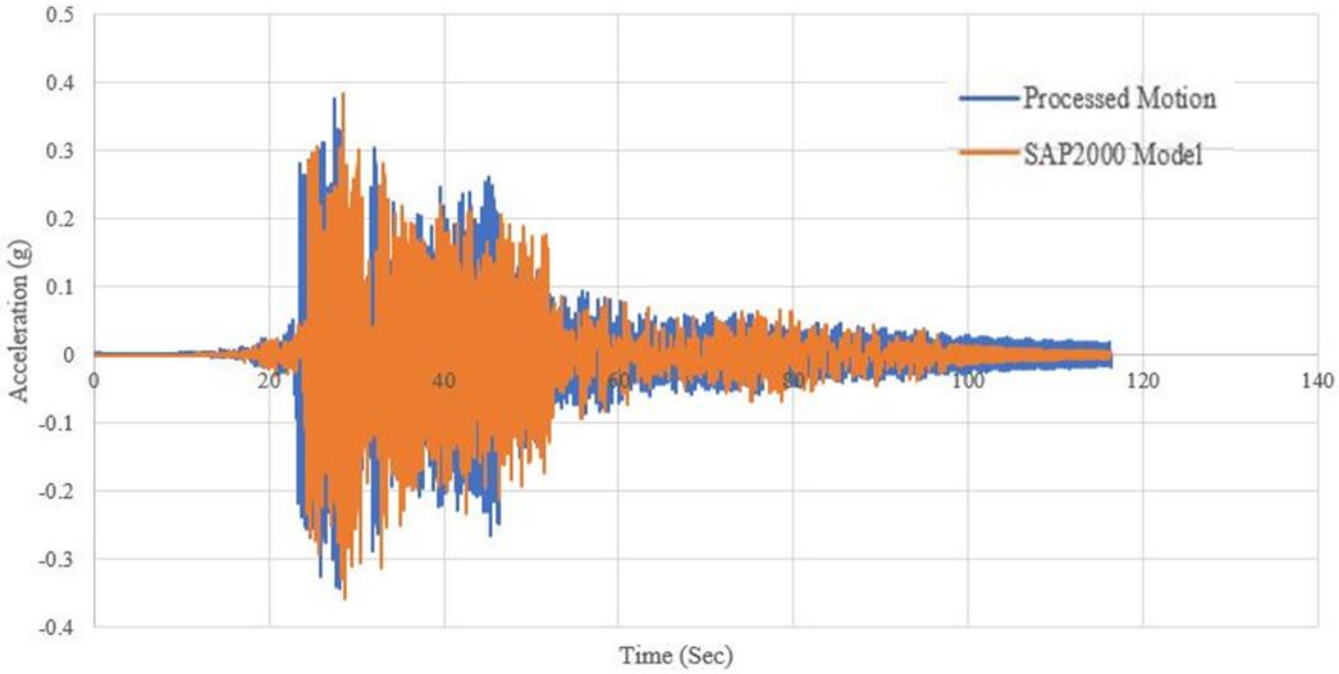

Figure 35. Final processed and SAP2000 accelerogram on the first floor

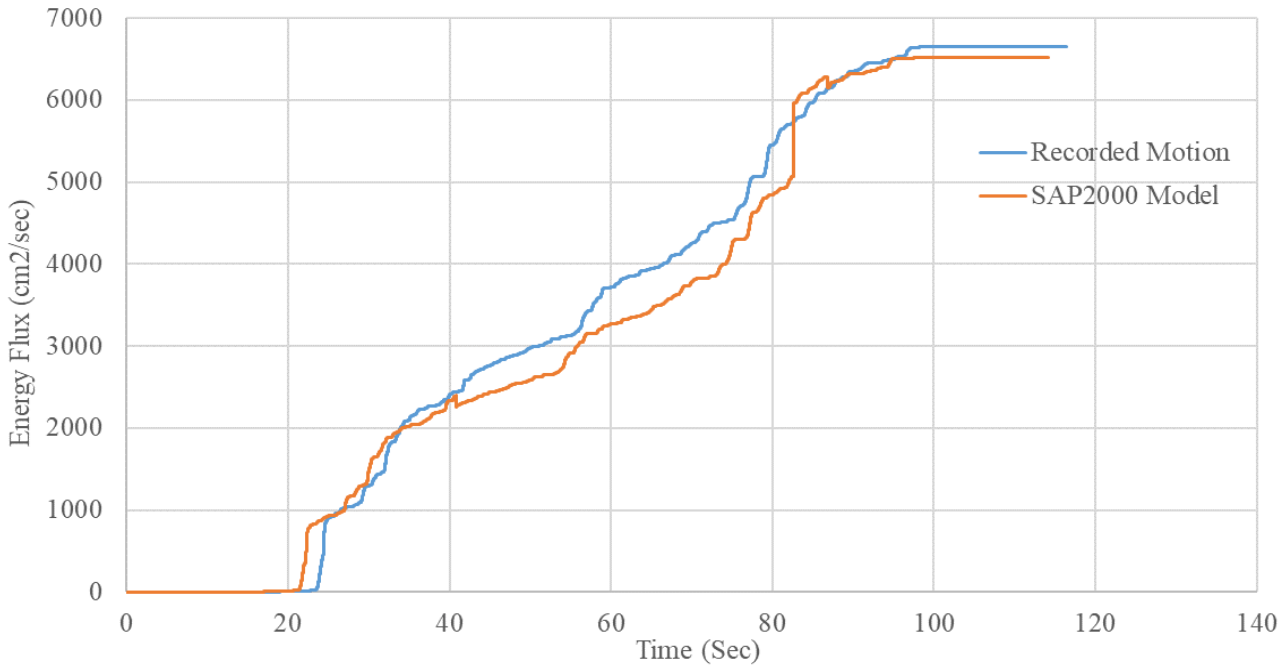

Figure 36. Recorded and SAP2000 model energy flux plot on the first floor

5.1.3 Second Floor

Figure 37 shows the raw and unprocessed acceleration history on the second floor of the model. The PGA of this unprocessed accelerogram is 0.42g and occurs at 28.485 sec. Figure 38 shows the processed record after application of baseline correction and filtering and the accelerogram on the second story predicted by the 2D three-story SAP2000 model. The PGA of the processed motion is 0.432g and occurs at 28.49 seconds; whereas; the PGA of the SAP2000 model is 0.44g and occurs at 28.495 seconds. With a further increase in floor number, SAP2000 seems to have overestimated the peak acceleration by 0.008g. Figure 39 shows the energy flux plots of the SAP2000 model and the recorded motion of the second floor. The SED of the recorded motion is observed to be 9565.315 cm^2/sec, and the SED of the SAP2000 model is observed to be 9374.015 cm^2/sec.

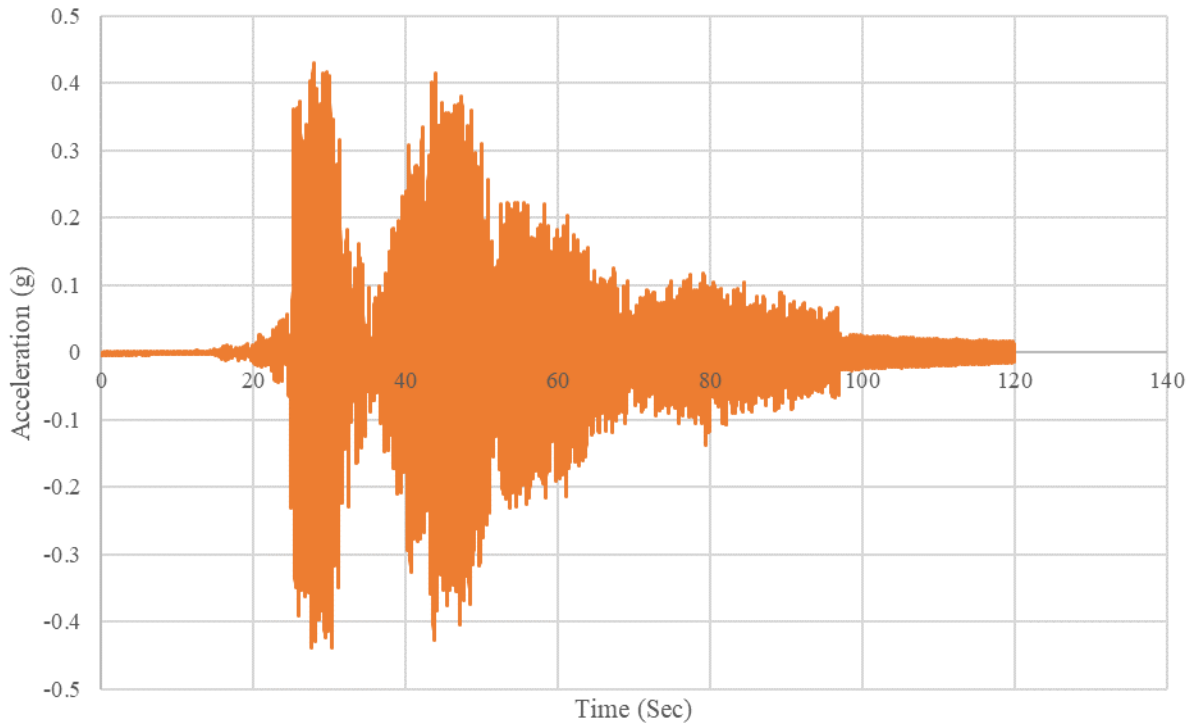

Figure 37. Raw accelerogram recorded on the second floor

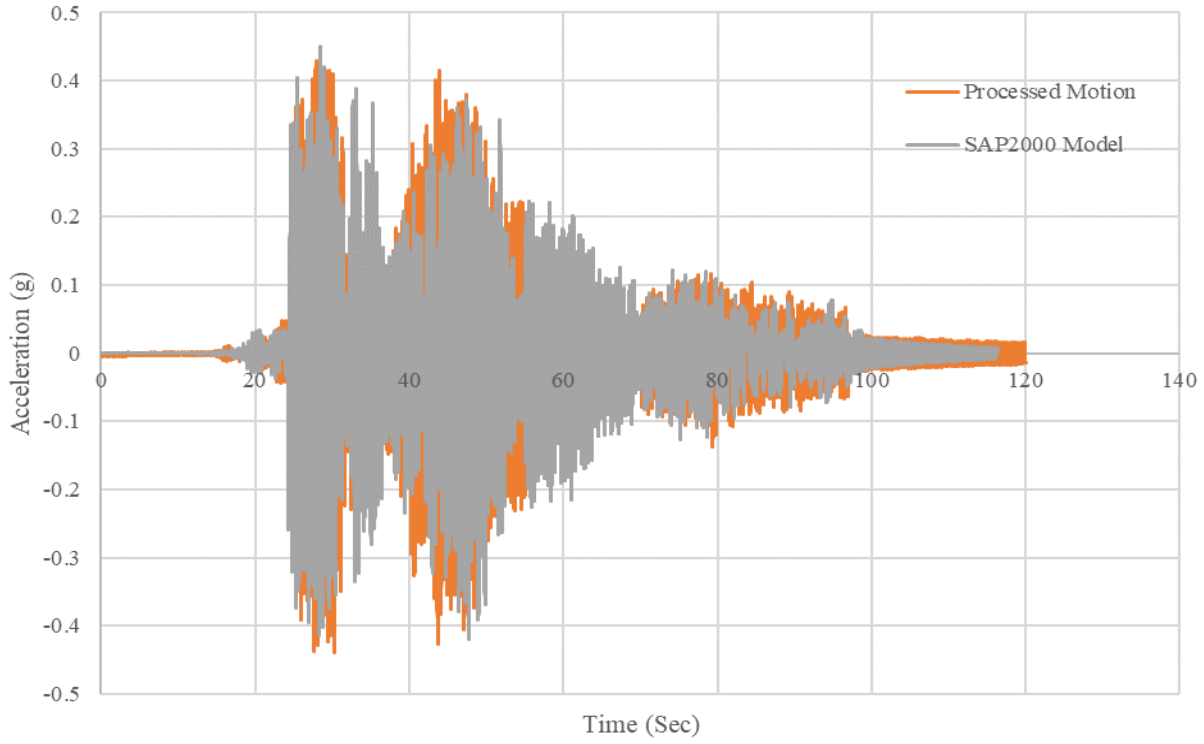

Figure 38. Final processed and recorded SAP2000 accelerogram on the second floor

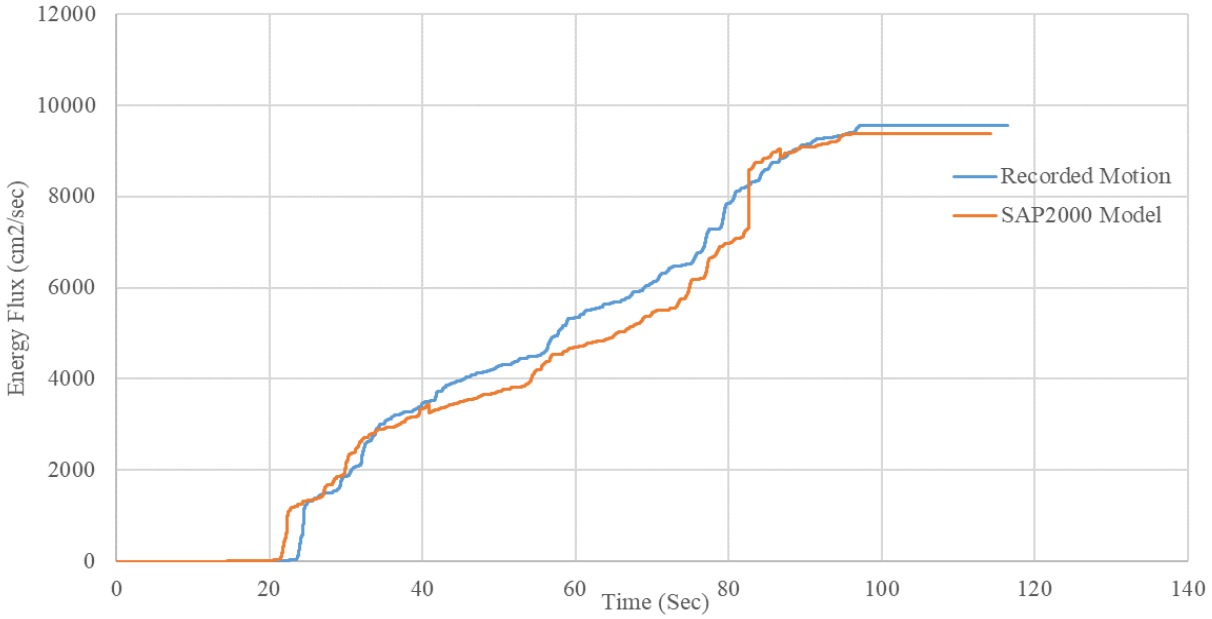

Figure 39. Recorded and SAP2000 model energy flux plot on the second floor

5.1.4 Top Floor

Figure 40 shows the raw and unprocessed acceleration history at the top/third floor of the model. The PGA of this unprocessed accelerogram is 0.485g and occurs at 29.335 sec.

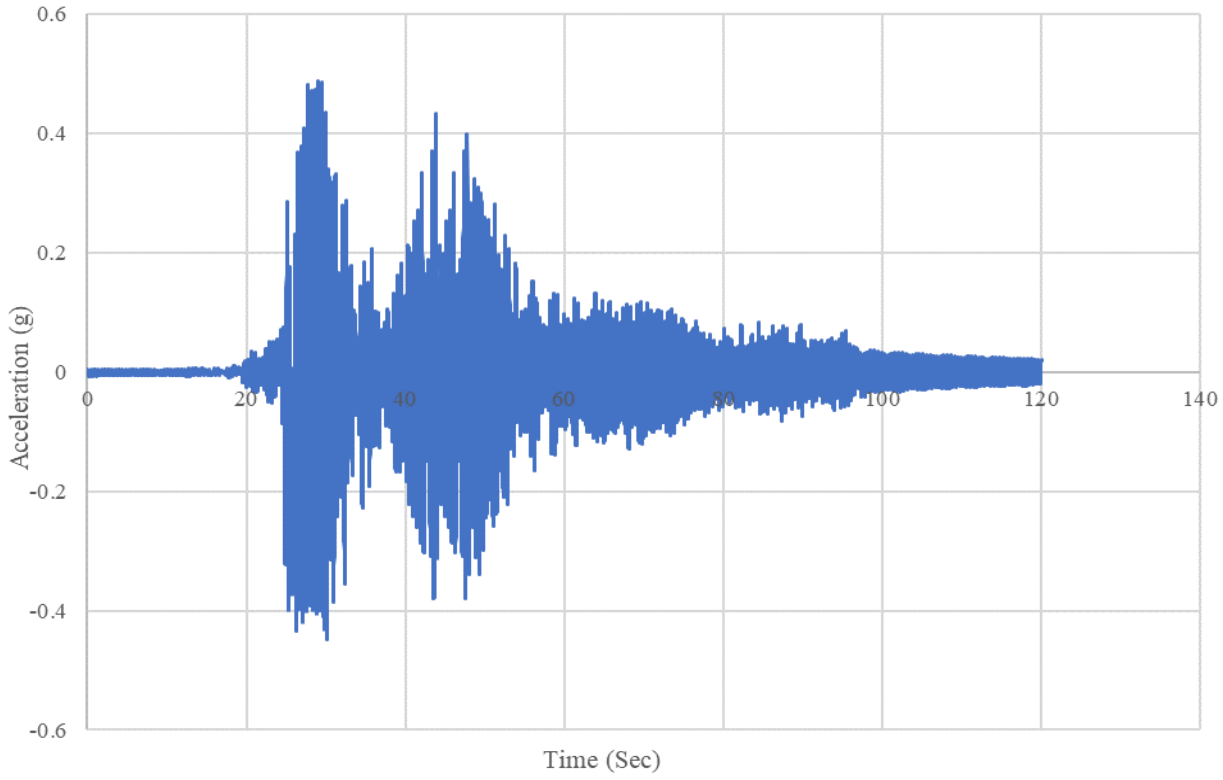

Figure 40. Raw accelerogram recorded at the top floor

Figure 41 shows the processed record after application of baseline correction and filtering and the accelerogram at the top story predicted by the 2D three-story, SAP2000 model. The PGA of the processed motion is 0.473g and occurs at 29.33 seconds; whereas, the PGA of the SAP2000 model is 0.482g and occurs at 29.335 seconds. A further increase in the discrepancy of 0.009g can be observed on the top floor of the three-story model. Figure 42 shows the energy flux plots of the SAP2000 model and the recorded motion of the top floor. The SED of the recorded motion is

observed to be 11764.4 cm^2/sec, and the SED of the SAP2000 model is observed to be 11294.17 cm^2/sec.

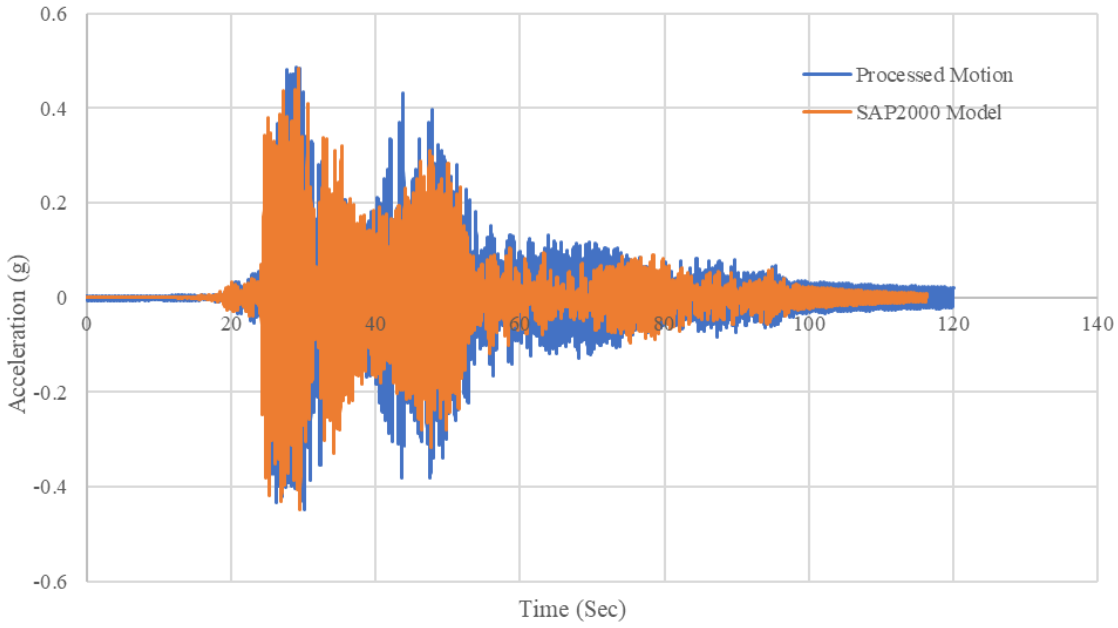

Figure 41. Final processed and SAP2000 accelerogram at the top floor

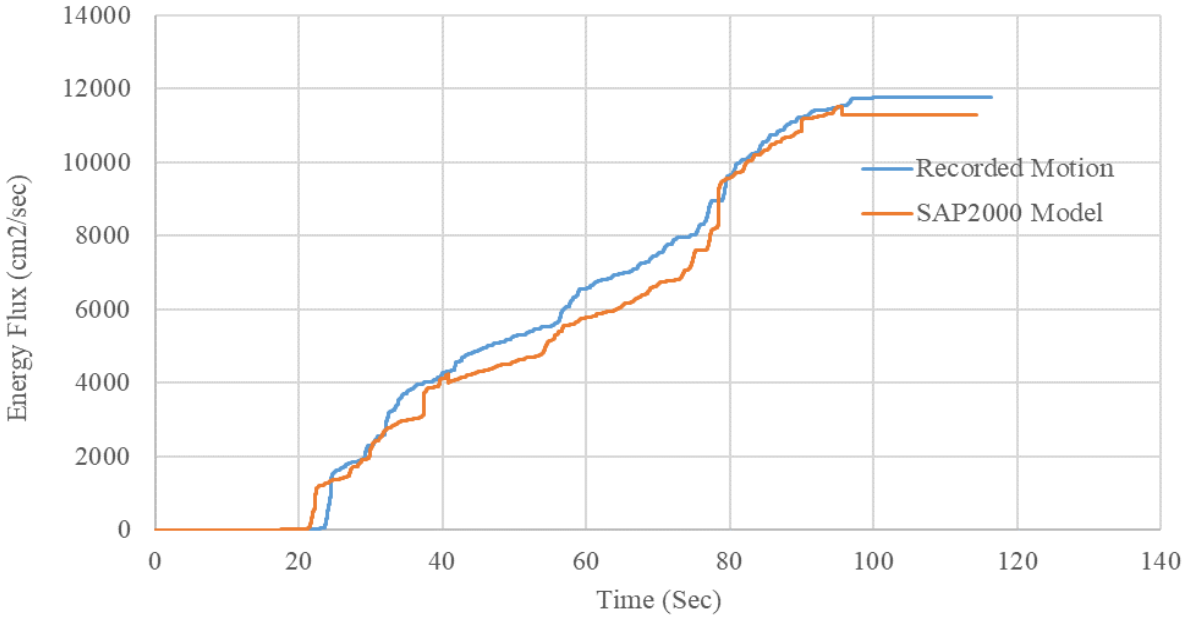

Figure 42. Recorded and SAP2000 Model Energy Flux Plot at the top floor

Table 2 lists the PGA values of the unprocessed, processed, and SAP2000 motions for every story of the three-story structure. Also, the table presents the percent variation in the PGAs of the processed data and the SAP2000 model. From the table, it can be interpreted that, with the increase in the floor height of the structure, the variation between the processed and SAP2000 results increases. The SAP2000 model slightly overestimates the peak motion in higher stories.

Table 2. PGAs from Unprocessed, Processed, and SAP2000 results

PGA (g)	Unprocessed	Processed	SAP2000	Variation (%)
Top	0.485g	0.473g	0.482g	1.902
Second	0.420g	0.432g	0.440g	1.851
First	0.381g	0.376g	0.380g	1.063
Ground	0.362g	0.368g	0.370g	0.543

5.2 Four-Story Structural Responses

5.2.1 Ground Floor

Figure 43 shows the raw and unprocessed acceleration history on the ground floor of the model. The PGA of this unprocessed accelerogram is 0.11g and occurs at 26.06 sec. Figure 44 shows the processed record after application of baseline correction and filtering and the actual ground motion as extracted from the PEER database. The PGA of the processed motion is 0.125g and occurs at 23.98 seconds. The PGA of the actual motion is 0.126g and occurs at 24.17 seconds.

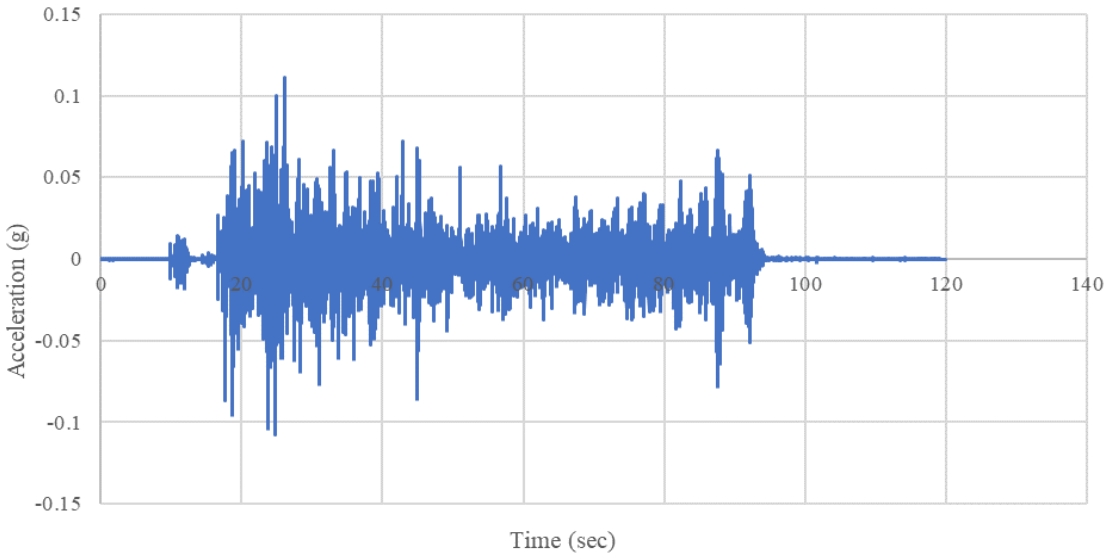

Figure 43. Raw accelerogram recorded at the ground floor

Figure 45 shows the energy flux plots of the actual and recorded motion. The SED of the recorded motion is observed to be 3580.602 cm^2/sec, and the SED of the actual motion is observed to be 3478.299 cm^2/sec.

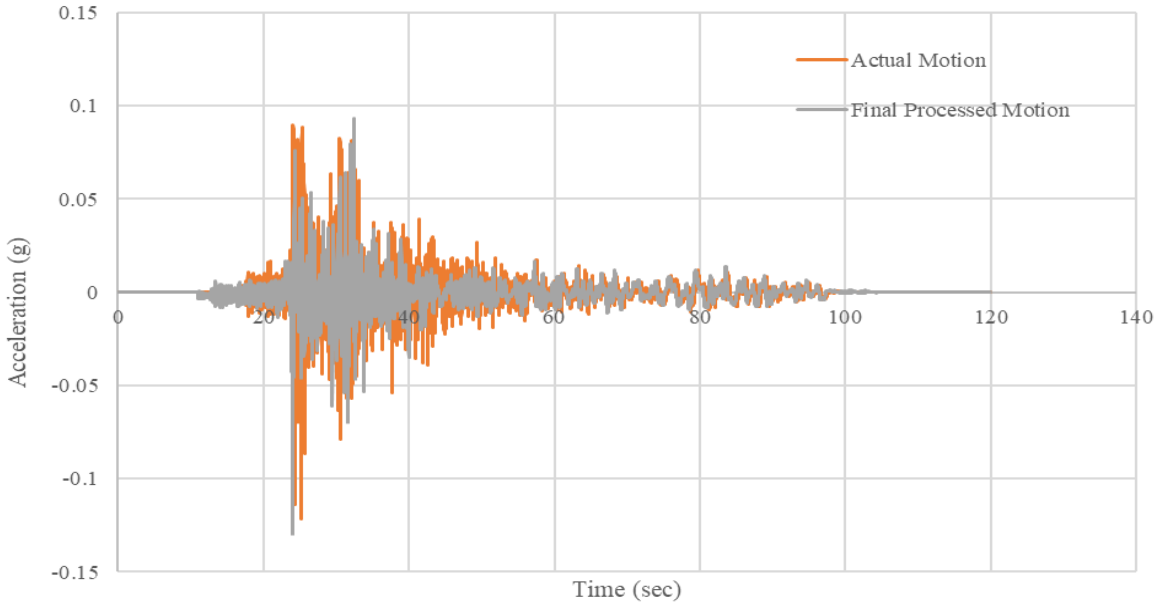

Figure 44. Final processed and actual accelerogram at the ground floor

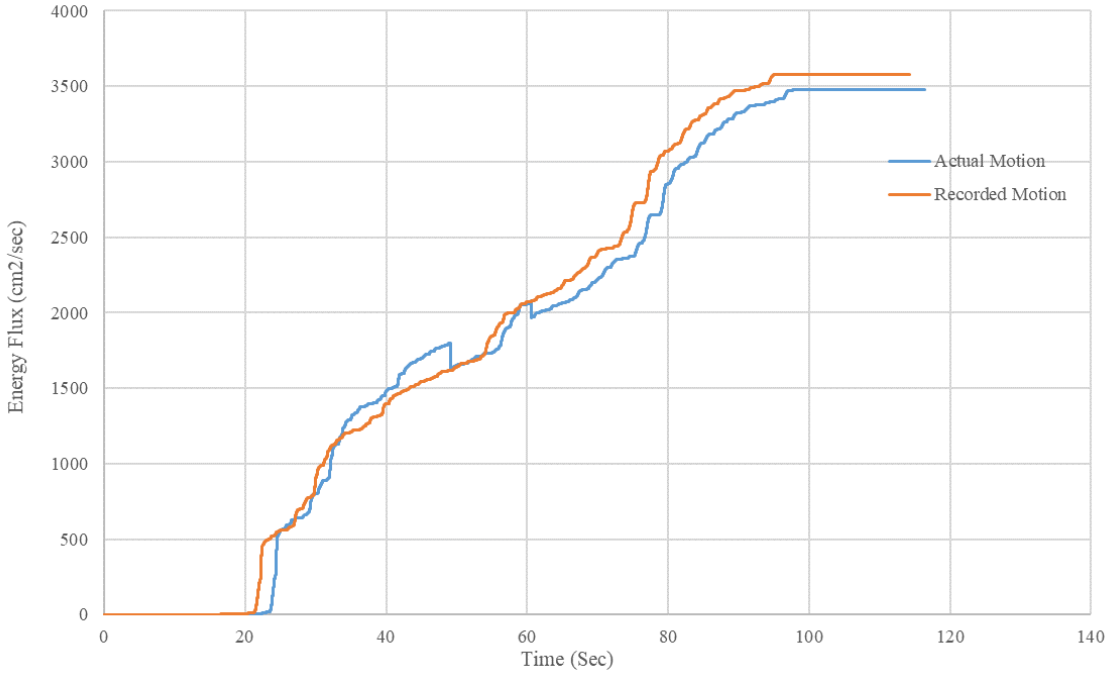

Figure 45. Recorded and Actual Energy Flux Plot at the ground floor

5.2.2 First Floor

Figure 46 shows the raw and unprocessed acceleration history on the first floor of the model. The peak ground acceleration (PGA) of this unprocessed accelerogram is 0.141g and occurs at 27.915 sec. Figure 47 shows the processed record after application of baseline correction and filtering and the accelerogram at the first story as predicted by the 2D four-story SAP2000 model. The PGA of the processed motion is 0.142g, occurring at 27.92 seconds, and the PGA of the SAP2000 model is 0.144g, occurring at 27.96 seconds. Figure 48 shows the energy flux plots of the SAP2000 model and the recorded motion of the first floor. The SED of the recorded motion is observed to be 4552.479 cm^2/sec, and the SED of the SAP2000 model is observed to be 4734.578 cm^2/sec.

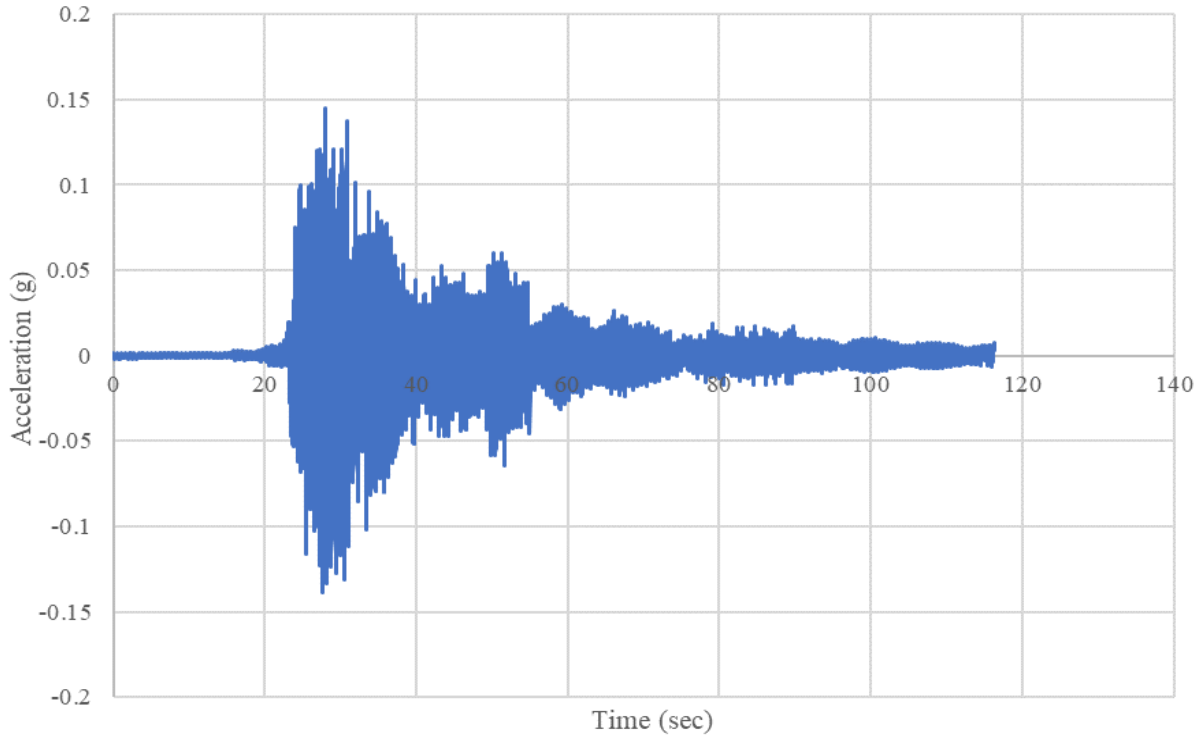

Figure 46. Raw accelerogram recorded at the first floor

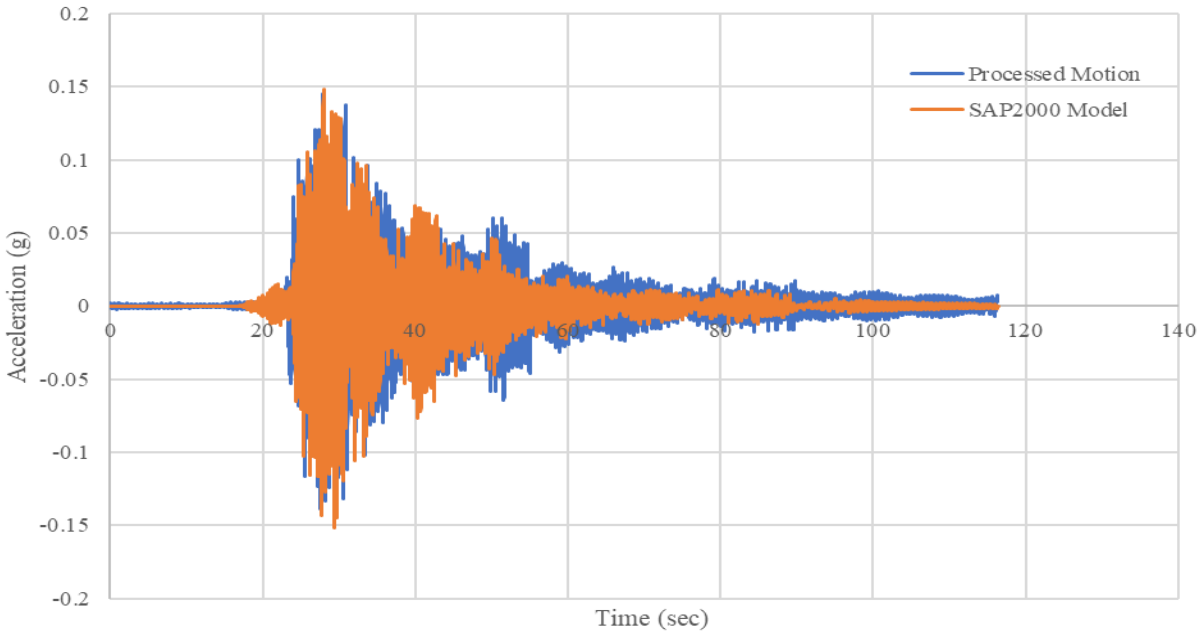

Figure 47. Final processed and SAP2000 accelerogram on the first floor

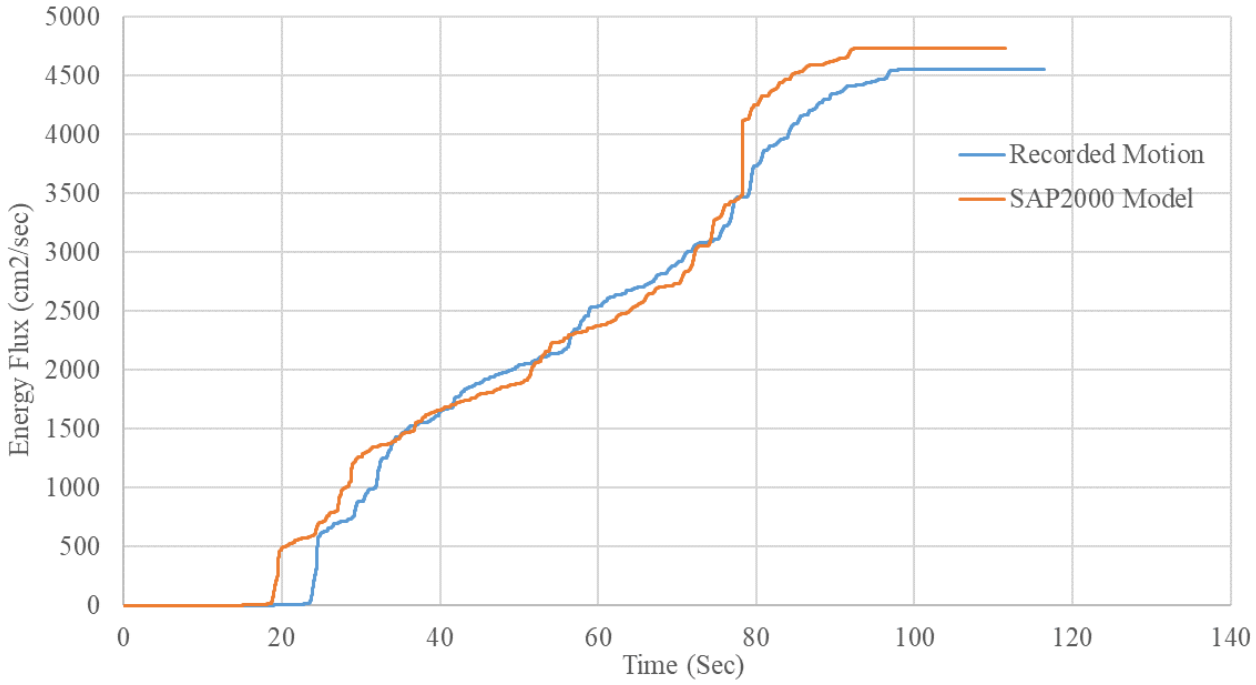

Figure 48. Recorded and SAP2000 model energy flux plot on the first floor

5.2.3 Second Floor

Figure 49 shows the raw and unprocessed acceleration history on the second floor of the model. The peak ground acceleration (PGA) of this unprocessed accelerogram is 0.176g and occurs at 29.68 sec. Figure 50 shows the processed record after application of baseline correction and filtering and the accelerogram at the second story as predicted by the 2D four-story SAP2000 model. The PGA of the processed motion is 0.176g, occurring at 29.685 seconds, and the PGA of the SAP2000 model is 0.179g, occurring at 29.67 seconds. Figure 51 shows the energy flux plots of the SAP2000 model and the recorded motion of the second floor. The SED of the recorded motion is observed to be 6649.689 cm^2/sec, and the SED of the SAP2000 model is observed to be 6516.6949 cm^2/sec.

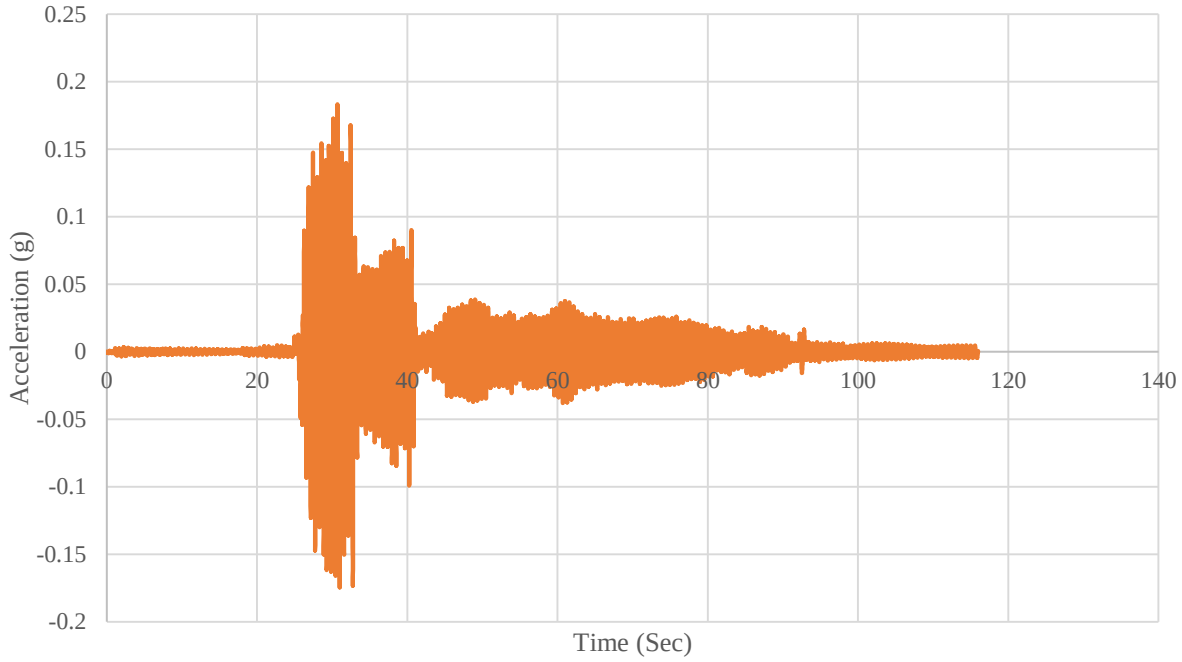

Figure 49. Raw accelerogram recorded on the second floor

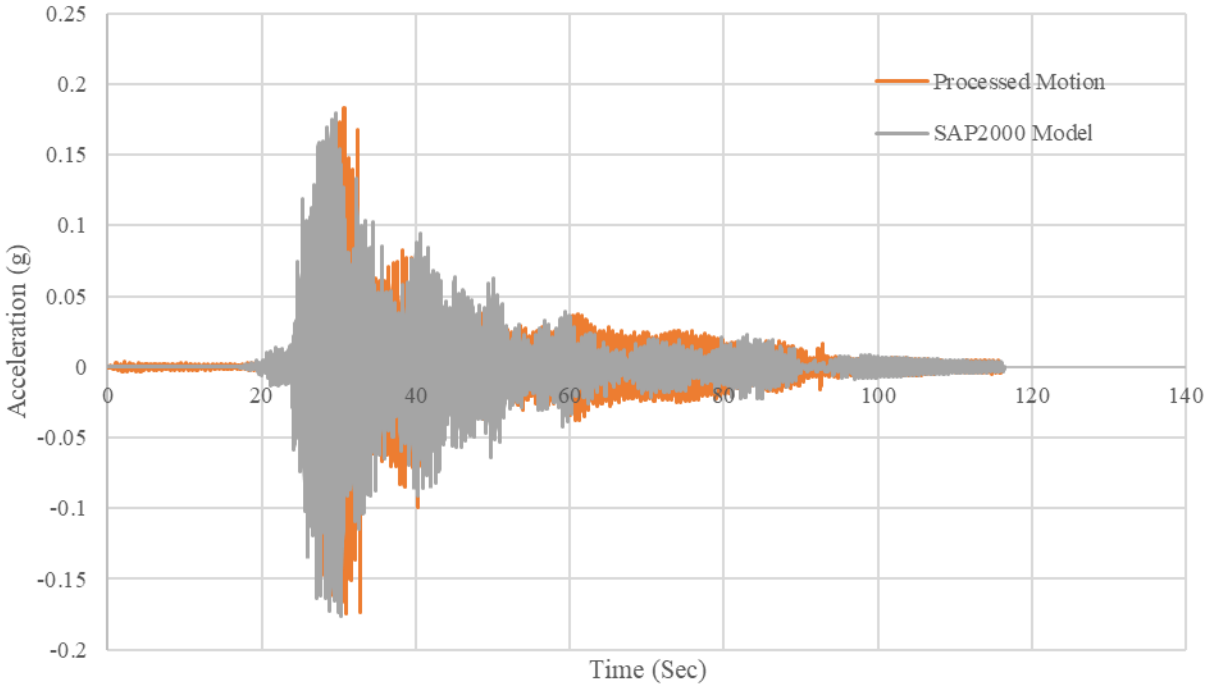

Figure 50. Final processed and SAP2000 accelerogram on the second floor

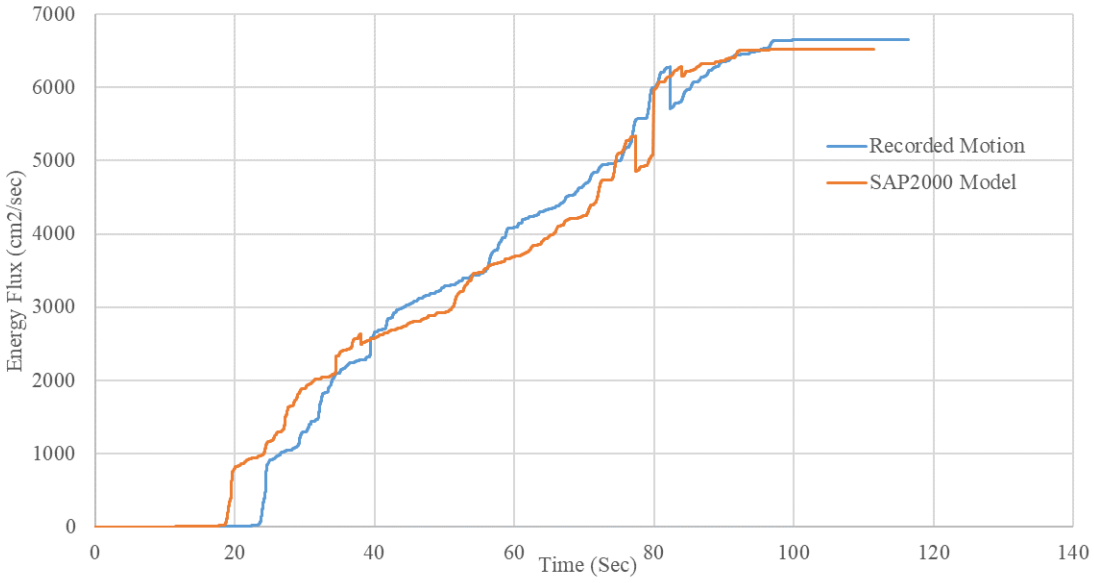

Figure 51. Recorded and SAP2000 model energy flux plot on the second floor

5.2.4 Third Floor

Figure 52 shows the raw and unprocessed acceleration history on the third floor of the model. The peak ground acceleration (PGA) of this unprocessed accelerogram is 0.308g and occurs at 29.2 sec. Figure 53 shows the processed record after application of baseline correction and filtering approach and the accelerogram at the third story as predicted by the 2D four-story SAP2000 model. The PGA of the processed motion is 0.333g, occurring at 30.005 seconds, and the PGA of the SAP2000 model is 0.34g, occurring at 29.855 seconds. Figure 54 shows the energy flux plots of the SAP2000 model and the recorded motion of the third floor. The SED of the recorded motion is observed to be 8184.232 cm^2/sec, and the SED of the SAP2000 model is observed to be 8347.913 cm^2/sec.

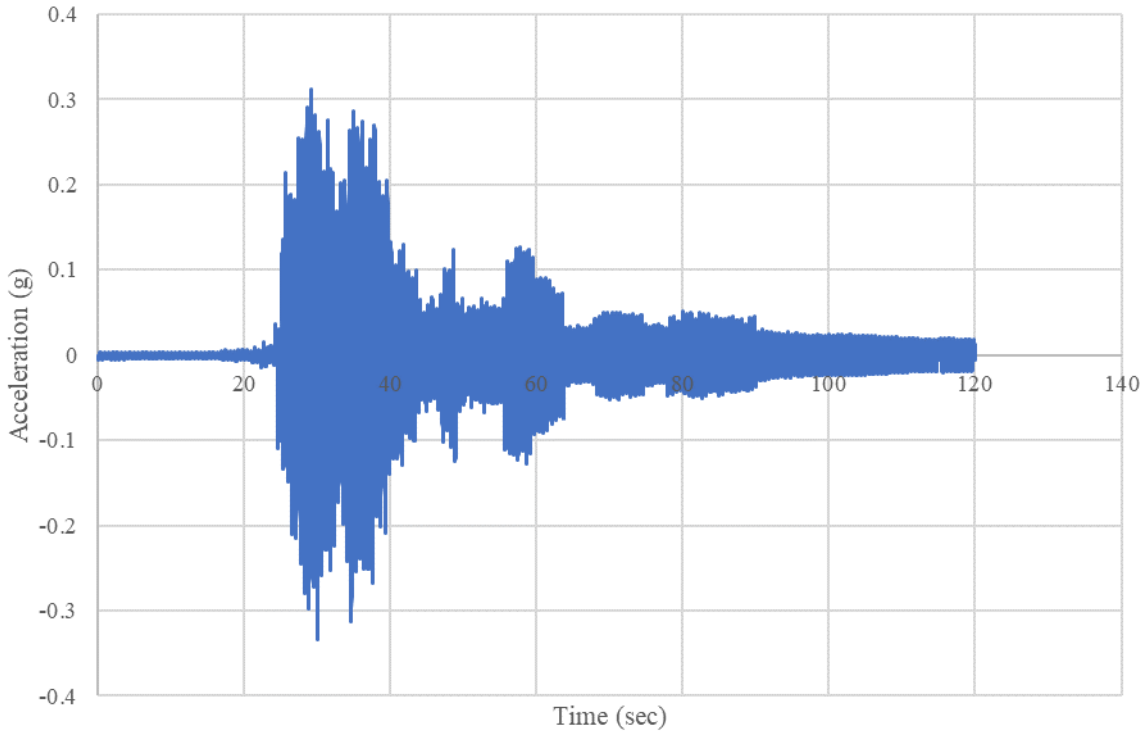

Figure 52. Raw accelerogram recorded on the third floor

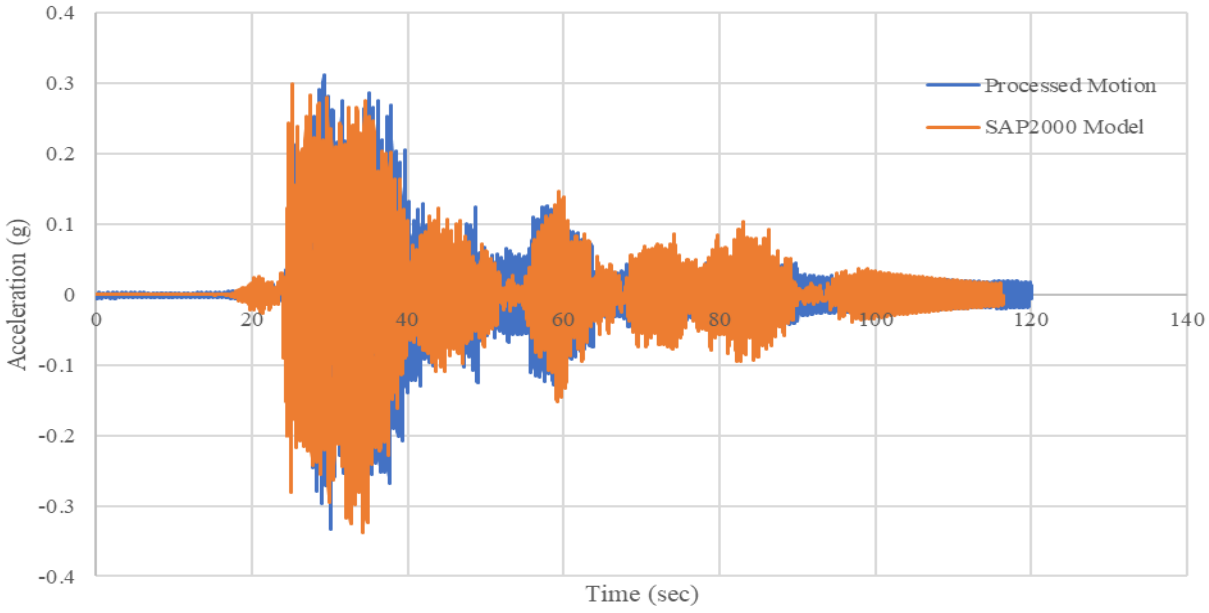

Figure 53. Final processed and SAP2000 accelerogram on the third floor

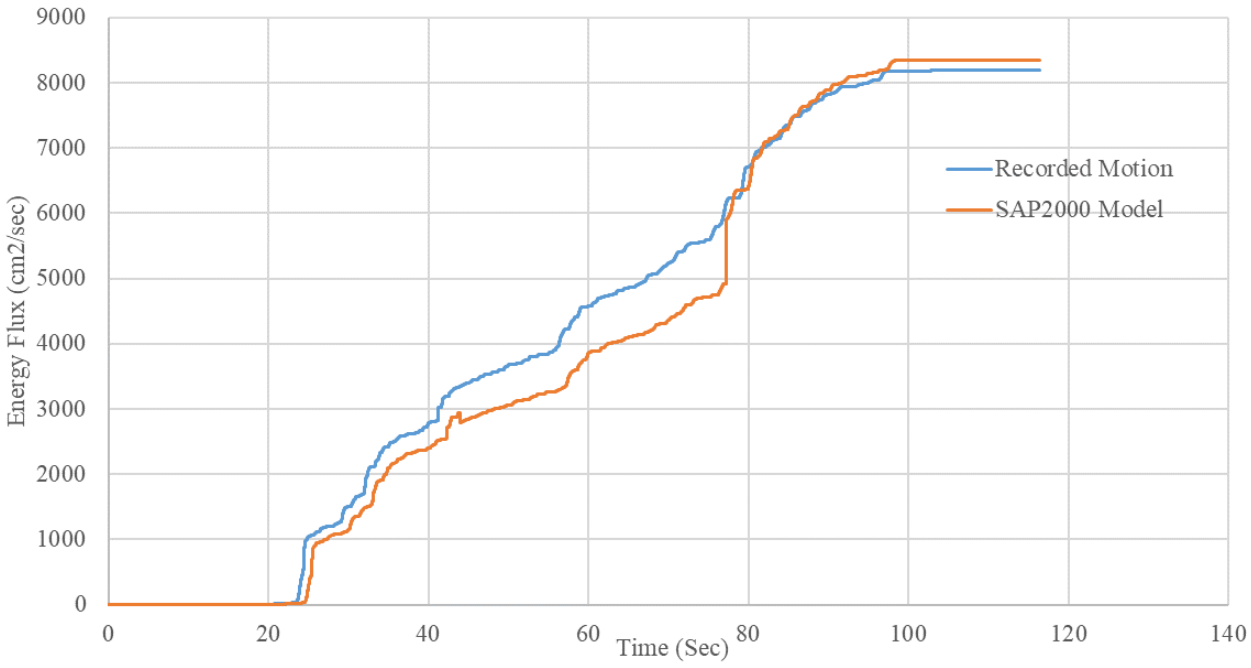

Figure 54. Recorded and SAP2000 model energy flux plot on the third floor

5.2.5 Top Floor

Figure 55 shows the raw and unprocessed acceleration history on the top floor of the model. The peak ground acceleration (PGA) of this unprocessed accelerogram is 0.37g and occurs at 30.045 sec. Figure 56 shows the processed record after application of baseline correction and filtering and the accelerogram at the top story as predicted by the 2D four-story SAP2000 model. The PGA of the processed motion is 0.385g, occurring at 30.055 seconds, and the PGA of the SAP2000 model is 0.41g, occurring at 30.255 seconds. Figure 57 shows the energy flux plots of the SAP2000 model and the recorded motion of the top floor. The SED of the recorded motion is observed to be 9974.533 cm^2/sec, and the SED of the SAP2000 model is observed to be 10423.39 cm^2/sec.

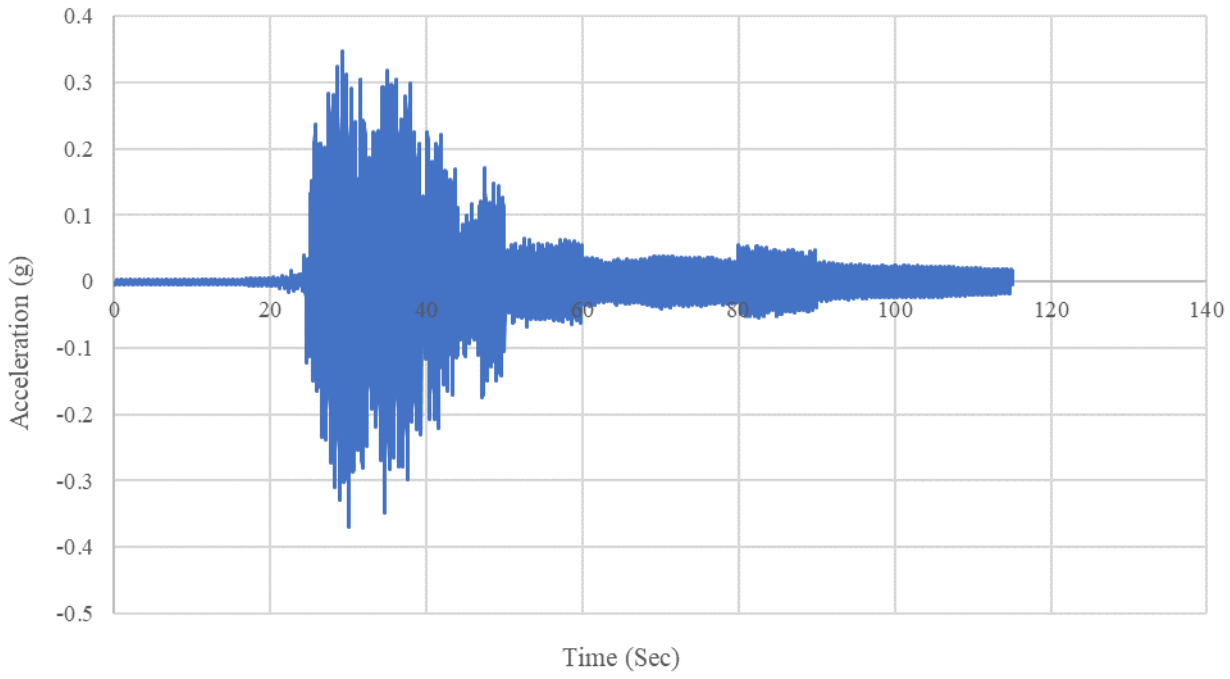

Figure 55. Raw accelerogram recorded at the top floor

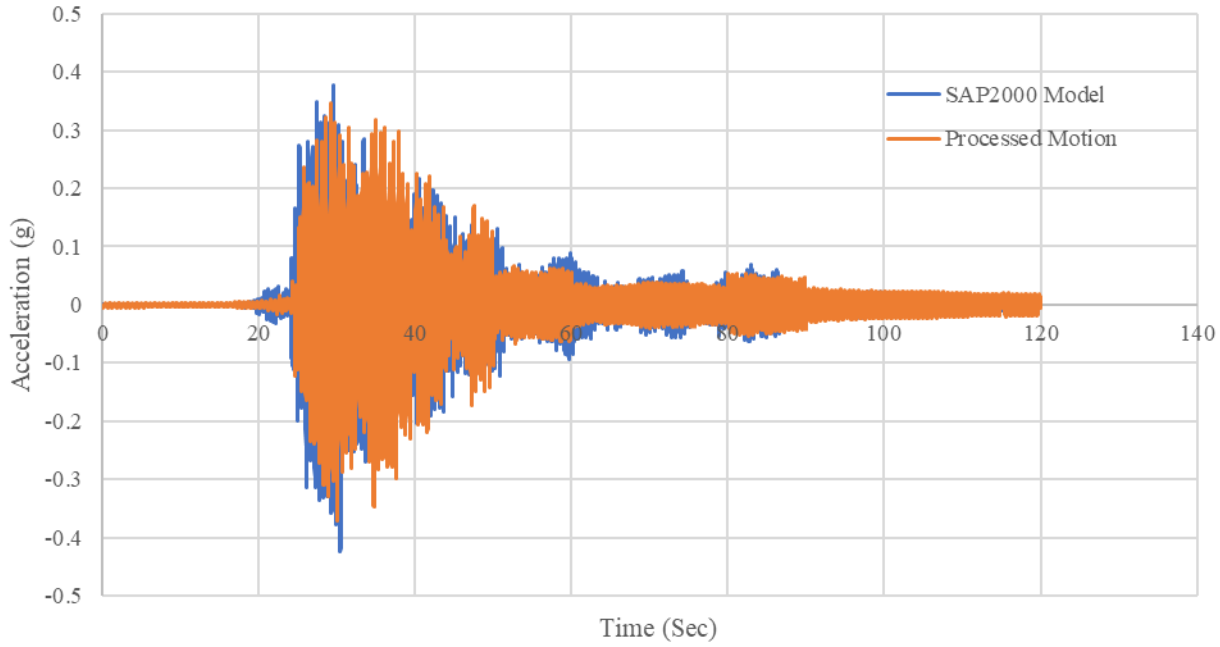

Figure 56. Final processed and SAP2000 accelerogram at the top floor

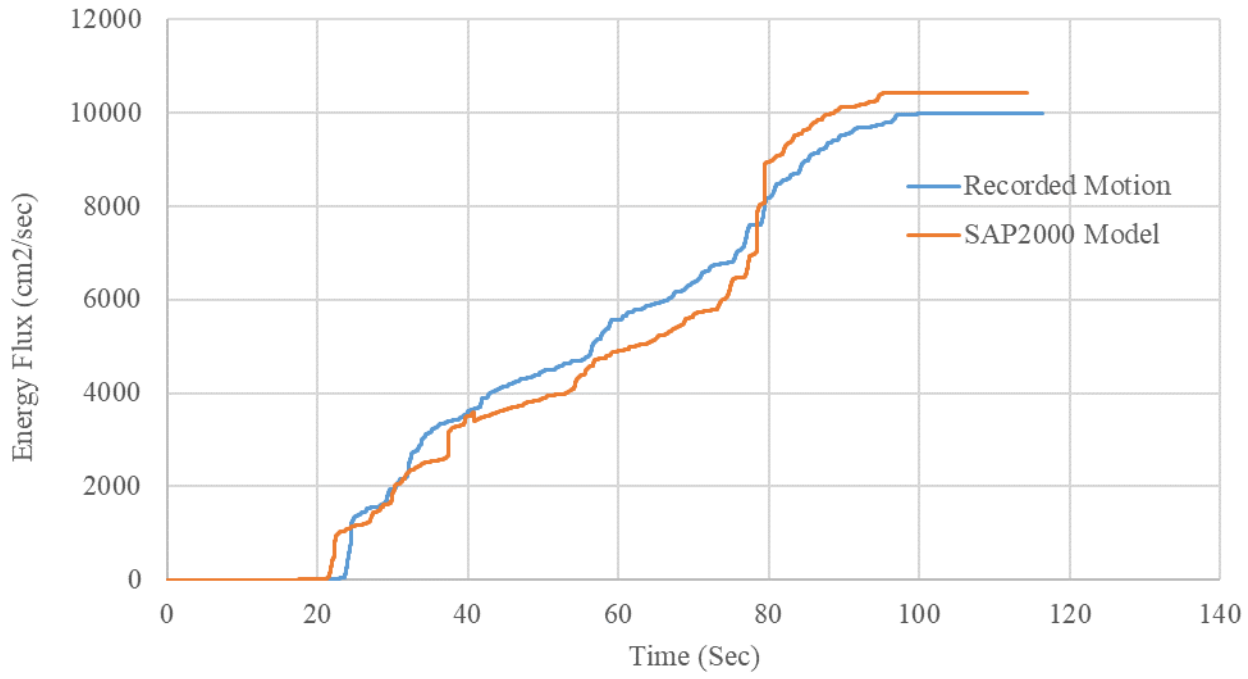

Figure 57. Recorded and SAP2000 Model Energy Flux Plot at the top floor

Table 3 lists the PGA values of the unprocessed, processed, and SAP2000 motions, and the percent variation in the PGAs of the processed data and the SAP2000 model, for every story of the four-story model.

Table 3. PGAs of Unprocessed, Processed, and SAP2000 recordings

PGA (g)	Unprocessed	Processed	SAP2000	Variation (%)
Top	0.37g	0.385g	0.41g	3.896
Third	0.308g	0.333g	0.34g	2.102
Second	0.176g	0.176g	0.179g	1.704
First	0.141g	0.142g	0.144g	1.408
Ground	0.11g	0.125g	0.126g	0.8

5.3 Five-Story Structural Responses

5.3.1 Ground Floor

Figure 58 shows the raw and unprocessed acceleration history on the ground floor of the model. The peak ground acceleration (PGA) of this unprocessed accelerogram is 0.083g and occurs at 26.06 sec. Figure 59 shows the processed record after application of baseline correction and filtering and the actual ground motion as extracted from the PEER database that is applied to the five-story structural model. The PGA of the processed motion is 0.082g, occurring at 23.98 seconds. The PGA of the actual motion is 0.09g, occurring at 24.17 seconds. Figure 60 shows the energy flux plots of the actual and recorded motion. The SED of the recorded motion is observed to be 5012.842 cm^2/sec, and the SED of the actual motion is observed to be 5115.07 cm^2/sec.

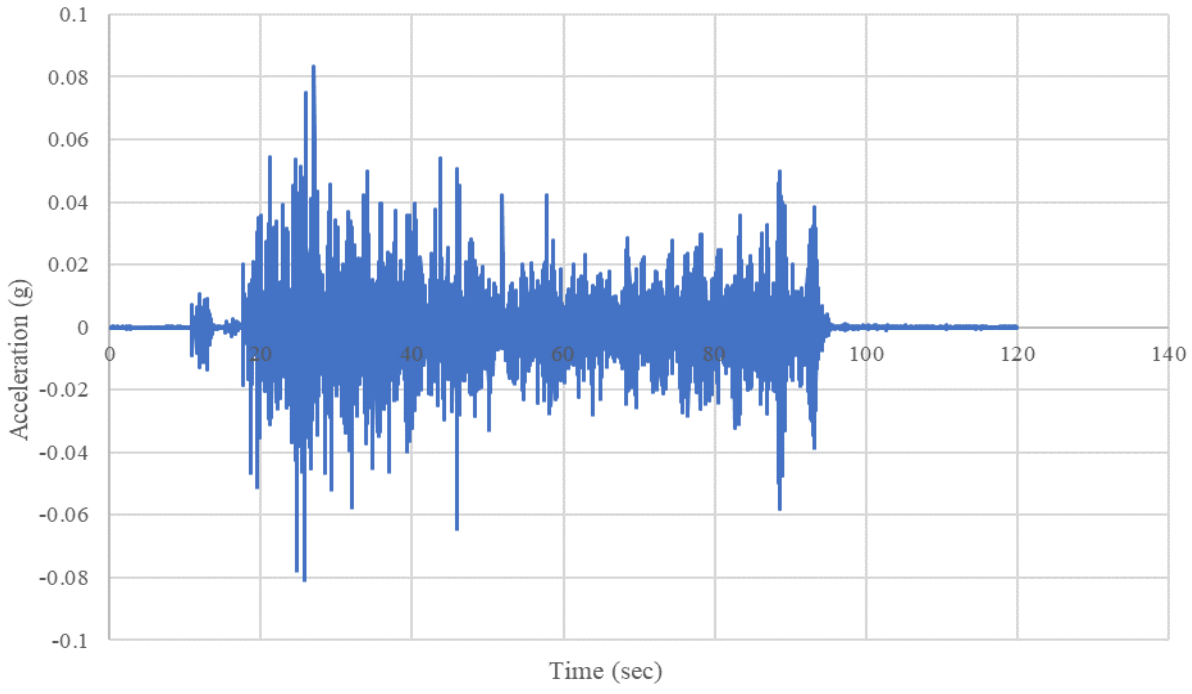

Figure 58. Raw accelerogram recorded at the ground floor

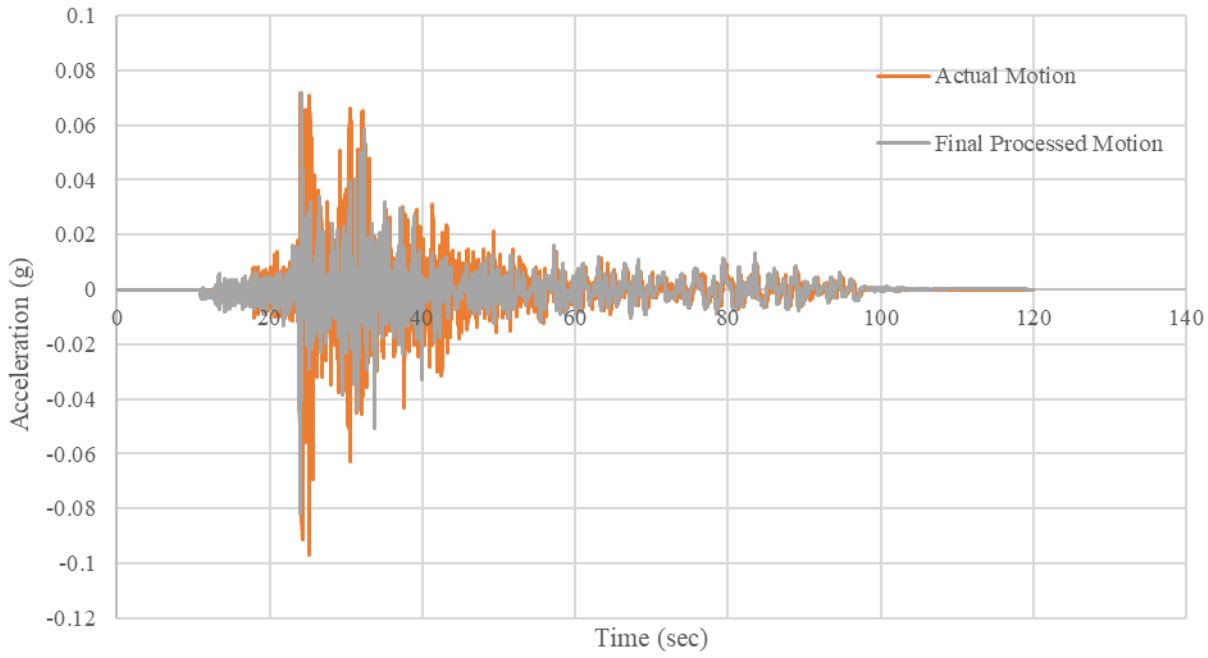

Figure 59. Final processed and actual accelerogram at the ground floor

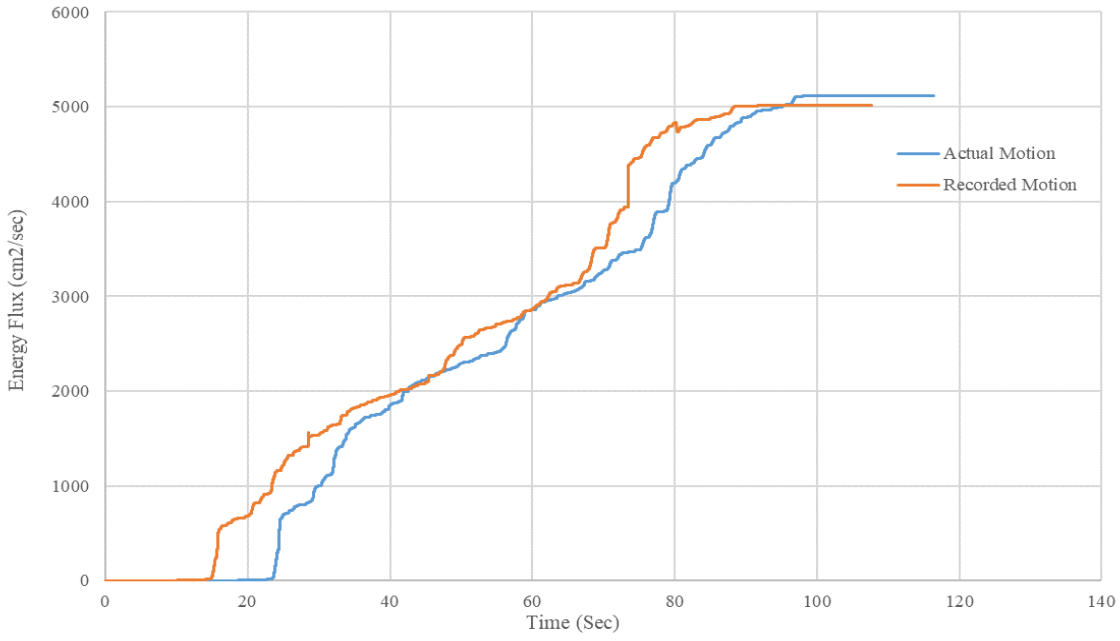

Figure 60. Recorded and Actual Energy Flux Plot at the ground floor

5.3.2 First Floor

Figure 61 shows the raw and unprocessed acceleration history on the first floor of the model. The peak ground acceleration (PGA) of this unprocessed accelerogram is 0.106g and occurs at 24.20 sec. Figure 62 shows the processed record after application of baseline correction and filtering and the accelerogram at the first story as predicted by the 2D five-story SAP2000 model. The PGA of the processed motion is 0.106g, occurring at 24.21 seconds, and the PGA of the SAP2000 model is 0.108g, occurring at 25.2 seconds. Figure 63 shows the energy flux plots of the SAP2000 model and the recorded motion of the first floor. The SED of the recorded motion is observed to be 6138.172 cm^2/sec, and the SED of the SAP2000 model is observed to be 6445.083 cm^2/sec.

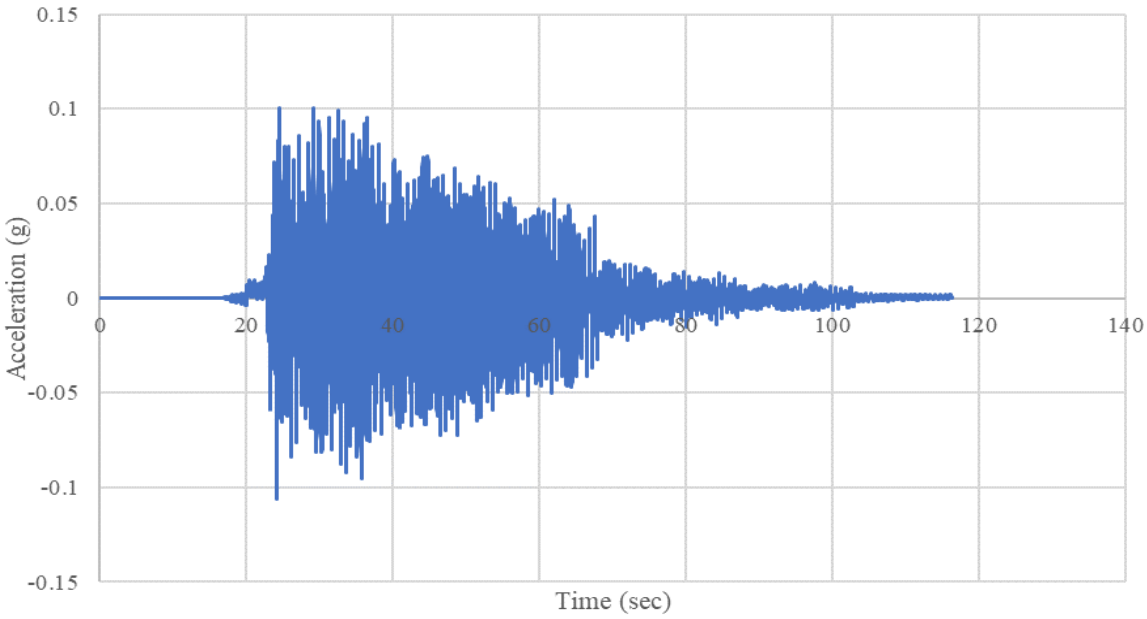

Figure 61. Raw accelerogram recorded at the first floor

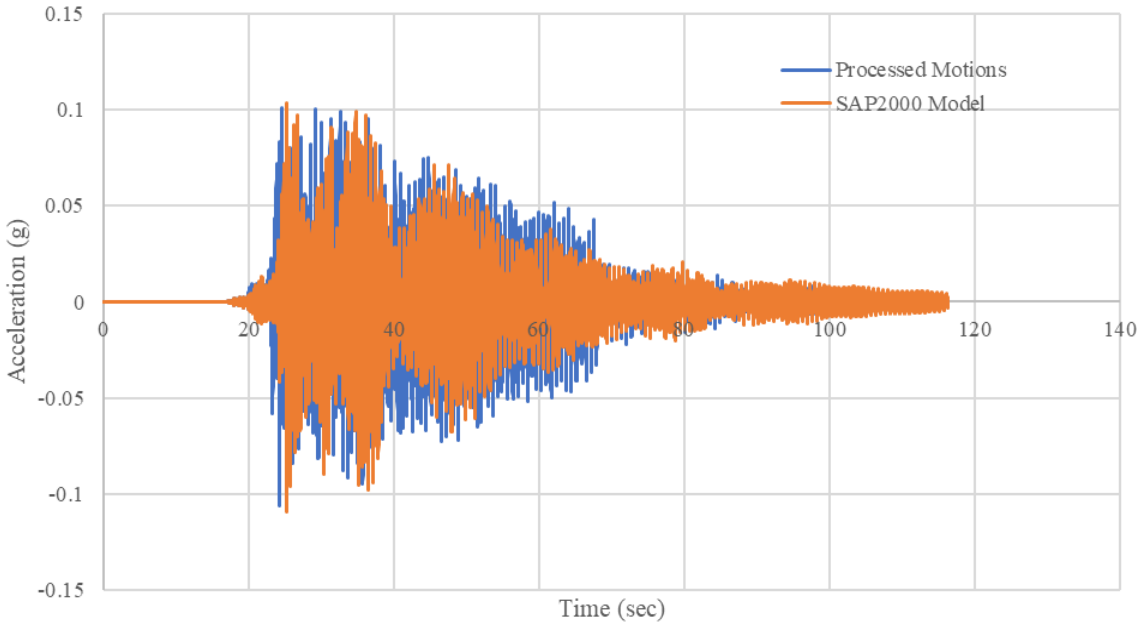

Figure 62. Final processed and SAP2000 accelerogram on the first floor

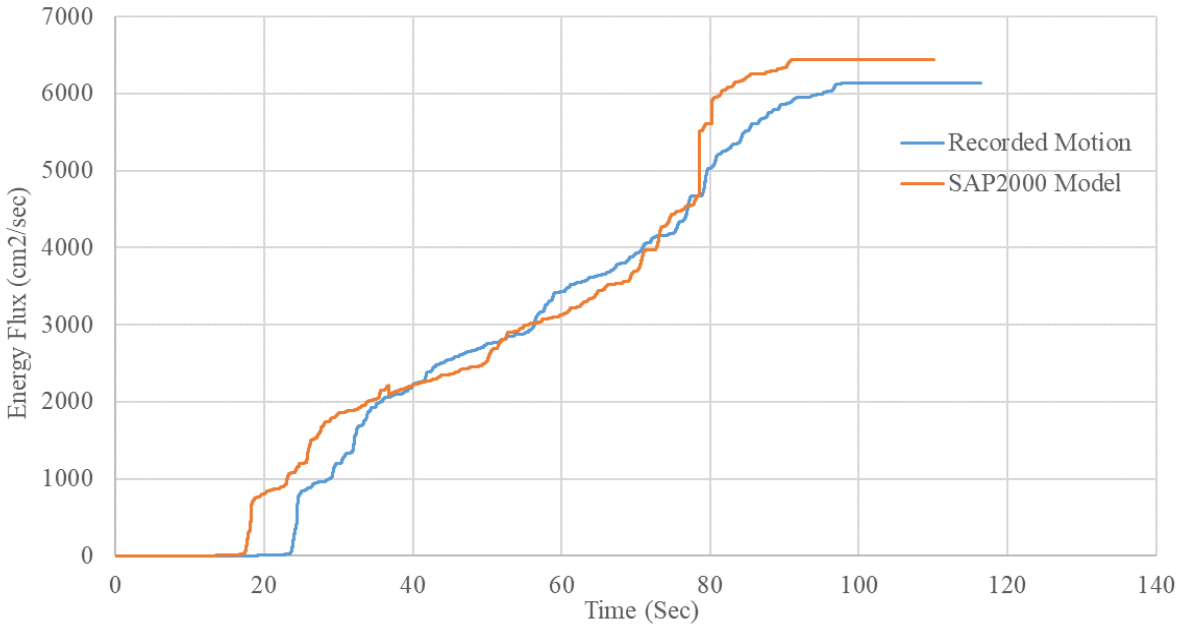

Figure 63. Recorded and SAP2000 model energy flux plot on the first floor

5.3.3 Second Floor

Figure 64 shows the raw and unprocessed acceleration history on the second floor of the model. The peak ground acceleration (PGA) of this unprocessed accelerogram is 0.11g and occurs at 27.33 sec. Figure 65 shows the processed record after application of baseline correction and filtering and the accelerogram at the second story as predicted by the 2D five-story SAP2000 model. The PGA of the processed motion is 0.113g, occurring at 27.35 seconds, and the PGA of the SAP2000 model is 0.116g, occurring at 27.48 seconds. Figure 66 shows the energy flux plots of the SAP2000 model and the recorded motion of the second floor. The SED of the recorded motion is observed to be 7672.587 cm^2/sec, and the SED of the SAP2000 model is observed to be 7097.259 cm^2/sec.

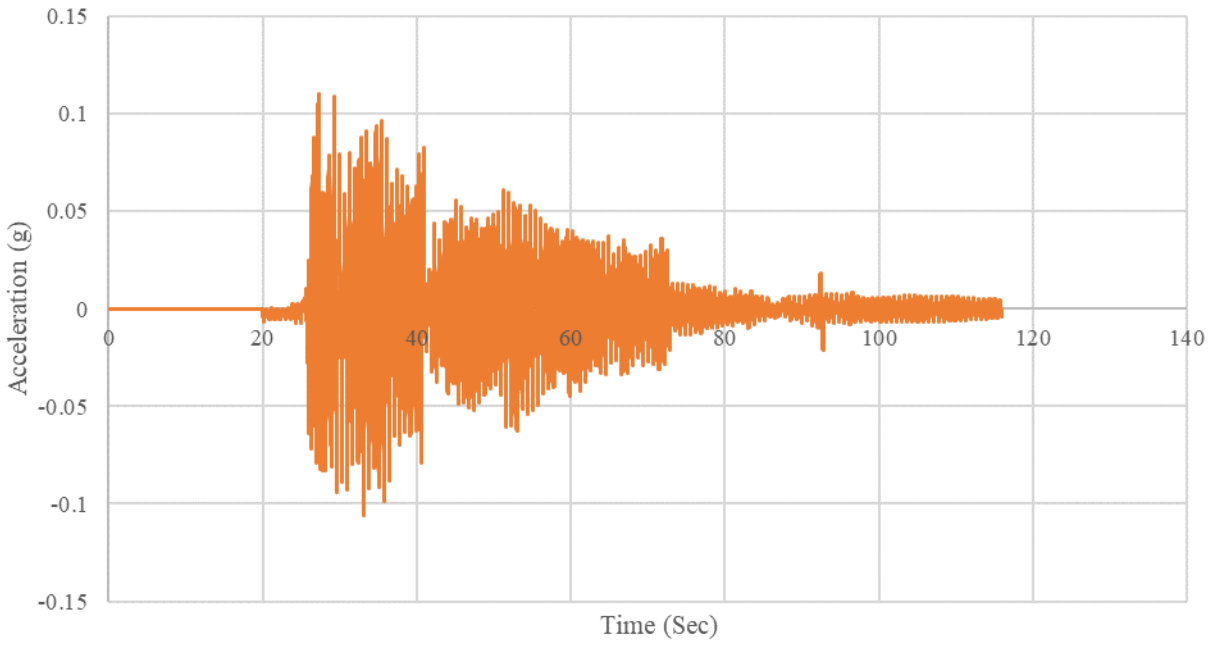

Figure 64. Raw accelerogram recorded on the second floor

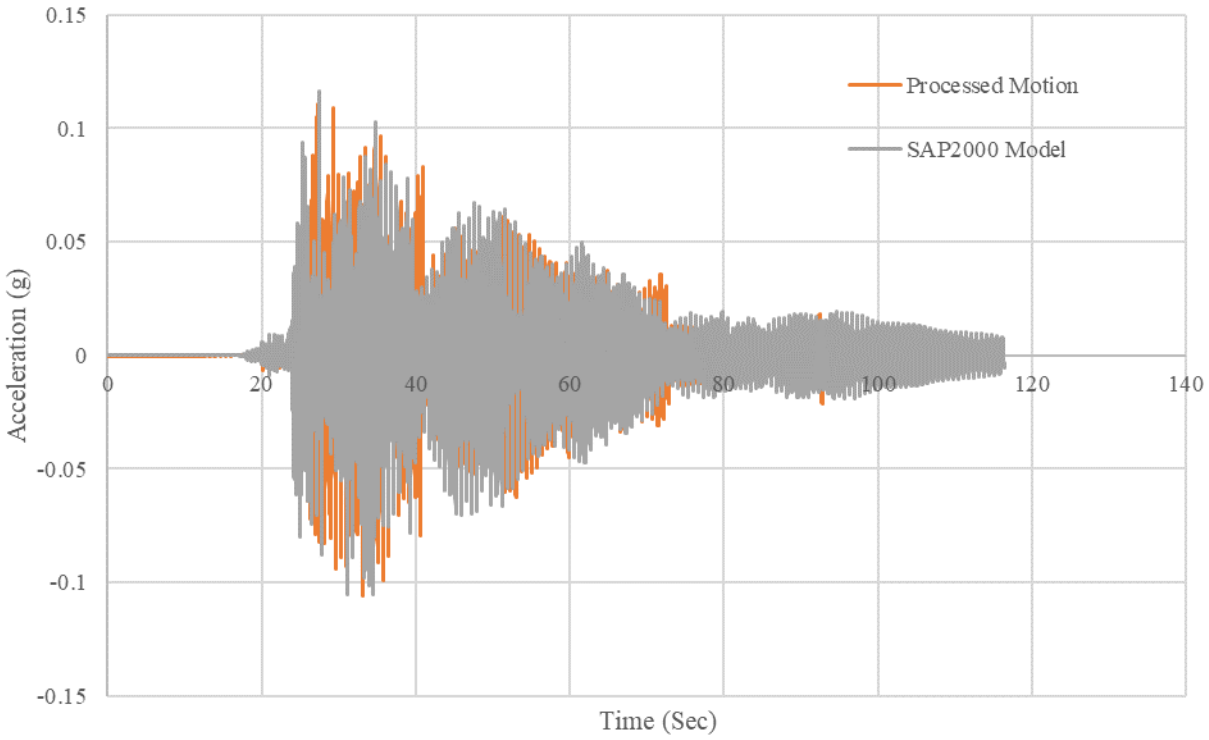

Figure 65. Final processed and SAP2000 accelerogram on the second floor

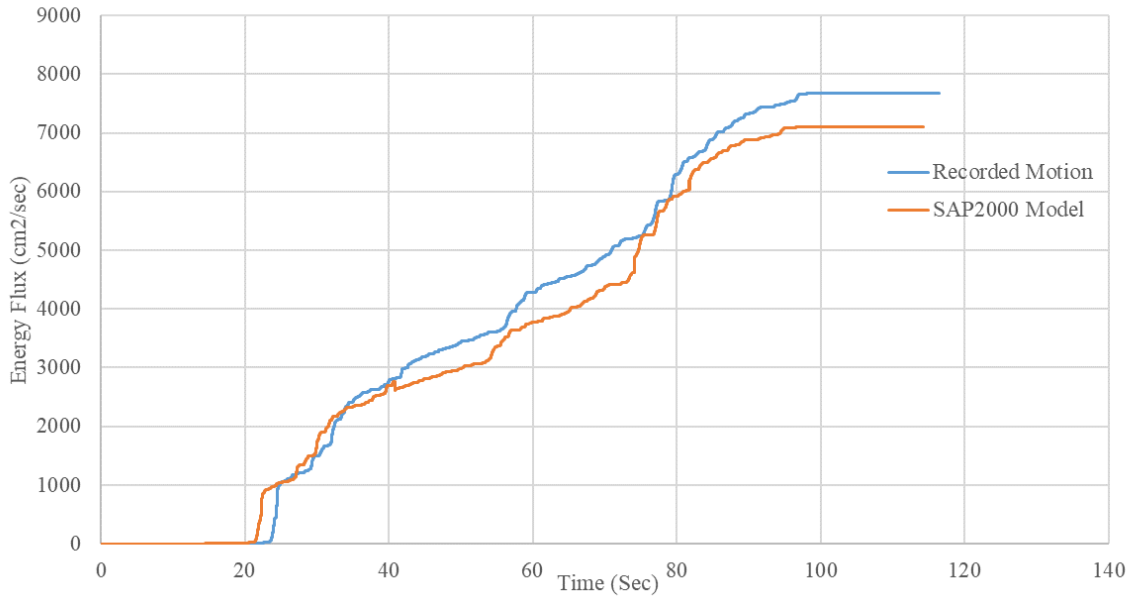

Figure 66. Recorded and SAP2000 model energy flux plot on the second floor

5.3.4 Third Floor

Figure 67 shows the raw and unprocessed acceleration history on the third floor of the model. The peak ground acceleration (PGA) of this unprocessed accelerogram is 0.256g and occurs at 26.83 sec. Figure 68 shows the processed record after application of baseline correction and filtering and the accelerogram at the third story as predicted by the 2D five-story SAP2000 model. The PGA of the processed motion is 0.242g, occurring at 25.75 seconds, and the PGA of the SAP2000 model is 0.249g, occurring at 25.85 seconds. Figure 69 shows the energy flux plots of the SAP2000 model and the recorded motion of the third floor. The SED of the recorded motion is observed to be 8695.747 cm^2/sec, and the SED of the SAP2000 model is observed to be 9202.273 cm^2/sec.

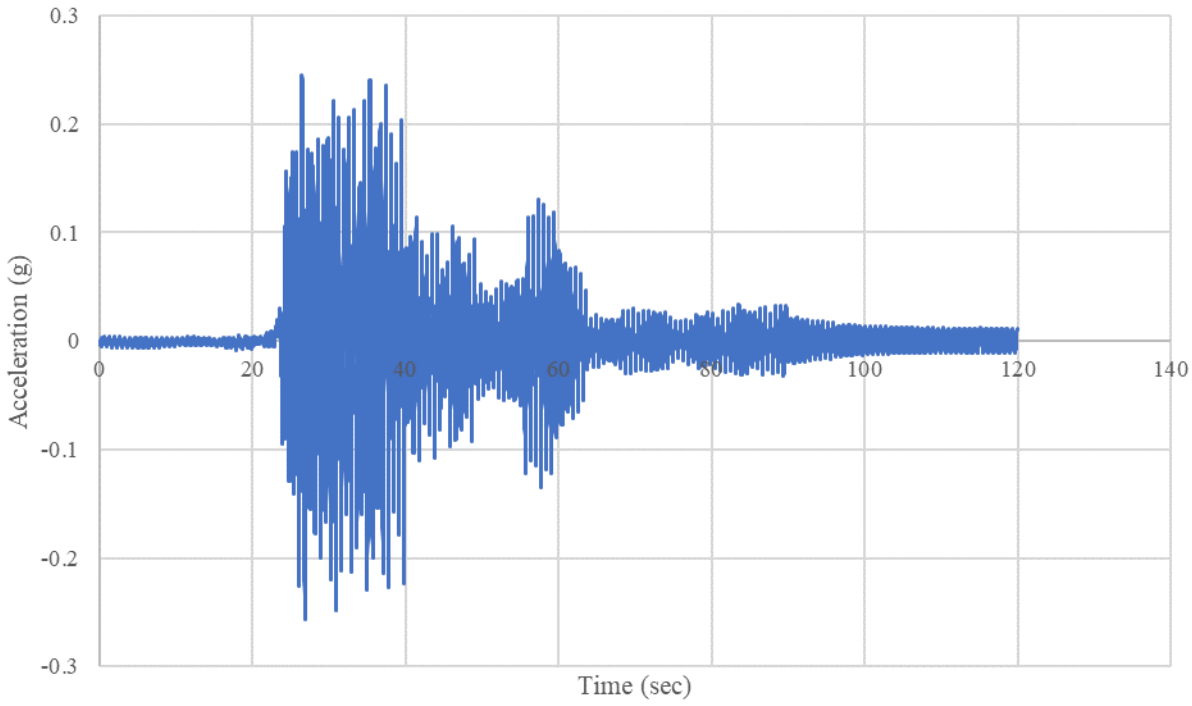

Figure 67. Raw accelerogram recorded on the third floor

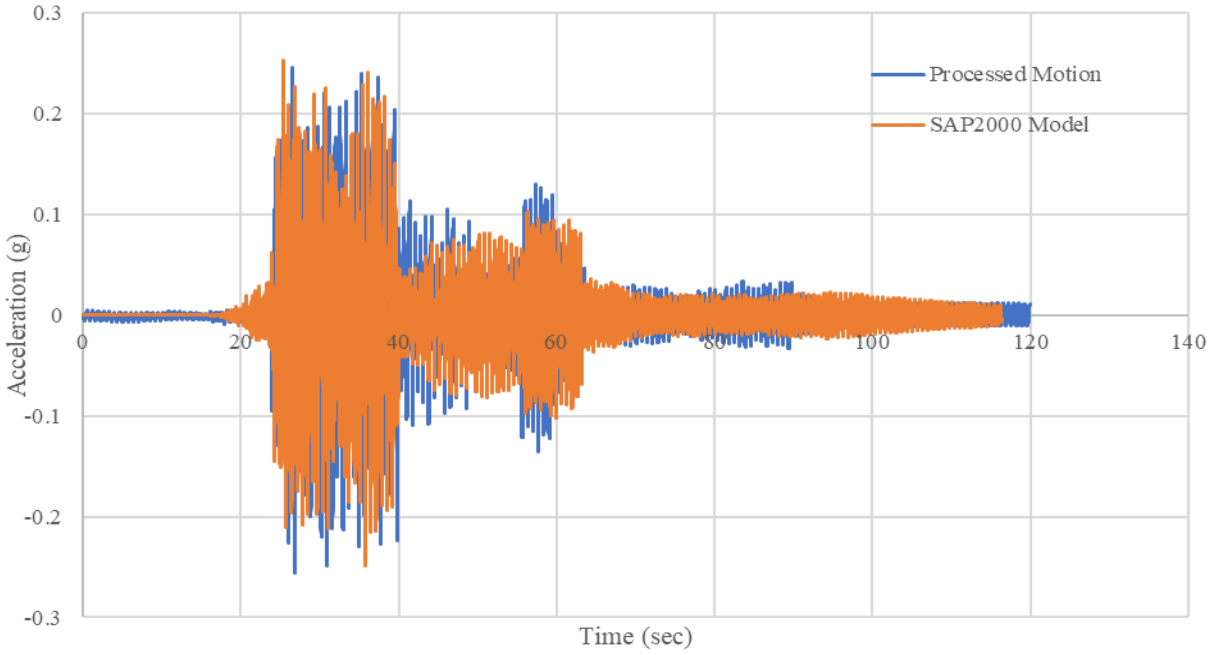

Figure 68. Final processed and SAP2000 accelerogram on the third floor

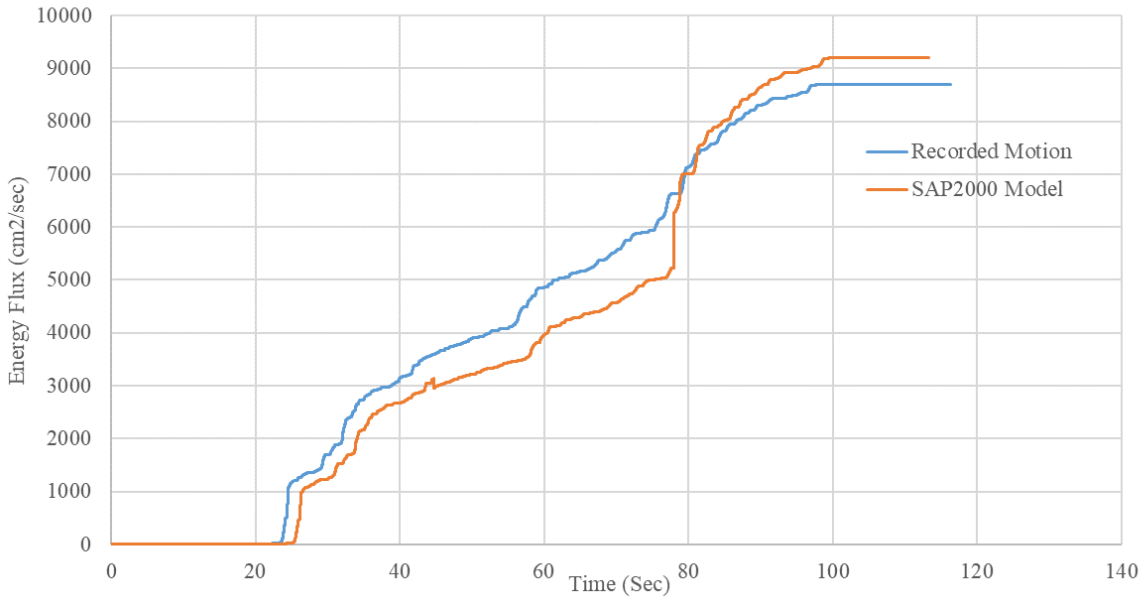

Figure 69. Recorded and SAP2000 model energy flux plot on the third floor

5.3.5 Fourth Floor

Figure 70 shows the raw and unprocessed acceleration history on the fourth floor of the model. The peak ground acceleration (PGA) of this unprocessed accelerogram is 0.268g and occurs at 30.4 sec. Figure 71 shows the processed record after application of baseline correction and filtering and the accelerogram at the fourth story as predicted by the 2D five-story SAP2000 model. The PGA of the processed motion is 0.268g, occurring at 30.45 seconds, and the PGA of the SAP2000 model is 0.277g, occurring at 30.445 seconds. Figure 72 shows the energy flux plots of the SAP2000 model and the recorded motion of the first floor. The SED of the recorded motion is observed to be 9718.776 cm^2/sec, and the SED of the SAP2000 model is observed to be 10287.894 cm^2/sec.

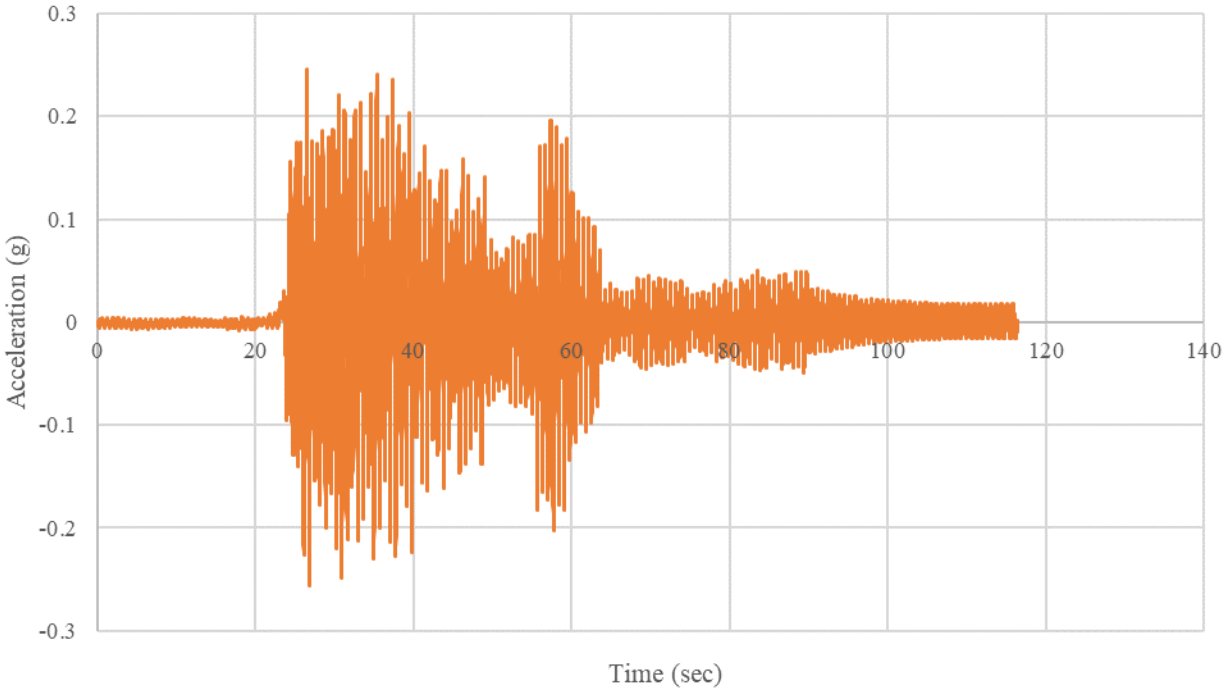

Figure 70. Raw accelerogram recorded on the fourth floor

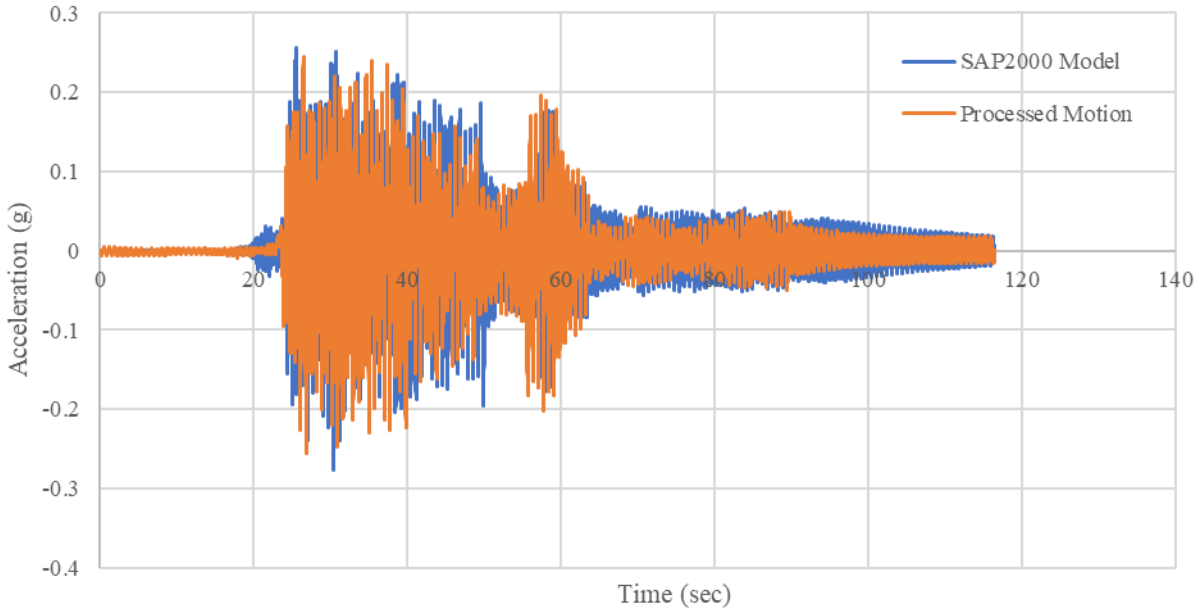

Figure 71. Final processed and recorded SAP2000 accelerogram on the fourth floor

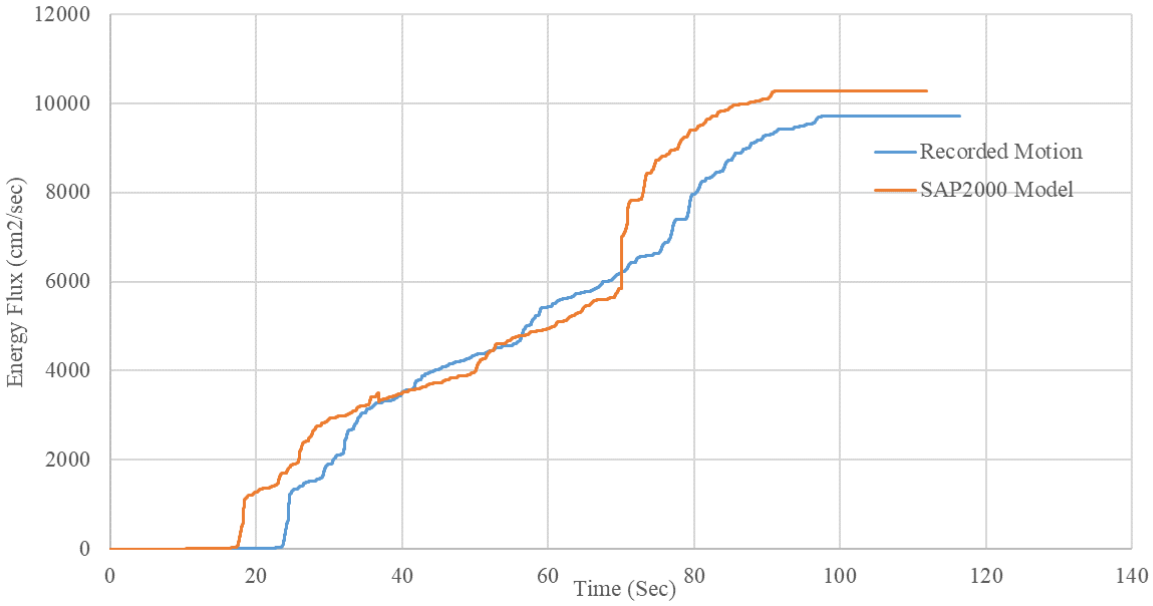

Figure 72. Recorded and SAP2000 model energy flux plot on the fourth floor

5.3.6 Top Floor

Figure 73 shows the raw and unprocessed acceleration history on the top floor of the model. The peak ground acceleration (PGA) of this unprocessed accelerogram is 0.355g and occurs at 33.2 sec. Figure 74 shows the processed record after application of baseline correction and filtering and the accelerogram at the top story as predicted by the 2D five-story SAP2000 model. The PGA of the processed motion is 0.351g, occurring at 33.255 seconds, and the PGA of the SAP2000 model is 0.37g, occurring at 32.8 seconds. Table 4 lists the PGA values of the unprocessed, processed, and SAP2000 motions, and the percent variation in the PGAs of the processed and SAP2000 model, for every story of the five-story model. Figure 75 shows the energy flux plots of the SAP2000 model and the recorded motion of the top floor. The SED of the recorded motion is observed to be 11654.86 cm^2/sec, and the SED of the SAP2000 model is observed to be 12532.11 cm^2/sec.

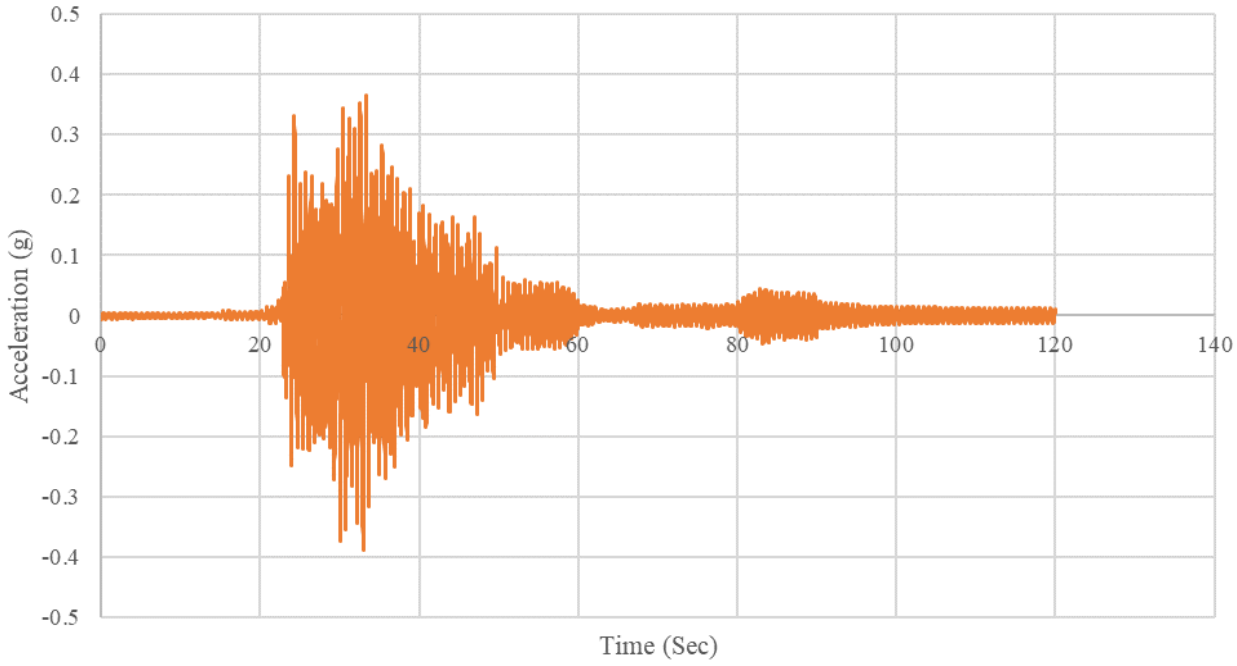

Figure 73. Raw accelerogram recorded at the top floor

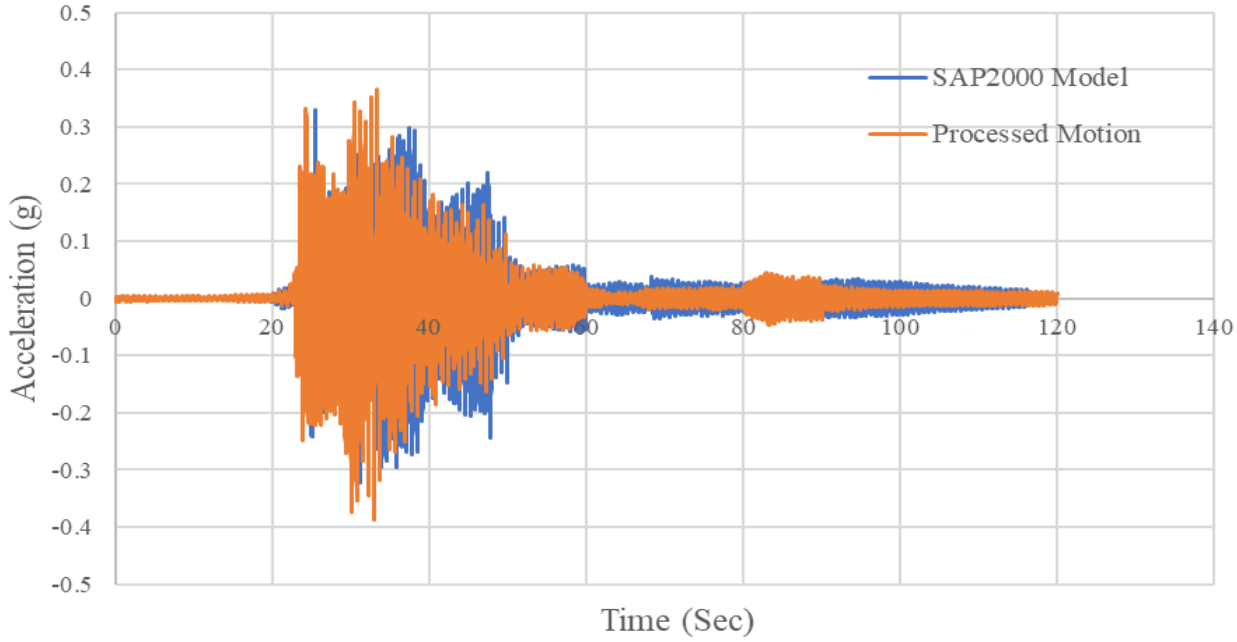

Figure 74. Final processed and recorded SAP2000 accelerogram at the top floor

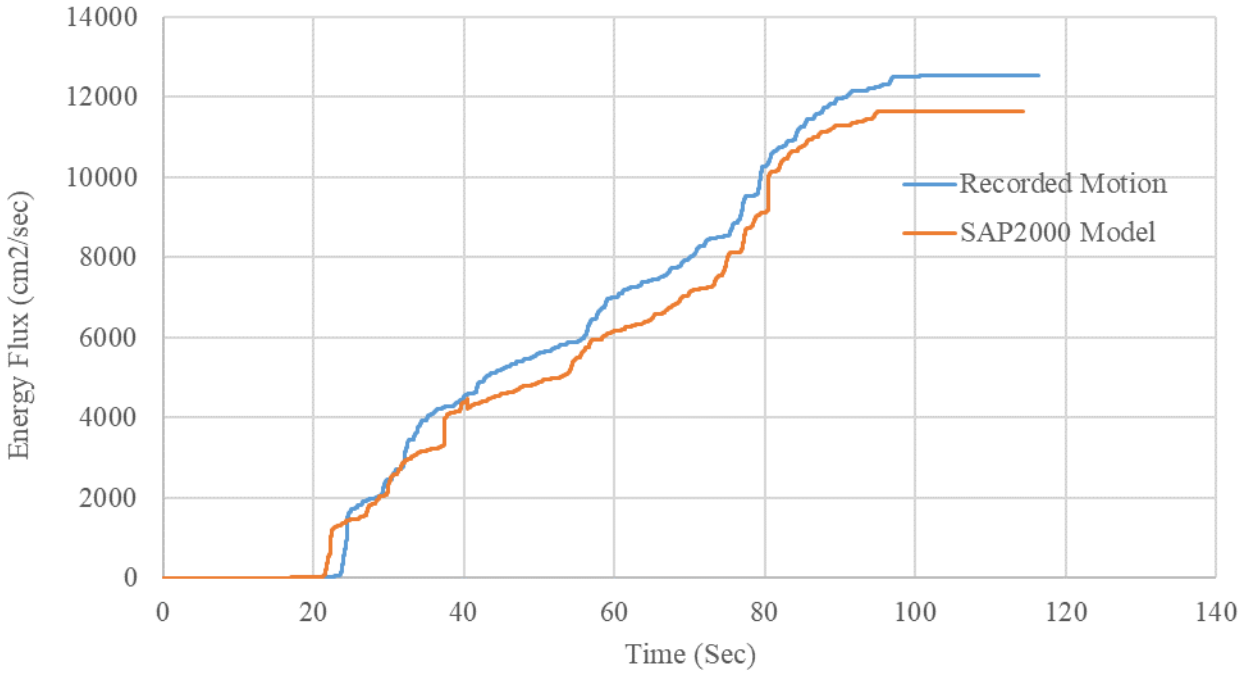

Figure 75. Recorded and SAP2000 model energy flux plot on the top floor

Table 4. PGAs of Unprocessed, Processed, and SAP2000 recordings

PGA (g)	Unprocessed	Processed	SAP2000	Variation (%)
Top	0.355g	0.351g	0.37g	5.413
Fourth	0.268g	0.268g	0.277g	3.335
Third	0.256g	0.242g	0.249g	2.892
Second	0.11g	0.113g	0.116g	2.654
First	0.106g	0.106g	0.108g	1.886
Ground	0.083g	0.082g	0.083g	1.219

Chapter 6. Summary

Three, four, and five-story scaled structural models were constructed, and an experimental setup with the necessary data acquisition system was assembled. Shake table experiments were performed on the scaled structural models using scaled ground motions. The purpose of this study was to measure structural responses such as acceleration at every story during a simulated earthquake event. 2D SAP2000 models were developed and used to predicted structural response and then compared with the actual processed motion. Although the PGAs recorded by the data acquisition system and those predicted by the SAP2000 models are comparable, an increase in the percentage of variation was observed in all the models with an increase in the number of stories. Also, there is an increase in percent variation between the structural models. SAP2000 model results slightly overestimated the response, especially at higher levels. The PGA at the ground floor of the three, four, and five-story models obtained using SAP2000 are 0.543%, 0.8%, and 1.219% higher, respectively than the response recorded by the data acquisition system. SAP2000 values for the PGA at the top floor of the three-story model are 1.902% higher than the response recorded by the data acquisition system. In the case of the four-story model, the response predicted by SAP2000 is 3.896% higher, and it is 5.413% higher for the five-story model. The results from the processed motions and SAP2000 models validate the functionality of the shake table used to perform this study.

Appendix

The following MATLAB scripts were used in order to perform baseline correction and filtering of the raw and unprocessed data. A Chebyshev filter of second order was used for filtering purposes. A subroutine to clear unwanted spikes from the accelerograms, developed by Aida Azari Sisi, was also used for this study.

```
clear all
clc
set (gca, 'FontName', 'Times New Roman')
acc=xlsread('filter','First','C3:C24002');
dt=0.005;
order=3;
L = length(acc);
t = linspace(0, L, L)*dt;
acc = fft(acc)/L;

vel=cumtrapz(t,acc);                % Obtaining Velocity and Displacement
dis=cumtrapz(t,vel);

dis_new=dis;                        % Applying Zero-padding
for i=length(dis)+1:length(dis)+0.1*length(dis)
    dis_new(i)=dis_new(length(dis));
end
t1=0:dt:(length(dis_new)-1)*dt;


P = polyfit(t,dis,3);                    %  Baseline Correction
po_va = polyval(P,t1);
dis = dis -po_va;

tb=20;                                   % Tapering
te=20;
n1 = (length(dis)*tb)/100;
 for i=1:n1
arg = pi*(i-1)/n1 + pi;
dis(i) = dis(i)*(1+cos(arg))/2;
end
n1 = (length(dis)*te)/100;
for i=1:n1
arg = pi*(i-1)/n1 + pi;
dis(length(dis)-i+1) = acc(length(dis)-i+1)*(1+cos(arg))/2;
end
Fs = 200;                                  % Filtering
Fn = Fs/2;
Ts = 1/Fs;
L = length(dis);
t = linspace(0, L, L)*Ts;
t=t';
figure(1)
plot(t, dis)
```

```
grid
Fdis = fft(dis)/L;
Fv = linspace(0, 1, fix(L/2)+1)*Fn;
Iv = 1:length(Fv);
figure(2)
semilogx(Fv, abs(Fdis(Iv))*2)
grid
xlabel('Frequency (Hz)')
ylabel('Fourier Amplitude')
Wp=0.01;
Ws=0.1;
Rp=0.25;
Rs =1;
[n,Ws] = cheb2ord(Wp,Ws,Rp,Rs);
[z,p,k] = cheby2(n,Rp,Wp);
[sosbp,gbp] = zp2sos(z,p,k);
figure(3)
freqz(sosbp, 2^16, Fs)
s_filt = filtfilt(sosbp,gbp, Fdis);
dis=s_filt:
t1=0:0.005:116.39;
plot(t1, dis, '-b')
hold on
plot(t, s_filt, '-r', 'LineWidth',1.5)
xlabel('Time(sec)')
ylabel('Displacement')
legend('Original', 'Filtered')
hold off
vel=diff(t,dis);                    % Obtaining Velocity and Acceleration
acc=diff(t,vel);
```

A subroutine to clear unusual spikes by Aida Azari Sisi:

```
clear all
clc
TimeData=xlsread('filter,'First','A3:A24002');
TimeData=TimeData';
AccelData_comp=xlsread('filter,'First','C3:C24002');
AccelData_comp=AccelData_comp';
plot(TimeData,AccelData_comp);ylabel('Acceleration,cm/s^2','FontSize',8);
xlabel('Time (s)','FontSize',8);
hold on;
disp('> Accelerogram of the record is ploted.');
disp(' ');
SampleInt=0.005;
comp_spike_index=input('- Does the record include any Spikes? (Y,N): ','s');
if length(comp_spike_index)<1
       while upper(comp_spike_index)=='Y' | upper(comp_spike_index)=='N'
       comp_spike_index=input('- Does the record include any Spikes? (Please
       enter Y or N): ','s');
       end
end
disp(' ');
comp_spike_index=upper(comp_spike_index);
if comp_spike_index=='Y'
        while comp_spike_index=='Y'
        %start_time=input('- Enter the starting time of the spike. t_start= ');
        %end_time=input('- Enter the ending time of the spike. t_end= ');

        start_index=start_time/SampleInt+1;
        end_index=end_time/SampleInt+1;

        max_acc=max(AccelData_comp(1,start_index:end_index));
        max_index=find(AccelData_comp(1,start_index:end_index)==max_acc);

        min_acc=min(AccelData_comp(1,start_index:end_index));
        min_index=find(AccelData_comp(1,start_index:end_index)==min_acc);

        if abs(max_acc)>abs(min_acc)
            pga_range=max_acc;
            s_index=max_index+start_index-1;
        else
            pga_range=min_acc;
            s_index=min_index+start_index-1;
        end
        t_spike=(s_index-1)*SampleInt;

        confirm_index=input(['> Spike: ',num2str(pga_range),'cm/sec^2 @
                    t=',num2str(t_spike),'sec. Do you want to delete? (Y/N): '],'s');
        if length(confirm_index)<1
            while upper(confirm_index)=='Y' | upper(confirm_index)=='N'
                confirm_index=input(['> Spike: ',num2str(pga_range),'cm/sec^2 @
                    t=',num2str(t_spike),'sec. Do you want to delete?
                    (Please enter Y or N): '],'s');
            end
        end
        disp(' ');
        confirm_index=upper(confirm_index);
        if confirm_index=='Y'
            mean_acc=(AccelData_comp(1,(s_index-1))+AccelData_comp(1,(s_index+1)))/2;
            AccelData_comp=[AccelData_comp(1,1:(s_index-1)),mean_acc,
                    AccelData_comp(1,(s_index+1):end)];
```

```
            plot(TimeData,AccelData_comp);ylabel('Acceleration,cm/s^2','FontSize',8);
            xlabel('Time (s)','FontSize',8);
            disp('> Accelerogram of the record is updated.');
            disp(' ');

            comp_spike_index=
                    input('- Does the record include any Spikes? (Y,N): ','s');
            if length(comp_spike_index)<1
                while upper(comp_spike_index)=='Y' | upper(comp_spike_index)=='N'
                    comp_spike_index=input('- Does the record include any Spikes?
                           (Please enter Y or N): ','s');
                end
            end
            disp(' ');
            comp_spike_index=upper(comp_spike_index);
        end
        end
end
close all;
AccelData_comp_spike_cleared_1=AccelData_comp;
AccelData_comp_spike_cleared=AccelData_comp_spike_cleared_1';
plot(TimeData,AccelData_comp)
hold off;
```

Manual

Start the SCSW Software:

1) Run “Startup NEW” From the desktop.
2) Make sure to turn on the tap water.
3) Check whether the E-stop button is glowing green before performing the experiment.
4) Also, make sure the system indicator button glows green.
5) Turn on the pump by clicking on HPS low, then HPS high.
6) Under Group 1, click on the “Start DAS.”
7) Click on the “ACT 3 Startup”.
8) Under logger, click on Setup then click on start to turn the A3 continuous logger.

Import Time history file to the SCSW Software:

1) Open “Startup NEW” From the desktop.
2) Under Function Generator, Type Time history.
3) Click on the “c” next to the function generator.
4) Click on Create Waveform.
5) Expand x(A3).
6) Right-click on the SWAF file.
7) Click on the properties.
8) Click on the “Convert ASCII FILE.”
9) Click on the “Set Source File” to import the desired time history.

10) Click on the “Set Target File” to create a converted ASCII file.

11) Make sure the units of time and displacements are as desired.

12) Enter the fixed sample interval in seconds.

13) If importing from a text file, make sure the Time column ignored is set to True, whereas Displacement Column ignored is set as False.

14) After the conversion, select the SWAF file to be loaded into the software.

15) Perform the soft start/ soft stop as necessary.

16) Click on ok and Run the test.

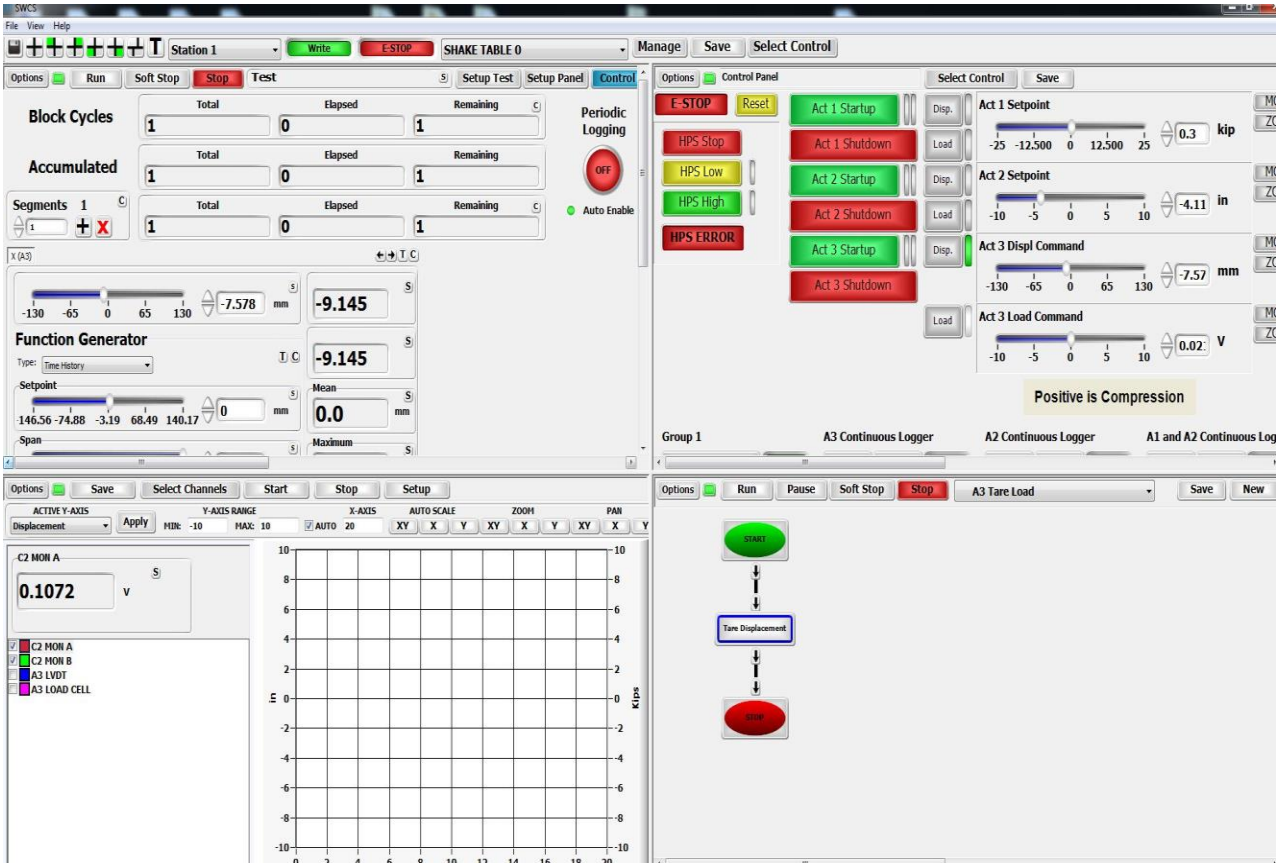

Figure: Working space of the SCSW Software

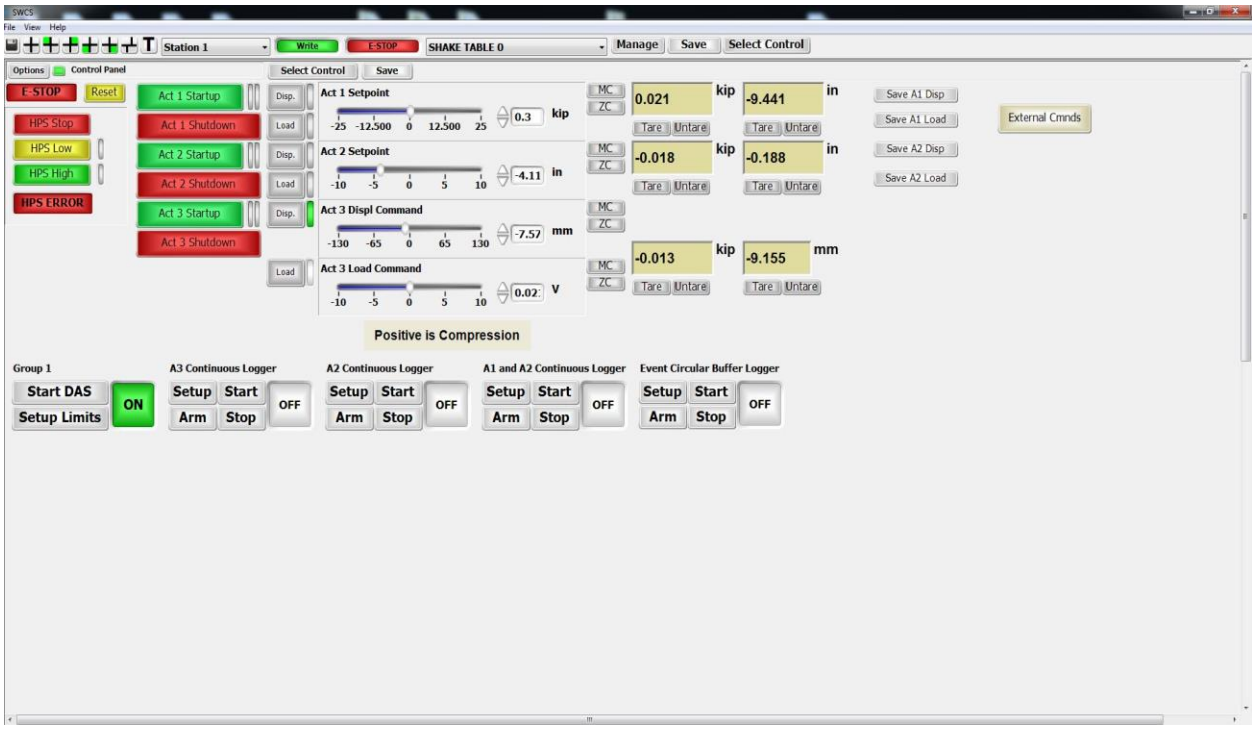

Figure: SCSW Software Logger Panel

Data Acquisition System:

1) Open Measurement and Automation (MAX).
2) Under Devices and interfaces, Open tree.
3) Right-click on VXI Slot 0.
4) Run the VXI Resource Manager.
5) Do not close but minimize the application.
6) Open the VEE Pro application.
7) Open SCSW file then “Biraj1”.
8) The main interface shows a block diagram with six channels.
9) The number of channels can be customized as desired.

10) In order to change the Time and Block size or the frequency of the data set, click on the Channel group block.
11) Right-click on the Channel group.
12) Click on the Edit user interface to customize time and frequency.
13) Double click on “Setup E1432”.
14) Here you can change the time and block size for your desired data collection range.
15) Click on Start to get on with the data collection process.
16) The status shows running while the data acquisition process is in progress.
17) Once the status shows ready, the data can be viewed.
18) Click on the Channel 1 Time to see the output at Channel 1.
19) The output gets stored in a default file or directory.
20) To change the destination file, Double click on the file and change the destination file or folder.

Figure: Data Acquisition System Assembly Setup

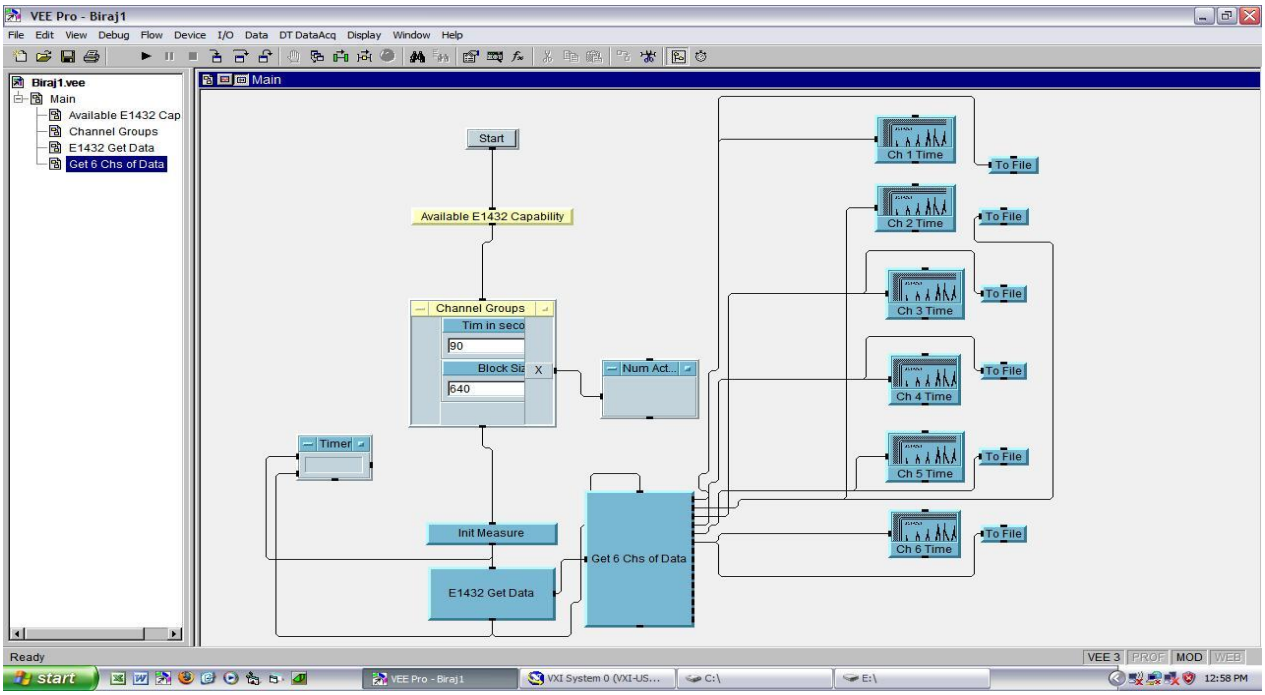

Figure: VEE Pro User interface with six channels

References

Abrahamson, N. A. (1992) “Non-stationary spectral matching.” Seismological Research Letters 63, 30.

ASCE (American Society of Civil Engineers) ASCE 7-16 (2017) “Minimum design loads for buildings and other structures.” Reston, Va.

Athanasiou A., Oliveto G., and Ponzo F. (2018) “Baseline Correction of Digital Accelerograms from Field Testing of a Seismically Isolated Building. Earthquake Spectra.” May 2018, Vol. 34, No. 2, pp. 915-939.

Bommer, J.J., Acevedo, A.B., and Douglas, J. (2003) “The selection and scaling of real earthquake accelerograms for use in seismic design and assessment.” Proceedings of ACI International Conference on Seismic Bridge Design and Retrofit, American Concrete Institute.

Boore, D. M. (1999) “Effect of baseline corrections on response spectra for two recordings of the 1999 Chi-Chi, Taiwan, earthquake.” U.S. Geological Survey, Open-File Rept. 99–545, 37 pp.

Boore, D. M. (2005) “On pads and filters: Processing strong-motion data.” Bull. Seism. Soc. Am. 95, 745-750.

Boore, D. M. and J. J. Bommer (2005) “Processing strong-motion accelerograms: Needs, options and consequences.” Soil Dynamics & Earthquake Engineering 25 (2), 93–115.

Chiu, Hung-Chie (1997) “Stable Baseline Correction of Digital Strong-Motion Data.” Bulletin of the Seismological Society of America, Vol. 87, No. 4, pp. 932-944.

Darragh, R.B., Silva, W.J., and Gregor, N. (2004) “Strong motion record processing procedures for the PEER center.” Proceedings of COSMOS Workshop on Strong-Motion Record Processing, Richmond, California, pp. 1–12.

Fahjan Y.M. and Ozdemir Z. (2008) “Scaling of Earthquake Accelerograms for Non-linear Dynamic Analyses to match the Earthquake Design Spectra.” 14th World Conference on Earthquake Engineering, October 12-17, 2008, Beijing, China.

Guorui, H. and Tao, L. (2015) “Review on Baseline Correction of Strong Motion Accelerogram,” International Journal of Science, Technology and Society 2015, 3(6): 309-314.

Haselton, C. B., Baker , J. W., Bozorgnia, Y., Goulet, C. A., Kalkan, E., Luco, N., Shantz, T., Shome, N., Stewart, J. P., Tothong, P., Watson-Lamprey, J., and Zareian, F. (2009) “Evaluation of Ground Motion Selection and Modification Methods: Predicting Median Inter-story Drift Response of Buildings.” PEER Technical Report 2009/01, Berkeley, California, 288p.

Mulchandani, H.K., Muthukumar, G., and Bansal, S. (2018) “Ground Motion Selection and Scaling using ASCE 7-16, Case Study on Town Alipur in Delhi Region.” 16th Symposium on Earthquake Engineering, December 20-22, 2018, IIT Roorkee, India, Paper No. 371.

Naeim, F. and Kelly, J.M. (1999) “Design of Seismic Isolated Structures: From Theory to Practice,” John Wiley & Sons.

Riddell, R., De La Llera, J.C. (1996) “Seismic Analyses and Design: Current Practice and Future Trends.” 11th World Conference on Earthquake Engineering, Paper No. 2010, ISBN: 0 08 042822 3.

Sextos, A.G., Katsanos, E., Elnashai, A. (2014) "Prediction of inelastic response periods of buildings based on intensity measures and analytical model parameters," Engineering Structures, 71, 161-177.

Shahbazian, A. and Pezeshk, S. (2010) “Improved Velocity and Displacement Time Histories in Frequency-Domain Spectral-Matching Procedures.” Bulletin of the Seismological Society of America, 100(6), pp. 3213-3223.

Thrainsson, H., Kiremidjian, AS., and Winterstein, S. (2000) “Modeling of Earthquake Ground Motion in the Frequency Domain.” John A Blume Earthquake Engineering Center Technical Report 134., Stanford Digital Repository.

Tokoro, K. and Menun, C. (2004) “Application of the modal Pushover Procedure to estimate Non-linear Response Envelopes,” 13th World Conference on Earthquake Engineering Vancouver, B.C., Canada, Paper No. 545.

Trifunac M. D. (1971) “Zero Baseline Correction of Strong Motion Accelerograms.” Bulletin of the Seismological Society of America, 61, 1201-1211.

Wang, L. (2002) “Illustration of Shake Table Experiments in Structural Engineering Curriculum.”, 2002 American Society for Engineering Education Annual Conference & Exposition.